EXPLORING THE TRANSCRIPTION PROGRAM OF INTESTINAL GOBLET CELL RESPONSE AND MUCIN PRODUCTION IN *TRICHURIS MURIS* INFECTION

EXPLORING THE TRANSCRIPTION PROGRAM OF INTESTINAL GOBLET CELL RESPONSE AND MUCIN PRODUCTION IN *TRICHURIS MURIS* INFECTION

By

ZARIN T. HAIDER, MBBS

A Thesis Submitted to the School of Graduate Studies in Partial Fulfillment of the Requirements for the Degree Master of Science

McMaster University

Descriptive notes

MASTER OF SCIENCE (2023) (MEDICAL SCIENCES)	McMaster University Hamilton, Ontario, Canada
TITLE	Exploring the transcription program of intestinal goblet cell response and mucin production in *Trichuris muris* infection
AUTHOR	Zarin T. Haider, MBBS
SUPERVISOR	Dr. Waliul I. Khan, MBBS, PhD, FRCPath
NUMBER OF PAGES	xviii, 123

Abstract

Goblet cells in the mucosal layer of the gastrointestinal tract are the primary source of gel-forming mucins, representing front-line defense. Sterile alpha motif-pointed domain ETS family transcription factor (SPDEF) has a crucial role in terminal differentiation, proliferation and maturation of goblet cells. Gut microbiota is an integral part of our internal environment. In a murine model of intestinal helminthic infection *Trichuris muris*, the interaction between host microbiota and parasite was seen to play critical roles in immune defense. This interaction is mediated through various mechanisms, including Toll-like receptor (TLR) and nucleotide-binding oligomerization domain (NOD)-like receptor signaling cascades. However, the precise role of intestinal microbiota and NOD/TLR signaling in regulating SPDEF is not yet understood. Hence, we investigated the role of SPDEF in intestinal goblet cell response, the role of helminth-microbiota axis and NOD/TLR signaling in modulating SPDEF during *T. muris* infection.

Experiments were conducted in wild-type (*SPDEF*$^{+/+}$) and SPDEF-deficient (*SPDEF*$^{-/-}$) mice on BALB/c background at different timepoints of *T. muris* infection. We observed increased PAS+ goblet cells and higher expression of SPDEF and Muc2 in *SPDEF*$^{+/+}$ mice following infection with elevated levels of IL-4 and IL-13. *SPDEF*$^{+/+}$ mice showed decreased worm burden from day 14 to 21 post-infection. Microbial analysis revealed altered composition in *SPDEF*$^{+/+}$ and *SPDEF*$^{-/-}$ after infection.

Microbiota was transplanted from naïve and *T. muris* infected mice to separate groups of antibiotic-treated (ABX-treated) mice. Increased PAS+ goblet cells and higher expression of SPDEF and Muc2 were observed in ABX-treated mice after receiving naive and *T. muris*-altered microbiota. Goblet cell number, the expression of SPDEF and Muc2 were higher in ABX-treated mice who

received *T. muris*-altered microbiota. Microbial analysis revealed differences in *T. muris*-altered microbiota compared to naïve microbiota.

In vitro experiment was conducted in human colonic mucin secreting LS174T cells where we observed stimulated mRNA expression of *SPDEF* and *MUC2* by *T. muris* excretory-secretory products. These findings reveal new information about major interactions among parasites, microbiota and SPDEF-mediated intestinal goblet cell response in the context of host defense.

Acknowledgements

First of all, my deepest gratitude goes to my supervisor Dr. Waliul Khan for being an amazing guide and mentor throughout the two years of my master's program at McMaster university. Coming all the way from Bangladesh to pursue my interest in research with very little prior experience, it has certainly been a beautiful and adventurous ride for me to have learnt new skills and gained knowledge which will forever be helpful for my research career. All throughout this journey, I received invaluable support and advice from Dr. Khan. I would also like to thank my committee members, Dr. Lesley MacNeil and Dr. Michael Surette, for their outstanding support, continuous guidance and valuable feedback on my research. Furthermore, I would like to express my gratitude to Surette lab members- Michelle Shah, Laura Rossi, Dr. Kate Kennedy, Dr. Michael Surette and others for guiding me in conducting microbial analysis of mice samples and answering countless questions regarding my experiments and research.

I would especially like to thank Huaqing Wang from Khan lab for his constant support, generosity and guidance in the process of my learning new research and laboratory skills from the very beginning. I could not have come all this way through this entire process without his unconditional support and direction from day one. My appreciation also goes to our previous lab members Dr. Suhrid Banskota, Dr. Sabah Haq, Dr. Eric Kwon, Yeganeh Yousefi, and to our current lab members Jensine Grondin, Tyler Seto and Sadrina Mowna for always being there for me through thick and thin. They have made my life at the lab a lot easier by helping me in every step of my learning process. I cannot thank them enough for their support.

Lastly, I would like to thank my family back home for being so supportive and proud of me despite all the circumstances. They have been constantly encouraging me from the very beginning, have

never lost faith in me and have empowered me to become the resilient human being that I am today by unconditionally inspiring me in pursuing my dream. I am eternally grateful to them.

Table of contents

List of figures

List of tables

List of abbreviations and symbols

5-HT	5-hydroxytryptamine
AAs	Amino acids
Ab	Antibody
ABX-treated	Antibiotic-treated
ABX-WT	Antibiotic-treated wild-type
ADCC	Antibody-dependent cellular cytotoxicity
Ags	Antigens
AMPs	Antimicrobial peptides
ANOVA	Analysis of variance
APCs	Antigen-presenting cells
AREB	Animal Research Ethics Board
ATOH-1	Atonal bHLH-1
bHLH	Basic helix-loop-helix
BMP	Bone morphogenic protein
BSA	Bovine serum antigen
CAF	Central animal facility
CHO	Carbohydrates
CID	Chronic inflammatory diarrhea
CREB4	CRE-binding domain-4
DAMPs	Damage-associated molecular patterns
DAPI	4’6-diamidino-2-phenylindole
DCs	Dendritic cells

DKO	Double knock-out
DMEM F-12	Dulbecco's modified Eagle-medium nutrient mixture F-12
EC	Enterochromaffin
EECs	Enteroendocrine cells
ELISA	Enzyme-linked immunosorbent assay
ER	Endoplasmic reticulum
ESPs	Excretory-secretory products
ETS	E-26 transformation specific
FBS	Fetal bovine serum
Fcgbp	Fc-γ binding proteins
FDR	False discovery rate
Fu	Fucose
GABA-α3	Gamma-aminobutyric acid α3
Gal	Galactose
GalNAc	N-acetylgalactosamine
GAPs	Goblet cell-associated antigen passages
GF	Germ-free
Gfi-1	Growth factor independent-1
GI	Gastrointestinal
GlcNAc	N-acetylglucosamine
HES-1	Hairy and enhancer of split-1
IBD	Inflammatory bowel disease
IFC	Immunofluorescence

IFN-γ	Interferon-γ
IgG	Immunoglobulin-G
IL	Interleukin
ILC-2	Innate lymphoid cell type-2
ISCs	Intestinal stem cells
KLF4	Kruppel-like factor-4
KO	Knock-out
LEFSe	Linear discriminant analysis effect size
LPS	Lipopolysaccharide
MAPK	Mitogen-activated protein kinase
Math-1	Mouse Atoh-1
MHC-II	Type-2 major histocompatibility complex
miRNA	Micro RNA
NF-κβ	Nuclear factor-κβ
NK	Natural killer
NLRP6	NOD receptor binding protein-6
NLRs	NOD-like receptors
NOD	Nucleotide-binding oligomerization domain
p.i.	Post-infection
PAMPs	Pathogen-associated molecular patterns
PAS	Periodic acid-Schiff
PBS	Phosphate buffer saline
PCoA	Principal coordinate analysis

PERMANOVA	Permutational multivariate ANOVA
PGN	Peptidoglycan
PI3K/AKT	Phosphatidylinositol 3-kinase/protein-B or AKT
PIC	Protease inhibitor cocktail
PRRs	Pattern recognition receptors
PSA	Prostate-specific antigen
PVDF	Polyvinylidene difluoride
RELBβ	Resistin-like molecule β
ROS	Reactive oxygen species
RT-qPCR	Real-time quantitative polymerase chain reaction
SA	Sialic acid
SAM	Sterile alpha motif
SCFAs	Short-chain fatty acids
SCID	Severe combined immunodeficiency
SEM	Standard error of means
SenGCs	Sentinel goblet cells
SPDEF	SAM-pointed domain ETS family transcription factor
SPF	Specific pathogen-free
STAT-6	Signal transducers and activators of transcription-6
STH	Soil-transmitted helminths
TA	Transit-amplifying
TBST	Tris-buffered saline Tween-20
TH1	Helper T cell type-1

TH2	Helper T cell type-2
TLRs	Toll-like receptors
Tregs	Regulatory T cells
TSLP	Thymic stromal lipoproteins
VNTR	Variable number tandem repeat
WT	Wild-type

Declaration of academic achievement

I, Zarin T. Haider, am the sole author of this thesis which has been designed by me and my supervisor, Dr. Waliul Khan. The research was conducted by me with technical support and cooperation from Huaqing Wang, past lab members Dr. Suhrid Banskota, Dr. Sabah Haq, Dr. Eric Kwon, Yeganeh Yousefi, and current lab member Jensine Grondin.

During the course of my master's program, I have had the pleasure to present a poster about my research at the Medical Sciences Research Day held on 25th April 2023 at McMaster Innovation Park.

Chapter 1: Introduction

1.1 Gastrointestinal (GI) tract and mucus membrane

The gastrointestinal or GI tract is composed of a long passageway of hollow organs extending from the mouth to the anus, which is a part of the digestive system. The complete digestive system is composed of the GI tract and other accessory solid organs including the liver, pancreas and gallbladder. The upper GI tract extends from mouth to small intestine (anatomically, from mouth to the suspensory ligament of Treitz between the third and fourth parts of duodenum), whereas the colon, rectum and anal canal form the lower GI tract. Other than digestion and absorption of food as its major functions, the GI tract performs many other functions, such as regulating the immune system, secreting enteroendocrine hormones and modulating inflammatory reactions. There are many factors that can affect the GI physiology and functions that include intestinal microbiota, inflammatory reactions, neural pathways, aging, neuroendocrine regulation, stress [1]. The histological structure of the GI tract includes a hollow lumen and the wall surrounding the lumen which consists of mucosa, submucosa, muscularis propria and serosa from inside outwards. The intestinal mucus membrane consists of epithelium coated with a mucus layer and the underlying lamina propria. The intestinal epithelium is composed of a variety of cells which include absorptive epithelial cells and secretory cells like goblet, Paneth and enteroendocrine cells (EECs) within the intestinal crypts. There is also a villus structure seen along the mucus membrane of small intestine as projections. The large intestine or colon lacks these villus projections and Paneth cells in their epithelium.

The mucus coat, epithelium, intercellular tight junctions and lamina propria form the protective intestinal barrier, protecting the wall against the luminal contents [2].

1.1.1 Goblet cells

Goblet cells are specialized cells originating from the secretory lineage that reside in the epithelial membrane of the GI tract, respiratory tract and conjunctiva. The mucosa of these systems is called the wet-surface mucosa due to the presence of these secretary goblet cells [3] [4]. The goblet cells are the main source of gel-forming mucins which are the major components of the mucus coating of the epithelium. Other than mucins, the goblet cells secrete a variety of factors which include trefoil factors, resistin-like molecule β (RELMβ) and Fc-γ binding proteins (Fcgbp), which also provide intestinal defense in the epithelial membrane along with mucins [2]. The goblet cells are the most abundant secretory cell-types originating from the intestinal stem cells (ISCs) located at the base of the intestinal crypts [5]. In the GI tract, the goblet cells are found in increasing numbers from the small intestine to the distal colon. In the colon, these cells contribute to forming a two-layered mucus gel which provides protection, lubrication and hydration to the membrane, and helps in the transportation of molecules [2] [4]. This mucus layer also harbors the gut flora in its loose outer layer, whereas its adherent and less porous inner layer usually acts as a sterile coverage. The inner layer protects the colon and maintains an almost bacteria-free environment, thus creating a barrier between the mucosal epithelium and gut microbiota [4].

1.1.2 Mucins

Mucins are high molecular weight glycoproteins that form the major building block of mucus. Around 21 different mucin genes have been identified [2] [4]. Mucins can be transmembrane/membrane-bound and secreted; the secreted mucins can be further classified into gel-forming and soluble/non-gel forming [6]. Transmembrane mucins are expressed on

enterocytes which include MUC1, MUC3, MUC4, MUC12, MUC13, MUC16, MUC17 [7]. The gel-forming secreted mucins, which include MUC2, MUC5AC, MUC5B, MUC6 form the skeleton of the mucus membrane, providing a protective lubricant blanket along the mucosal epithelium [5] [7].

The structure of mucins is highly hydrophilic, polymeric and viscoelastic with an average mass of $2x10^6$ Daltons, which forms a gel-like covering in the mucus membrane by binding with H_2O [2] [5]. This gel covering prevents contact between the epithelium and the contents inside the gut lumen, the disruption of which may lead to abnormal immune responses in the host leading to various inflammatory conditions and infections [2]. More than 80% of its contents are carbohydrates (CHO) which are concentrated into mucin domains [5]. The mucin domains represent the key element of its chemical structure surrounded by *O*-glycans, forming a central protein core [5]. The protein sequence of these domains is rich in amino acids (AAs) proline, threonine and serine, which is why they are also called the PTS domains, organized as variable number tandem repeat (VNTR) [7] [8]. Serine and threonine are the most prevalent AAs. With the help of their hydroxyl groups, this protein core is linked with the oligosaccharide chains around the core via *O*-glycosidic bonds. There are five types of sugars in the oligosaccharide chains which include fucose (Fu), galactose (Gal), N-acetylglucosamine (GlcNAc). N-acetylgalactosamine (GalNAc) and sialic acid (SA) [5].

The mucins are synthesized in the endoplasmic reticulum (ER) where they undergo *N*-linked glycosylation followed by transportation into the Golgi complex and *O*-linked glycosylation. They are then stored into the secretory mucinogen granules where they become highly concentrated and are eventually secreted from the granules after they merge with the plasma membrane. The secretory granules account for 75% of the cytoplasmic volume and are the

source of secreted mucins from the cells [2]. The secretion of mucins from the granules happens in two ways: the continued constitutive secretion under normal physiological condition, and stimulated secretion in response to various factors or stimuli [2] [4]. During stimulated secretion, more or the entire secretory content is secreted from the granules. These factors include microbial factors, inflammatory cytokines, growth factors, neuropeptides, autonomic neural pathways, and lipids [2] [9] [10] [11] [12] [13]. The secretion of mucins can also be regulated by various cellular responses like nucleotide-binding oligomerization domain-like (NOD) receptors binding protein 6 (NLRP-6) mediated activation of the inflammasome, autophagy, production of reactive oxygen species (ROS) and endocytosis [2]. In terms of worm infection, the gel-covering in the mucus membrane formed by mucins helps in lubrication, traps the worms in the viscoelastic mucus layer, and inhibits their motility and feeding capacity [14].

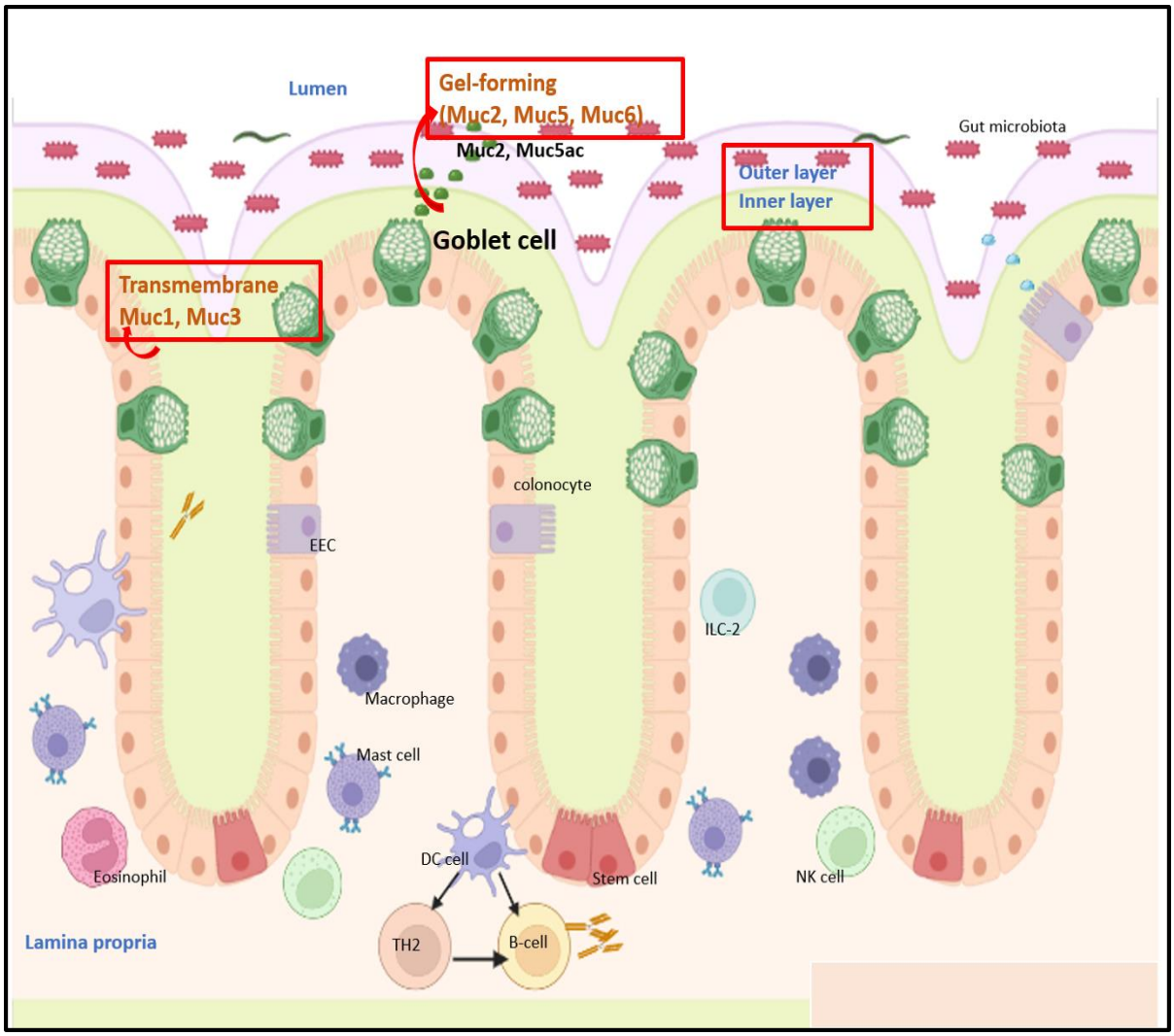

Figure 1. Intestinal mucus barrier and different kinds of mucins

The gastrointestinal epithelium is a double-layered mucus membrane, majorly formed by gel-forming mucins secreted by the goblet cells and transmembrane mucins expressed on the enterocytes. The outer mucus layer is in close proximity to the intestinal lumen containing gut flora, while the inner layer is almost bacteria-free. Various kinds of immune cells are located in the lamina propria underneath the mucosal layer, which show immune and inflammatory responses to infections and other stimuli. The picture is generated by the author.

1.2 Goblet cell differentiation and transcription program

The intestinal crypts of small and large intestine contain intestinal stem cells or ISCs, also known as progenitor cells. In the colon, the multipotent, undifferentiated ISCs of monoclonal origin reside at the base of the intestinal crypts (at the lower 2/3rd), and the upper 1/3rd of the crypts towards the luminal side contains the differentiated epithelial cells [15]. These intestinal stem cells produce rapidly proliferating daughter cells, also called the transit-amplifying (TA) cells, which generate precursor cells. The precursor cells differentiate into 2 lineages- the absorptive lineage giving rise to the enterocytes (called colonocytes in the colon) and secretory lineages that differentiates into goblet, Paneth (in small intestine) and enteroendocrine cells (EECs) [16]. The differentiation of ISCs into four major types of cells (enterocytes, goblet cells, Paneth cells and EECs) requires a variety of complex pathways, namely Wnt β-catenin (canonical), Notch, bone morphogenetic protein (BMP) and phosphatidylinositol 3-kinase (PI3K)/protein kinase B (AKT) pathways [2]. Wnt β-catenin and Notch cascades are the key regulators in determining the cell-fate of ISCs into the secretory and absorptive lineages respectively [17] [18]. Hairy and enhancer of split or HES family basic helix-loop-helix (bHLH) Transcription Factor-1 or HES-1 acts as the downstream component of Notch that determines the cell fate of ISCs into the absorptive enterocytes. Atonal bHLH Transcription Factor-1 (ATOH-1) is the downstream component of β-catenin that activates several transcription factors like sterile alpha motif (SAM) pointed domain ETS family transcription factor (also termed as SPDEF), growth factor independent-1 (Gfi-1) and regulates the cell-fate of ISCs into the secretory goblet cells [19].

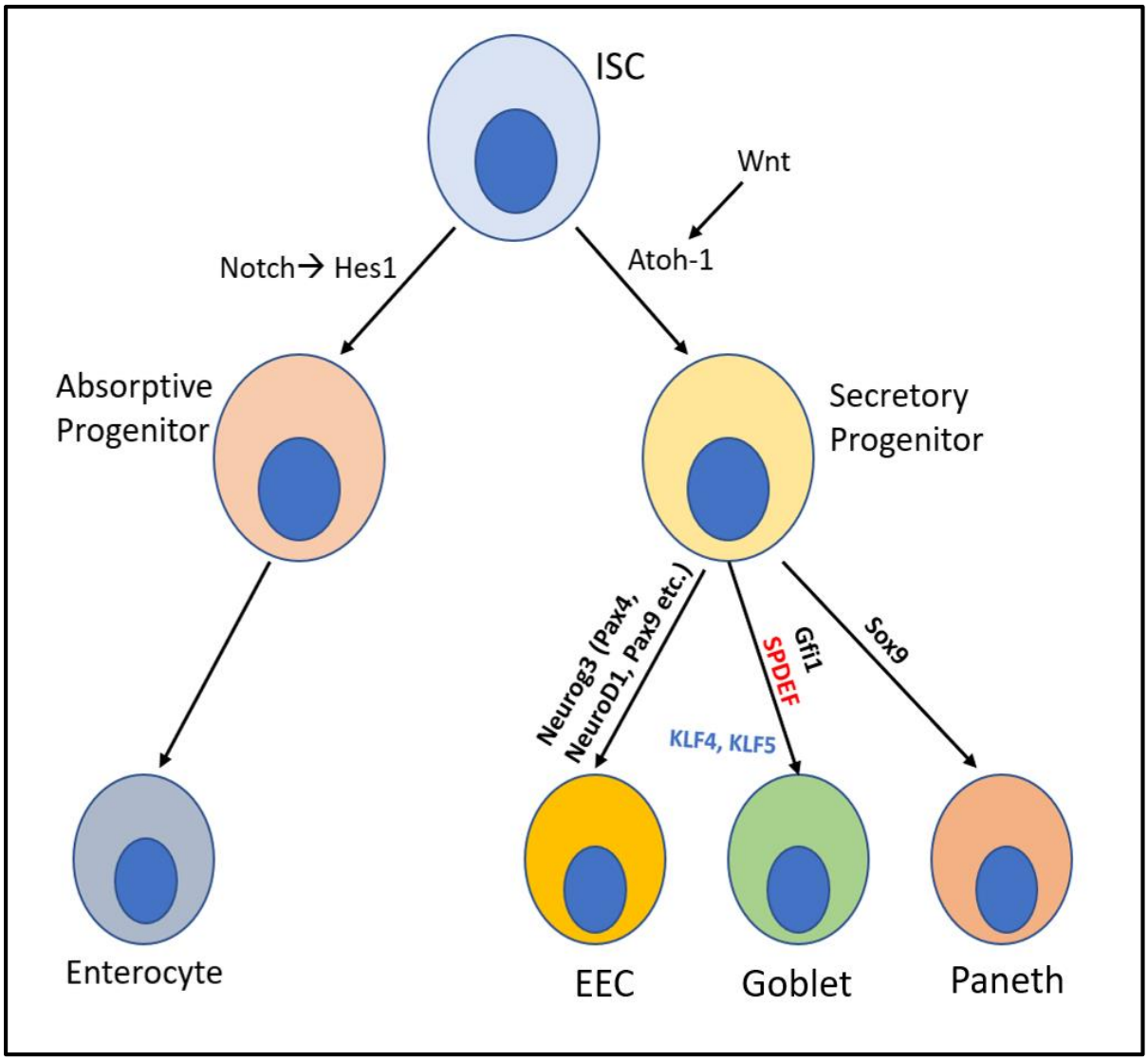

Figure 2. Differentiation of intestinal stem cells (ISCs)

The ISCs differentiate into absorptive and secretory lineage giving rise to enterocytes, goblet cells, Paneth cells and enteroendocrine cells (EECs) via Wnt and Notch signaling pathways and their transcription factor networks. The picture is generated by the author.

1.2.1 Role of SPDEF in goblet cell differentiation

SPDEF is an epithelium specific ETS family transcription factor, also known as the ESE family protein. The ESE family of transcription factors is a subgroup of E-26 transformation specific transcription factors or ETS family of proteins [20]. The ETS family proteins bind the GGAA/T regulatory sequence of DNA with their H3-helix of DNA binding domain, which has 85 amino acids [20]. SPDEF, a Wnt responsive transcription factor was first described as a prostate-derived transcription factor and was later found to be also expressed in breasts, intestine, lungs, salivary glands and conjunctiva [20] [21] [22]. SPDEF was seen to interact with androgen receptor *in vitro* which regulates the expression of prostate specific antigen (PSA) promoter [21]. Twenty seven types of different mammalian ETS proteins have been identified [22]. Several studies have indicated that SPDEF regulates the terminal differentiation, homeostasis and maturation of intestinal goblet cells. A study conducted in mice showed that the inactivation of SPDEF does not impair the cell-fate determination of the ISCs into the secretory lineage, but the maturation and terminal differentiation of the secretory cells were hampered leading to the accumulation of immature secretory cells [19] [23]. CRE-binding protein-4 (CREB4), an endoplasmic reticulum or ER stress transducer has also been seen to act as a downstream component of SPDEF to promote the terminal differentiation and maturation of goblet cells in mice [19].

1.3 Goblet cell response in enteric parasitic infection

Previous studies have shown that goblet cells at the colonic crypts can go through non-specific endocytosis and convert into sentinel goblet cells (senGCs). The endocytosed senGCs are killed, undergo complex exocytosis and are expelled into the gut lumen [24]. The goblet cells

in small and large intestine form goblet cell-associated antigen passages or GAPs, through which they deliver the luminal antigens (Ags) to the dendritic cells (DCs) in the lamina propria [25]. The DCs and macrophages provide the processed Ags to naïve CD4+ T cells and convert them into helper T cell type-2 or TH2 cells [2] [25]. Alterations in the goblet cell response and mucin production have been seen in many intestinal infections including parasites, bacteria and virus [5]. Hyperplasia of mucus secreting goblet cells has been observed in intestinal parasitic infections such as *Ascaris galli*, *Trichinella spiralis, Trichuris muris and Nippostrongylus brasiliensis,* which helps in providing innate defense to the host [5] [26]. Qualitative changes in mucins were also observed in parasitic infections, namely *N. brasiliensis*, which include alteration in the composition of mucins from neutral to acidic nature and change in terminal sugars [5]. Elevated levels of Muc2 and Muc4 were observed in *T. spiralis* infection in mice [5]. MUC2 (in human) or Muc2 (in mice), also called the goblet cell mucin expressed in both small and large intestine, is an important component of innate defense in nematode infection. During *T. muris* infection, significantly higher number of goblet cells and increased secretion of Muc2 were observed in resistant BALB/c mice than in susceptible AKR mice, correlating with worm expulsion [27]. Genetic background of mice plays an important role is determining resistance or susceptibility to *T. muris* and in C57BL/6 resistant strain, delayed worm expulsion due to the absence of Muc2 was observed following *T. muris* infection [27]. Muc5ac, also called gastric foveolar mucin which is normally expressed in the stomach and lungs has been seen to increase in the colon only in resistant mice following *T. muris* infection, and around the time of worm expulsion, a remarkable increase in Muc5ac was found in Muc2 deficient mice [27] [28]. Muc5ac was also seen to be critical for worm expulsion, whereas its lacking resulted in susceptibility to chronic infection [26]. Other

mucins such as Muc4, Muc13 and Muc17 were also seen to increase during *T. muris* infection in a study conducted on BALB/c mice, which resulted in increased thickness of glycocalyx, the carbohydrate-rich zone projecting from the apical surface of the epithelium composed of glycoproteins like mucins [26].

Intestinal parasitic infections induce TH2 immune response that triggers worm expulsion by a variety of pathways [29]. TH2 immune response can mediate the release of cytokines or interleukins, which include IL-4, IL-5, IL-9, IL-13. During parasitic infection in mice model, IL-13 was seen to cause goblet cell proliferation via signal transducers and activators of transcription-6 or STAT-6 pathway triggering worm expulsion [27]. Also, overexpression of exogenous IL-25 and IL-9 was associated with goblet cell proliferation and mucin expression. Several studies indicated that IL-13 also helps in upregulation of Muc5ac [27]. In human colonic cancer cell lines, IL-4 and IL-13 induced the expression of trefoil factors and mucins. IL-17, a TH17 cytokine and IL-6 were seen to promote overexpression of Muc5ac and Muc5b [24]. Another TH17 cytokine IL-22 was seen to help in goblet cell proliferation and mucin expression. TH1 cytokine tumor necrosis factor-α or TNF-α has been observed to increase Muc2 by nuclear factor-kappa beta or NF-κβ-inducing kinase (NIK) and Akt/PI3 pathways [24].

1.4 Mucin and host intestinal microbiota

The microbiota is an integral part of the internal environment of our body and has a major role in its maintenance. This microbial environment resides throughout our body. Among them, the intestinal microbiota is composed of trillions of microorganisms including bacteria, viruses, protozoa and fungi. The gut microbiome not only helps in the development and maintenance

of normal gut architecture, but it also plays roles in immune system maintenance, host nutrition, homeostasis and energy balance such as production of short-chain fatty acids (SCFAs), vitamin synthesis and amino acid metabolism [30]. In the GI tract, microbial density gradually increases from the proximal to distal [31]. In the colon, there are approximately 10^{12} microbial cells per gram of intestinal contents and they are composed of bacteria of approximately 1000 different species [32] [33]. The most abundant intestinal microbiota are from the phyla Bacteroidetes and Firmicutes [34]. The highest number of bacterial species from the gut has been found to reside in the lumen of the gut, whereas from the lumen to the epithelial membrane, the bacterial density decreases [31]. Again, from the luminal to the distal portion of the mucus membrane, the microbial density has been seen to decrease due to the increasing thickness of the mucus. The luminal microbiota shows differences in their diversity and ecosystem as opposed to the microbiota residing in the mucus membrane [31].

The colon has two layers of mucus. Usually, the outer layer contains all the bacteria, which are mostly mucolytic or mucin-degrading microbes like *Bacteroides,* whereas the inner mucus layer, even though generally bacteria-free since the mucin polymers stagger on top of each to form a net against the invasion; has still shown the presence of some bacteria along the colonic crypts, most of which are from the *Actinobacter* species and Proteobacteria [35] [36] [37]. Also, α-diversity was found to be higher in the inner colonic mucus layer than the fecal sample. The composition of luminal, mucosa-associated and fecal microbial composition also shows differences between small and large intestine [35] [36].

Gut microbiota helps in the proper formation of intestinal mucus [31]. In the germ-free (GF) mice, the colonic mucus layer was found to be thinner and more penetrable to bacteria with fewer number of filled goblet cells than the conventionally raised mice [3]. The glycosylation

profile of mucus was also different in two groups [38]. When certain bacterial products like lipopolysaccharide (LPS) or peptidoglycan (PGN) were introduced into the GF mice, they showed higher mucus secretion, similar to conventionally raised mice [4]. The inner colonic mucus layer of GF mice showed penetrability to bacteria-sized particles, which showed an impenetrable characteristic after 7 weeks of receiving microbiota transplant [37]. Revealing non-penetrable property by the colonic of GF mice after being transplanted with cecal microbiota indicates the importance of gut microbiota in the maturation and development of the mucus [10] [11] [38]. One possible mechanism by which the microbiota can modulate the mucus can be that the microbiota helps in shaping the glycan profile and expressing glycosyltransferases in the mucus [41] [42]. This glycan profile of the mucus changes from species to species, also from small gut to large gut [41] [42].

The gut microbiota and the mucus layer of the host share a symbiotic relationship. The presence of glycan helps the microbiota to adhere to the mucus [7] [43] [44]. The microorganisms have their glycan binding capacity, which helps them to colonize in the mucus [44] [45] [46]. This glycan binding capacity also depends on the glycan profile of the mucus. There are other bacterial outer membrane proteins like lectins, adhesins, capsules and appendages like pili or flagella that also contribute to the adherence of the microorganisms to the mucus [13] [45] [46]. Other factors such as O_2 gradient, diet, antimicrobials and antimicrobial peptides (AMPs), invasion by pathogenic bacteria, physiological and metabolic state of the host, host genetics, age of the host and host immune system also play roles in the distribution of the gut microbiota [31] [33]. This glycan can also act as a source of nutrients for certain mucolytic or mucin degrading bacteria, who ingest the glycan by their glycosidase or glycan-degrading enzyme [32] [47] [48]. When the glycan binding enzyme removes all the glycans from the mucin-

glycan chain, protein core of the mucin is degraded, leading to mucus degradation [49] [50]. While using glycan as an energy source, SCFAs from the glycan-degrading enzymes are created that are absorbed by the colonocytes and the energy spent for the synthesis and secretion of mucin is partly recovered this way [49] [50]. Some of these mucolytic bacteria are helpful for the maintenance of the mucus, some can modulate the immune system by forming capsular polymer with the help of glycan [31]. This also confirms the bidirectional relationship between the host and the commensal microbiota.

1.5 Intestinal helminth and host microbiota interaction

Intestinal parasites are among the most prevalent pathogens infecting the animal kingdom worldwide affecting health, productivity and agriculture [51] [52]. Among the intestinal parasites, intestinal helminths, the multicellular parasitic worms, are the most common and they are persisting now as a worldwide health concern [51] [53]. Helminths are multicellular parasitic worms and a matter of global health concern that can cause long-lasting infection by modulating host immunity. This alteration of host immune response can help them persist inside the host for a long time and avoid immune-mediated expulsion [53]. Over 1.5 billion people worldwide along with many other mammalian species are infected with at least one species of intestinal helminths with their eggs and larvae, which happens either due to the chronicity of the infection or when the host is unable to prevent re-infection[34] [51] [54] [55]. Even though these helminths have been largely eradicated from developed countries and the tropical-subtropical regions, about one-fourth of the population remain at risk [56]. Most of the intestinal helminths that cause infection in humans are soil-transmitted helminths (STH).

The parasites and host microbiome share a bidirectional relationship. The helminths can modulate the changes in the bacterial diversity and community composition following infection which can vary from parasites to parasites [33]. One study has shown that the murine helminth *Heligmosomoides polygyrous* causes increased abundance in the species of *Lactobacillaeceae* family in small intestine, while no change was seen in the cecal bacterial community [57]. Chronic infection by the soil transmitted murine helminth *T. muris* in naive mice showed decreased bacterial diversity and increased relative abundance of *Lactobacilli* [58] [59].

Some indirect factors can also contribute to the alteration of gut microbial environment, which include the glycosylation profile and secretion of mucus, pH alteration, epithelial damage, parasitic worms and their eggs, and intestinal motility [56]. There are also direct factors that can modulate the microbial composition by parasites. The *T. muris* eggshell has a component named chitin that acts as an energy source for bacteria and its dietary supplementation into the mice and pigs showed altered bacterial composition [56]. Moreover, adult worms can directly compete with the microbiome for nutrients. The secreted products from the parasites like acetate and lactate are utilized by some bacteria as their energy source, leading to a change in their growth [60]. The helminths also compete with the microbiota for nutrient like glucose, which can affect its availability for the bacteria [61]. The helminths secrete AMPs that can alter microbial communities [62]. The intestinal microbiota also produces and utilize many intestinal metabolites (SCFAs) including acetate, butyrate and propionate, which help in immune system development [53]. The SCFAs are released when the microbiota carries out anaerobic fermentation of carbohydrates in the intestine, so their altered composition following helminthic infection can also alter carbohydrate metabolism, observed in *Trichuris suis* model

in pigs [53]. In naïve mice, the most abundant microbiota was found to be from the phylum Bacteroidetes, which breaks down fiber to SCFAs. These act as energy sources for the host [63]. The SCFAs are also anti-inflammatory and can stimulate the differentiation and suppressive capacity of FOXp3+ Treg cells (Regulatory T cells) [61]. They can also decrease the release of inflammatory cytokines by inhibiting NF-kB pathway, stimulate mucus production, and decrease allergic airway inflammation and IL-10 expression in mesenteric lymph nodes in mice [53]. The direct alteration of these intestinal metabolites can alter immune response and the colonization of pathogens as well [53].

The microbial bacterial environment also helps in establishment of infectivity by the intestinal parasites. The bacteria can associate with the egg-polar plug of the intestinal helminths, contributing to the emergence of their infective larvae [33]. Again, to facilitate the worm-growth, the parasites alter the bacterial community for their advantage [33]. It was observed in a study that, a high burden of helminthic infection in humans during early life in endemic areas altered the composition and stability of microbiota [64] [65]. Since the microbial composition has been observed to play a role in the establishment of parasitic infestation, it may be suggested that regulation of the microbial components play a role in controlling parasitic infection [34].

1.6 Effect of helminth-microbiota interaction on host immunity

The intestinal microbiota is an important part of the functional innate immune system. The interaction between parasitic helminths and gut microbiota has influence on homeostasis and host immune response [30]. The GI helminths have immune-suppressive properties, which changes immune-mediated response [54]. It can be said that, this microbiota-parasite-host

interaction forms a three-way synergy [66]. Also, due to host-parasite interaction, the immune and structural cells of humans and other mammals achieve 'tolerance', the ability to restrict the tissue damage actively without creating an impact on the parasite-load, for the maintenance of the host's fitness [52]. The intestinal helminths can cause long-term infection by avoiding immune-mediated expulsion, which helps them not only to persist in the body, but also they can impair the immune system, observed in both humans and mice models [56]. Studies suggested that the parasite mediated TH2 response was associated with some changes in the mucosal environment with subsequent changes in the gut microbial environment. As mentioned before, the mucosal environment also has impact on host microbiota [66]. Furthermore, changes in the microbiome have revealed its association with some inflammatory diseases like inflammatory bowel disease (IBD), diabetes, allergy [67]. Live helminthic infection is associated with decreased prevalence of allergic disease in humans and decreased allergic airway inflammation in mice [68] [69]. The decrease in parasite infections in the developed world may be a cause for the rise in the frequency of immune associated disorders in these populations [56]. Even without the infection, the helminth-altered microbiota can also modulate host immunity. Some studies revealed that the transfer of altered microbiota in the absence of live infection was associated with decreased airway inflammation in mice [53].

The intestinal helminths usually are expulsed through TH2 effector mechanism, but sometimes, this type-2 immune response is not able to cause the complete expulsion of the worms. This is because some helminths show certain regulatory mechanisms [61]. The helminths can secrete excretory-secretory products (ESPs) like immunomodulatory proteins, defensins, glycoproteins and microRNA (miRNA), that can modulate the immune cells of the host's body and can also directly induce certain regulatory cells like FOXp3+ Tregs. This gives

them the opportunity to survive longer in the host and increases host susceptibility to infections and inflammation [61]. The helminths can modulate microbial composition through their ESPs and AMPs. Toll-like receptors (TLRs) and nucleotide-binding oligomerization domain (NOD)-like receptors are pattern recognition receptors (PRRs) that can detect the metabolites secreted by intestinal microbiota [61]. The helminths and their derived products can also change the expression of these PRRs, which modulate host recognition of microbes. Thus, the helminths, microbes and host immunity, all act interpersonally and modulate each other [61].

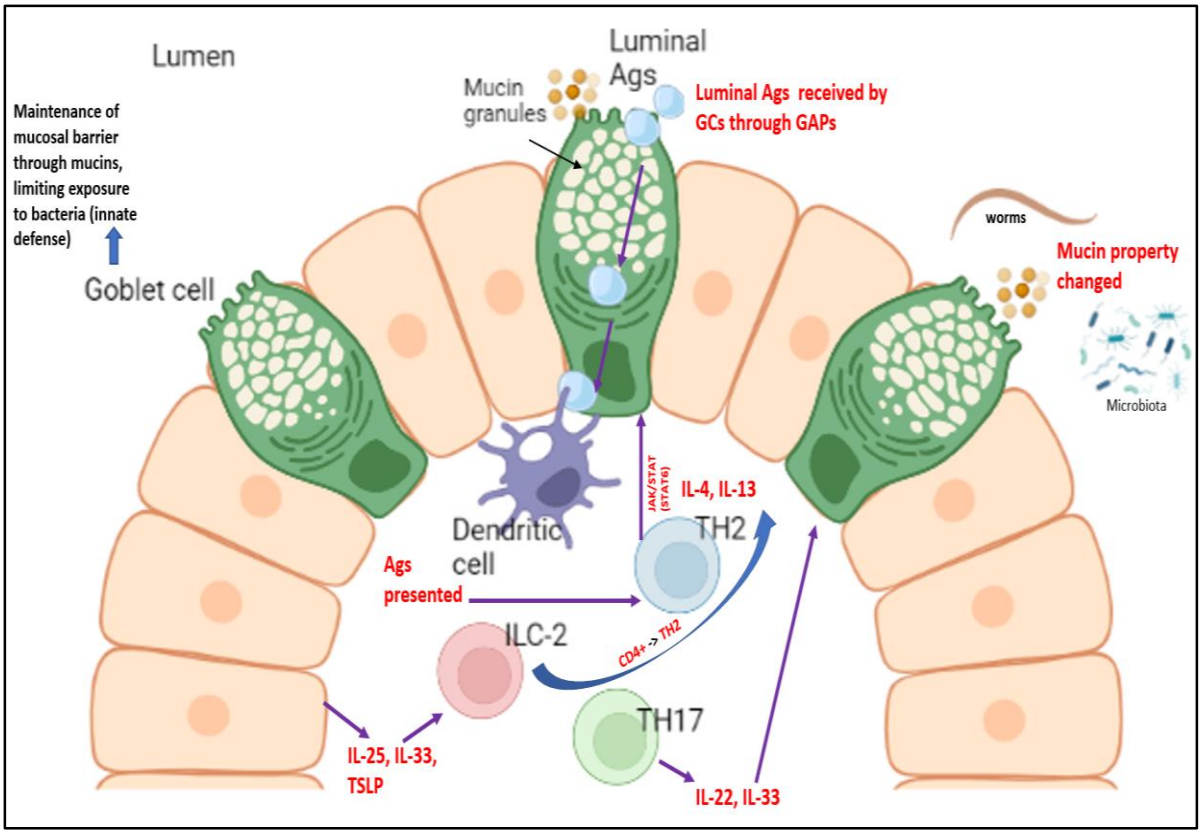

Figure 3. Immunological Regulation of Goblet Cell Function and Role of Microbiota in Enteric Parasitic Infection

The goblet cells present antigens (Ags) through GAPs to the antigen-presenting cells (APCs) in the lamina propria, which include dendritic cells (DCs) [2] [25]. The DCs process Ags, present them to the CD4+ T-cells and convert them into TH2 cells, which secrete various cytokines (IL-4, IL-13) that cause goblet cell hyperplasia through a STAT-dependent pathway and increase mucin secretion, providing immunity to the host [2] [27]. Cytokines secreted from enterocytes and other types of immune cells in the lamina propria (innate lymphoid cell-2/ILC-2, TH17) can also induce goblet cell hyperplasia directly or indirectly by inducing TH2-mediated cytokine secretion. The microbiota in the gut lumen can induce changes in the mucin property secreted by the goblet cells in response to a parasite. The parasites can modulate changes in the microbial community and the microbiota also plays important roles in parasitic

establishment, indicating a synergistic relationship between the parasite and the microbiota. The picture is generated by the author.

1.7 Intestinal parasitic nematode (Trichuris muris)

Soil-transmitted helminths or STH affect more than 1 billion people worldwide [51]. *Trichuris muris* is a soil-transmitted helminth and murine pathogen having similarities in genomic, transcriptomic and morphological aspects with *Trichuris trichiura*, which is the most common intestinal whipworm causing gastrointestinal infection in humans around the world [26] [27] [29]. *Trichuris* species are epithelial dwelling parasites that can infect humans, livestock and mammals, also potentially showing relative drug resistance and re-infection [51]. *T. trichiura* itself infects around 800 million people worldwide, most of them being children who show symptoms of malnutrition and intellectual retardation [51] [70] [71]. *T. muris* in mice is a common laboratory model used to study the various pathophysiological, immunological, microbiological and inflammatory changes that occur in the GI tract following infection [72] [73]. *T. muris* secrete ESPs by which they invade the host tissue and promote microbiological alteration, tissue remodeling, and evasion of immunological and inflammatory responses [53].

1.7.1 Life cycle of T. muris

The infection with *T. muris* occurs after the ingestion of eggs excreted through the feces of the infective hosts [29]. The eggs excreted through the feces become embryonated in a period of approximately two months, which cause the infection [51]. In the large intestine, the eggs mostly hatch in the wall of caecum and proximal colon, where they undergo 4 larval molting, namely L1, L2, L3 and L4. The first larval molting occurs within 90

minutes of infection and the subsequent stages happen around 9-11, 17 and 22 post-infection (p.i.) days respectively [29]. The expulsion of worms starts from day 14 p.i. and by day 21, most of the worms are expelled from the gut in resistant mice [28]. After 21 days, worm expulsion gradually decreases [63]. Between day 32 and 35 post-infection, full larval development occurs and the adult worms are released from the epithelial wall of the caecum and proximal colon into the gut lumen [51] [63]. By day 35 p.i., complete worm expulsion occurs in resistant strains of mice, although the susceptible strains may harbor worms after 35 days [27] [63]. The anterior part of the adult worms is covered by parasite-modified epithelial cells forming a structure similar to 'syncytial tunnel'. An electron microscopy study showed that adult worms live in direct contact with the modified epithelial cell cytoplasm [51].

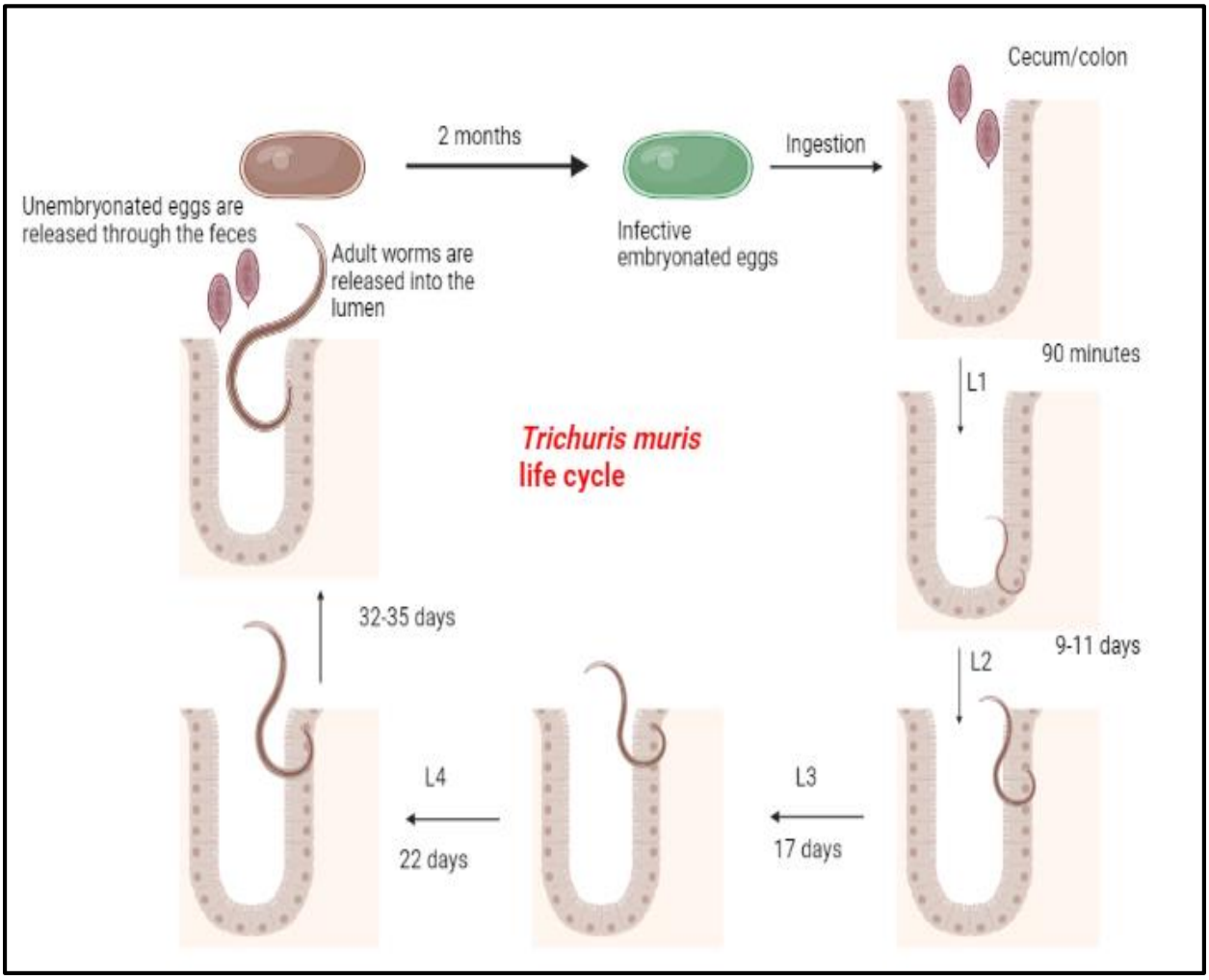

Figure 4. Life cycle of T. muris

The infection with *T. muris* is initiated by ingestion of embryonated eggs. The hatching of the eggs in the cecal epithelium is facilitated by the intestinal microbiota, where they undergo 4 larval molting stages (L1-L4). After 32 days, the larvae become adult worms and can be found in the cecal and colonic lumen. The unembryonated eggs are released into the environment with the feces and take around 2 months to become embryonated. The picture is generated by the author, adapted from Klementowicz et al., (2012) [51].

1.7.2 Responses to T. muris by resistant and susceptible strains

The intestinal helminth *T. muris* survives in the host by eliciting a Helper T-cell type-1 or TH1 immune response, whereas the resistance to *T. muris* is achieved by TH2 immune response. A study conducted on BALB/c mice showed that a high dose infection with more than 150 eggs of *T. muris* resulted in expulsion of worms by TH2 immune response and a low-dose infection with less than 15 eggs resulted in chronic infection in mice resulting from their survival in the gut [26]. More than 70% of the mouse strains such as BALB/c, BALB/k, C57BL/6 are resistant to *T. muris* who expel the worms by day 35 p.i. by eliciting TH2 immune response if high infective dose is given, whereas the susceptible strains such as AKR and B10Br elicit TH1 immune response and cannot expel *T. muris* worms resulting in chronicity [29]. Also, C57BL/6 and BALB/c are susceptible to *T. muris* chronic infection if low infective dose is given [29].

1.8 Effects of T. muris on host immunity

1.8.1 Effects on goblet cells and mucins

The intestinal mucus forms part of the front-line defense. In acute *T. muris* infection, activation of transcription factors leading to goblet cell hyperplasia was observed [26] [27]. Following *T. muris* infection, hyperproliferation of goblet cells was seen in the mice models who were able to expel the worms, and hyperproliferation of enterocytes was seen in the mice who could not expel the worms resulting in chronic infection [26] [27] [74] [75]. Although the goblet cell hyperplasia is considered largely under the control of TH2 immune response, IL-4/IL-13 independent hyperplasia of goblet cells can also happen according to some studies [76] [77] [78].

In the resistant BALB/c mice during acute infection with high dose of *T. muris* eggs, significant upregulation of Math-1 (mouse Atoh-1) and SPDEF was observed leading to increased differentiation and number of goblet cells, whereas during chronic infection with low dose of *T. muris* eggs in the same strain of mice, there was increased expression of Hes-1 leading towards the enterocyte differentiation [26]. Acute infection in mice also led to increased thickness of glycocalyx layer composed of glycans and various cell-surface mucins compared to WT mice and mice with chronic infection. Although hypersecretion of glycoprotein was observed in both acute and chronic infections, the IL-13 regulated glycoprotein hypersecretion mediated by GABA-α3 receptors was more pronounced in acute infection versus chronic after 21 p.i. days [26]. The glycosylation profile also altered after infection which showed mucins with relatively more charge in acute compared to chronic infection, which might have increased the barrier function of the mucus leading to worm expulsion [26]. Muc2 mucin, the major secretory mucin of goblet cells showed significant upregulation with increased goblet cell numbers in *T. muris* infected resistant BALB/c mice during day 21 and 35 p.i. as opposed to infected susceptible AKR strain. This also correlated with worm expulsion in resistant mice [27]. Muc2 deficiency in mice resulted in not only a delay in worm expulsion, but also an aberrant loss of goblet cell phenotype, abnormal mucosal morphology in the colon, and perpetuation of dextran sulphate sodium-induced colitis [27] [79]. Goblet cell hyperplasia mostly is mediated by TH2 cytokines IL-4 and IL-13 through STAT-6 dependent pathway. A previous study has shown that *Stat-6*$^{-/-}$ mice during *T. spiralis* infection presented with diminished goblet cell number and impairment in worm expulsion compared to WT mice [77]. Muc5ac, which is normally expressed in the stomach and lungs was seen to be a critical mediator for worm expulsion of the resistant C57BL/6 mice with *T. muris* infection [28]. In

infected WT mice, hypersecretion of IL-13 induced Muc5ac was observed, whereas *Muc5ac*$^{-/-}$ mice, despite having a prominent TH2 response, showed high susceptibility to *T. muris* harboring chronic infection with lower goblet cell number and Muc2 expression compared to infected WT [28]. In the same study it was seen using human colon cancer cell lines that worms are creating less ATP (adenosine triphosphate) in MUC5AC producing cells, which is thought to be an important mediator for worm viability.

1.8.2 Effects on other innate immune cells

Other than goblet cells in the mucus barrier and PRRs (which are discussed later), various types of innate immune cells provide protection against *T. muris*, some of which include APCs like dendritic cells (DCs), natural killer (NK) cells, macrophages, innate lymphoid cell type-2 (ILC-2), basophils and mast cells [51]. Epithelial cells have also been seen to provide immunity against *T. muris* and to act as a bridge between innate and adaptive arms. Intestinal epithelial cells secrete IL-25, IL-33 and thymic stromal lipoprotein (TSLP) which were seen to induce ILC-2 and multipotent progenitor (MPP) cells and they subsequently promoted CD4+ T-cell proliferation and differentiation towards TH2 phenotype resulting in increased IL-4, IL-5, IL-13 during *T. muris* infection [29] [80] [81]. Resistant mice were seen to secrete higher amount of IL-33 from enterocytes on day 3 p.i. and recombinant IL-33 administration into the susceptible mice at an early stage of infection helped the mice to expel the worms, the phenomenon which was otherwise not observed if administered during the late stage of infection or into the severe combined immunodeficiency (SCID) mice [80] [82] [83].

The DCs are potent APCs which take up the Ags and present them to T-cells promoting TH2 differentiation and releasing of cytokines. The DCs express class-II major histocompatibility

complex (MHC-II), CD80, CD86, CCR7 and lower endocytic activity [84]. DCs migrate to the mesenteric lymph nodes (MLNs) in the lamina propria where the naïve T-cells are located to stimulate TH2 differentiation. These recruited DCs mature at the site of infection on day 7 p.i. in the resistant mice following *T. muris* infection [29]. This mobilization of the DCs to the site of the infection in resistant mice is stimulated by certain chemokines, such as CCL2, CCL3, CCL4, CCL20 and TSLP [84]. There are various subsets of DCs that can show varied responses to infection and among them, CD11b+ DCs have been seen to enhance TH2 response during *T. muris* infection [85].

Previous study has shown that NK cells can also produce IL-4 and IL-13 and activate TH2 cells during *T. muris* infection [51]. They were also seen to play a role in sex-based differences during *T. muris* infection where these cells in male IL-$4^{-/-}$ mice showed increased expression of CXCR3 receptor that enhances interferon- γ (IFN-γ) secretion and TH1 immunity resulting in susceptibility [86] [87]. The DX5+ NK cells in female IL-$4^{-/-}$ mice, on the other hand, produced more IL-13 and expelled the worms [88].

Mast cells and eosinophils are some of the hallmarks of parasitic infection and their accumulation was also seen at the site of *T. muris* infection in resistant mice [29]. Both types of cells have been seen to promote TH2-mediated response in acute *T. muris* infection [29] [89]. The basophils have also been seen to produce some TH2-inducing cytokines that facilitated DC-mediated TH2 differentiation leading to resistance to infection [51].

1.8.3 Effects on adaptive immune response

There are several studies that have already shown that intestinal helminth *T. muris* survives in the host by eliciting a type-1 (TH1) immune response, whereas the resistance to *T. muris* is

achieved by TH2 immune response. Lee et. al. showed that when naïve mice receive T-cells but not B-cells, they show resistance to *T. muris* [90]. In another study, it was seen that the nude or T-cell deficient mice who showed susceptibility to *T. muris* partially restored resistance and showed worm expulsion after they received splenocytes or MLNs or thymocytes [91]. The deficiency of CD4+ T-cells in mice causes susceptibility to *T. muris* and the adoptive transfer of these cells from BALB/c to SCID mice showed worm expulsion [51] [92]. The mice with chronic infection secrete IFN-γ from the TH1 cells with the production of immunoglobulin-G2a (IgG2a) that helps in survival of the worms and with the administration of anti-IFN-γ-antibody (Ab) or recombinant TH2 cytokine IL-4, they showed resistant phenotype [93].

The susceptible mice produce high levels of TH1 cytokines such as IFN-γ, IL-18, IL-12 and pro-inflammatory mediators like TNF-α and IL-17 that can lead to prolonged inflammatory reactions resulting from chronicity [93] [92] [95] [96]. TH2 cytokines IL-4 and IL-13 play the major role in worm expulsion in resistant mice and their deficiency cause susceptibility to *T. muris* [97] [98]. B-cells and their antibodies also represent the adaptive arm of the immune system and it was seen in resistant mice that T-cells can stimulate B-cells to secrete antibodies that can facilitate antibody-dependent cellular cytotoxicity (ADCC) process, providing more immunity to *T. muris* [29]. The susceptible strains, however, showed higher IgG2a production which is a TH1-associated Ab, whereas the resistant strain produced more TH2-associated Ab IgG1 [29] [99].

1.8.4 Effects on PRR-mediated signaling

NOD-like receptors (NLRs) and Toll-like receptors (TLRs) are pattern recognition receptors (PRRs) expressed in the cytoplasm or on the surface of various immune and non-immune cells

including macrophages, DCs, NK cells, neutrophils, epithelial and endothelial cells. They recognize the pathogen-associated molecular patterns (PAMPs) or damage-associated molecular patterns (DAMPs) that act as ligands for the receptors. The PRRs provide first-line defense against microbes by acting as a bridge between innate and adaptive host defense, leading to the subsequent activation of adaptive response [100]. To date, there are ten human and thirteen murine subtypes of TLRs that have been identified, most of which are transmembrane proteins [101]. The NLRs, on the other hand, are intracellular proteins that have twenty three subtypes in humans and thirty four in mice [102].

Goblet cells in the colon express high levels of TLR1/2, TLR4 and TLR5 on their surface, and NOD1 and NOD2 intracellularly [103]. Previous studies have shown that ESPs from certain helminths like *Hymenolepis diminuta* increased the expression of TLR2 and TLR4 in the mouse intestine and increased TLR2 in murine colonic DCs was also observed in *Schistosoma japonicum* infection [104] [105]. In the context of *T. muris*, research from our lab has shown both *in vivo* and *in vitro* that *T. muris* ESPs can directly act through the TLR2 receptors in NF-κβ dependent pathway to cause increased 5-hydroxytryptamine (5-HT) or serotonin production from the enterochromaffin (EC) cells in the gut [103].

The NOD2 receptor plays an important role in colonic epithelial cell response to *T. muris* and in recruitment of colonic DCs to the site of infection [106]. Our lab has demonstrated that *T. muris* infected NOD1/2- DKO (double knock-out) C57BL/6 mice had decreased number of goblet and Muc2-expressing cells in the colon along with decreased IL-4 secretion and increased worm burden in contrast to infected WT mice [107]. When the naïve mice were treated with NOD1 and NOD2 agonists, they showed an increase in goblet cell number and *Muc2* expression [107]. The human colonic adenocarcinoma cell line LS174T has goblet cell-

like properties and secretes high levels of MUC2 [108]. Our study has also shown *in vitro* that there was increased expression of MUC2 in this cell line when treated with NOD1 and NOD2 agonists [107]. However, whether the *T. muris* ESPs can directly act through the NOD receptors in enhancing SPDEF and mucin expression is yet to be determined.

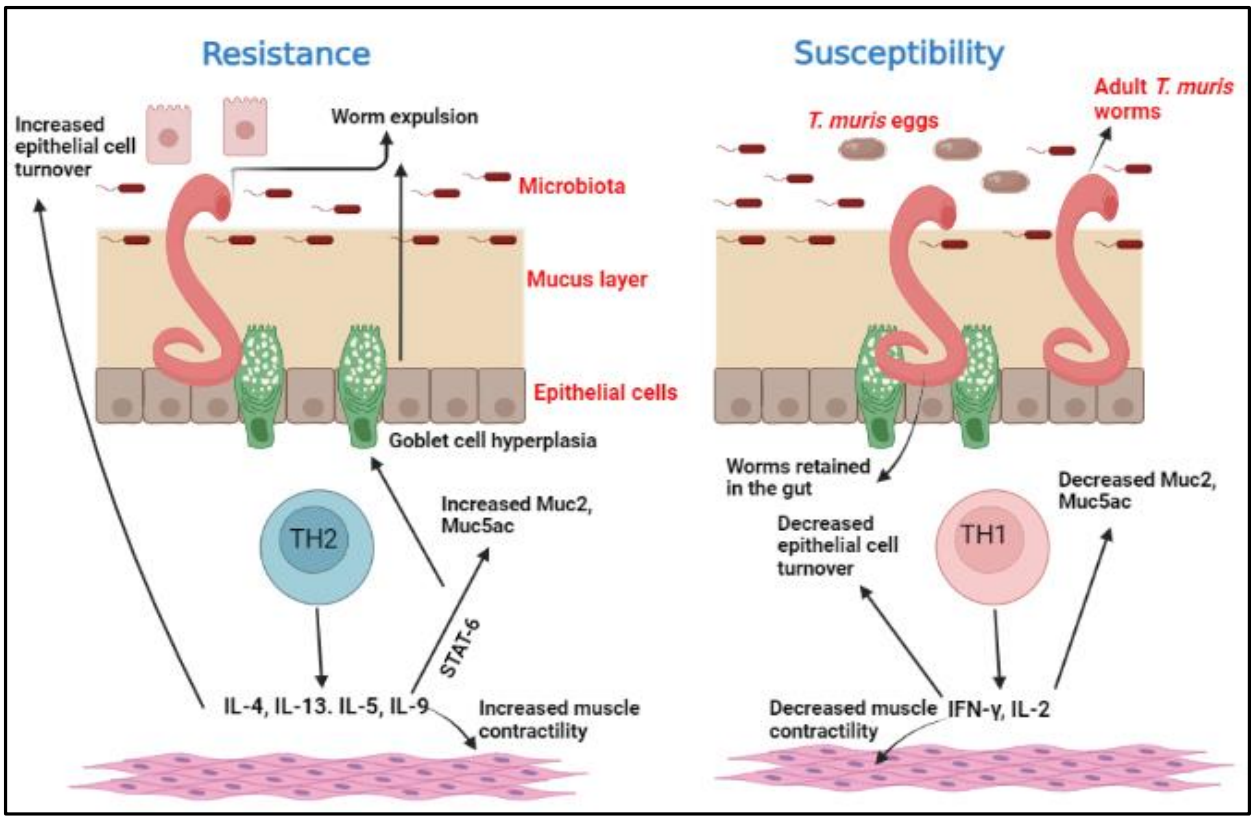
Resistance
Susceptibility
Increased epithelial cell turnover
Worm expulsion
Microbiota
Mucus layer
Epithelial cells
Goblet cell hyperplasia
Increased Muc2, Muc5ac
TH2
STAT-6
IL-4, IL-13. IL-5, IL-9
Increased muscle contractility
T. muris eggs
Adult T. muris worms
Worms retained in the gut
Decreased Muc2, Muc5ac
Decreased epithelial cell turnover
TH1
Decreased muscle contractility
IFN-γ, IL-2

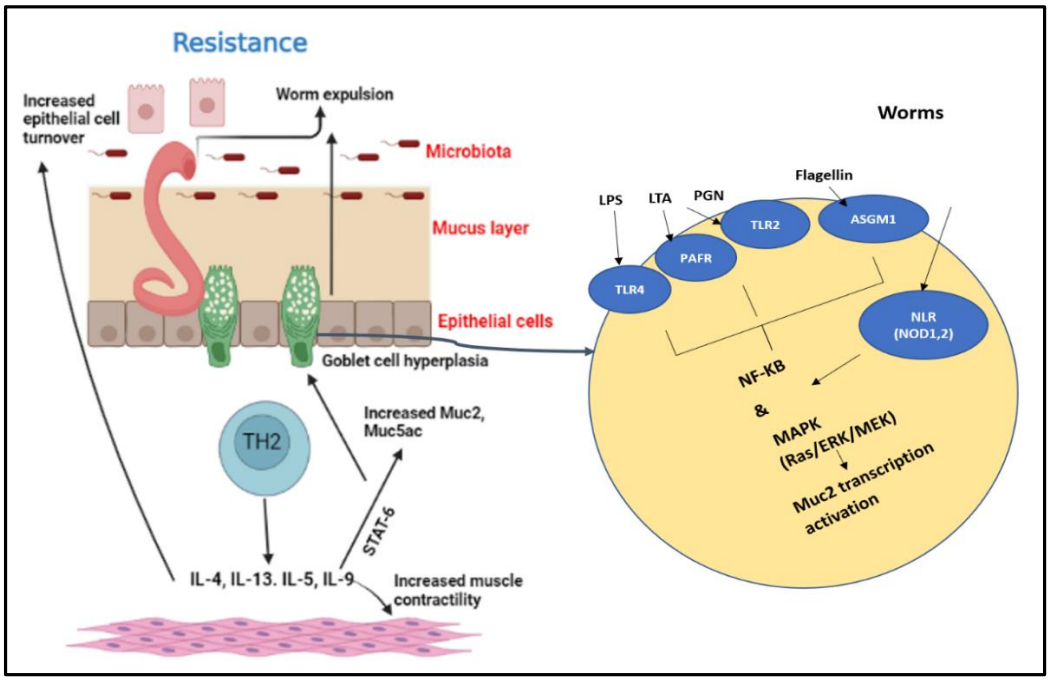
Resistance
Increased epithelial cell turnover
Worm expulsion
Microbiota
Mucus layer
Epithelial cells
Goblet cell hyperplasia
Increased Muc2, Muc5ac
TH2
STAT-6
IL-4, IL-13. IL-5, IL-9
Increased muscle contractility
Worms
Flagellin
LPS
LTA
PGN
TLR2
ASGM1
PAFR
TLR4
NLR (NOD1,2)
NF-KB
&
MAPK (Ras/ERK/MEK)
Muc2 transcription activation

Figure 5. Immune responses generated against T. muris infection in resistant and susceptible mice

The resistant strains of mice generate TH2-mediated immune response with production of IL-4, IL-5, IL-9 and IL-13 from activated TH2 cells. The TH2 response facilitates worm expulsion by causing hyperplasia of goblet cells, increased Muc2 and Muc5ac secretion from the goblet cells, accelerated epithelial cell turnover and increased smooth muscle contractility of the colon. These effector mechanisms are reversed in susceptible strains of mice where TH1-mediated immune response is observed with production of IFN-γ, which causes chronic infection due to failure in worm expulsion. The goblet cells in the colon express a variety of PRRs (TLR2, TLR4, NOD1, NOD2) [103]. These receptors bind with a couple of ligands that include bacterial LPS, LTA, PGN and flagellin, and ESPs from *T. muris* worms. The receptor-ligand binding generates downstream intracellular signaling pathways (NF-κβ, MAPK), which help in transcriptional activation of Muc2. The pictures are generated by the author.

1.9 T. muris and host microbiota interaction

The interaction between the intestinal parasite and host microbiota has been the most studied in the context of GI worms, like the *Trichuris* species [30]. The microbiota acts as an essential component in the establishment of worms in the gut and the worms can subsequently alter the microbial composition. In acute *T. muris* infection in mice, the gut microbiota contributes to the establishment of worms by facilitating their egg hatching. The established *T. muris* infection alters the microbial environment into a less favorable condition, and this altered microbiota facilitates chronic infection by inhibiting the hatching of eggs of a second dose of infection [51]. A study conducted in C57BL/6 mice demonstrated that pre-treatment of mice with antibiotics before the ingestion of eggs resulted in reduced infection level [63]. *T. muris* can alter gut microbiota in different ways that include alteration of the mucus, physiological changes in the internal environment and secretion of AMPs like Ang4. Housing condition of the animal model can also cause changes in the internal microbial environment [51]. A chronic inflammatory diarrhea (CID) model in macaques showed that *T. trichiura* infection was associated with an increase in α-diversity of gut microbiota, altered the microbial composition and abundance and decreased the clinical signs of CID [30].

Adult *T. muris* worms reside in the cecum and colonic mucosa on the GI tract, the highest abundance being in the proximal colon [51]. It was noticed that chronic *T. muris* infection in mice caused by low infective dose resulted in diminished α-diversity in cecal and colonic microbiota and changes in the abundance of bacterial taxa, whereas acute *T. muris* infection with high infective dose did not show any significant change in the α or β-diversity [63] [109] [110]. In chronic *T. muris* infection in C57BL/6 mice, the changes in the microbial composition and α, β-diversities of microbiota in stool samples started appearing as significant between 14

and 28 p.i. days, and were maintained until the end of experiment after 91 days [63]. A different species of *Trichuris*, a *T. suis* model study conducted in pigs showed that infection with *T. suis* was associated with an increased abundance of *Prevotellaceae* family and *Mucispirillum* genus. *Mucispirillum* colonizes in the GI mucus layer, so its increased abundance resulted in increased production of mucus following infection, indicating an association between alteration of mucus production and microbial change [109] [111].

Intestinal luminal microbes help *T. muris* larvae to properly hatch in the colonic epithelium. Oral administration of *Lactobacillus casei* in mice can increase the susceptibility to *T. muris* [112] [113]. Reducing the number of bacteria in the gut resulted in significant decline in the number of hatched *T. muris* eggs [112]. In a study, *T. muris* eggs were hatched *in vitro* and incubated at 37°C with mouse cecal explants containing four different species of bacteria- *Escherichia coli*, *Staphylococcus aureus*, *Salmonella typhimurium* and *Pseudomonas aeruginosa*. It was observed that *T. muris* eggs could hatch successfully almost at a similar rate in every bacterial suspension, whereas the removal of bacteria through filtration or their structural disruption prevented hatching of the eggs [112]. This suggests that not only the presence of bacteria, but also their intact morphology play key roles in the establishment of parasitic infections [112]. Administration of antibiotics into the mice can reduce aerobic and anaerobic bacteria, subsequently affecting the hatching of *T. muris* eggs [114]. All these findings suggest how crucial the gut microbial environment is for the survival of the intestinal dwelling parasites and how the parasites can also modulate a change in the microbial community.

1.10 Effects of T. muris in SPDEF-mediated transcription program

The role of SPDEF in goblet cell hyperplasia and mucin hypersecretion, and its induction through TH2-mediated inflammatory response in the airway and conjunctiva have been previously studied, along with its role in the intestine [115] [116] [115]. It has already been observed that transcription factors Atoh-1 and SPDEF were upregulated in acute *T. muris* infection in BALB/c mice around the time of the worm expulsion and the transcription factor Hes-1 which helps in enterocyte differentiation was upregulated in chronic infection [26]. This indicates a bias towards higher goblet cell differentiation in mice during acute *T. muris* infection.

Although upregulation of SPDEF around the time of worm expulsion is observed in resistant mice during *T. muris* infection, the precise role of SPDEF in worm expulsion and the role of interaction between intestinal microbiota and NOD/TLR innate immune signaling in activation of SPDEF during *T. muris* infection remain to be determined.

Chapter 2: Hypothesis and aims

Based on the literature presented on the role of SPDEF in goblet cell response, the innate and adaptive immune responses in *T. muris* parasitic infection, and the changes in microbial diversity and composition by the parasite; this thesis hypothesizes that *T. muris* infection modulates intestinal goblet cell response and mucin production by activating SPDEF mediated transcription program.

Aim 1

To determine the role of SPDEF in intestinal goblet cell response and mucin production during *T. muris* infection

Rationale: In previous studies, as discussed in Chapter 1, upregulation of SPDEF was observed in BALB/c mice during acute *T. muris* infection in association with increased colonic goblet cell numbers [26]. However, the precise role of SPDEF in goblet cell response and in *T. muris* expulsion remains to be determined. Herein, we investigated the role of SPDEF in regulation of goblet cell response and production of mucins (Muc2, Muc5ac), worm expulsion and generation of TH2 cytokines (IL-4, IL-13) following acute *T. muris* infection utilizing SPDEF-deficient ($SPDEF^{-/-}$) mice and WT counterparts on BALB/c background. Microbial analysis was also performed in *T. muris* infected WT and $SPDEF^{-/-}$ mice.

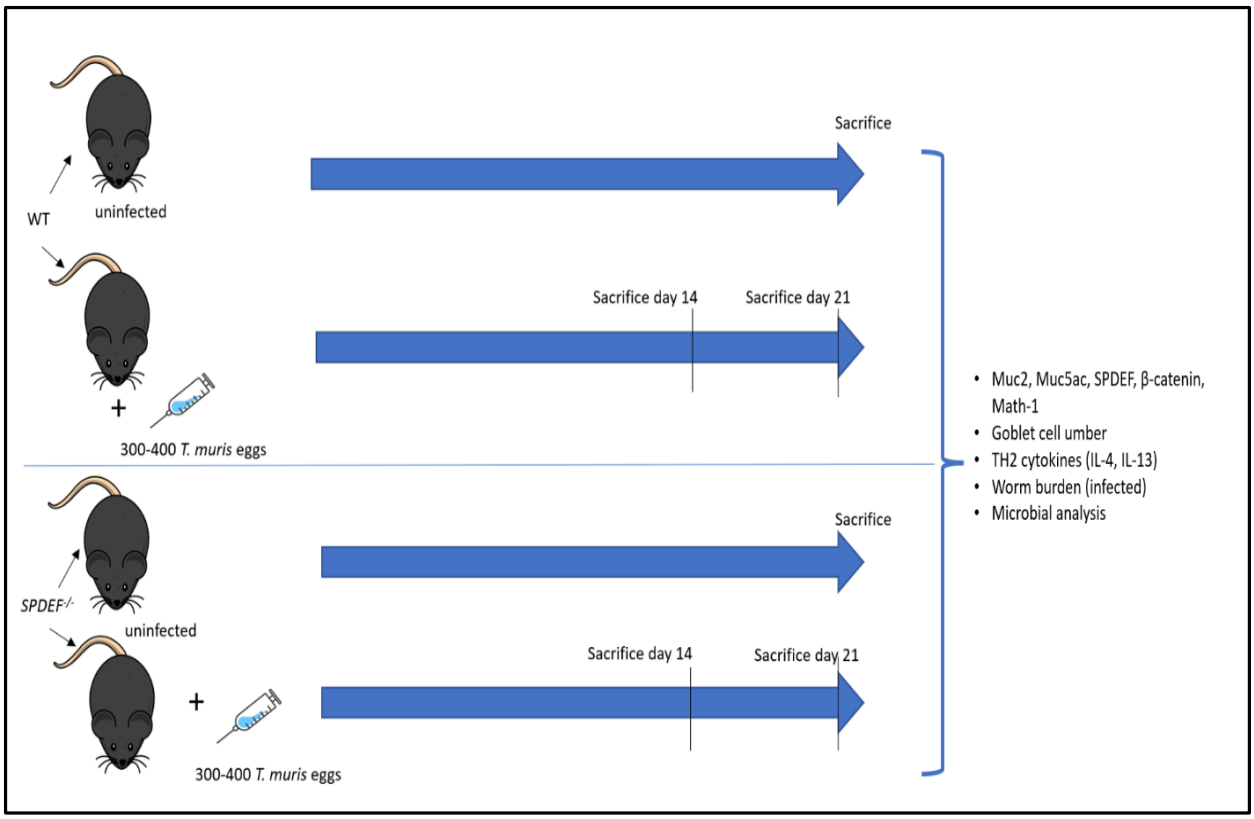

Figure 6. The experimental plan carried out between WT (SPDEF$^{+/+}$) and SPDEF-deficient (SPDEF$^{-/-}$) mice to observe the role of SPDEF in goblet cell response in T. muris infection

Aim 2

To understand the role of *T. muris*-microbiota axis in activating SPDEF to regulate goblet cell response and mucin production

Rationale: The changes in microbial composition and diversity in *T. muris* infection and its role in parasite establishment in the gut are well-documented [51] [63] [109] [110]. The relationship between parasite and host microbiome is mediated by a variety of mechanisms, which include ESPs and AMPs secreted by the parasite, worm-induced TH1/TH2 immune responses leading to mucosal and bacterial changes and modulation of PRR-mediated signaling pathways [9] [117]. In this aim, we investigated the effects of adoptive microbial transfer from naïve and *T. muris* infected

mice to antibiotic-treated (ABX-treated) mice in regulation of SPDEF and mucin production. We also performed microbial analysis to observe the differences in ABX-treated groups with or without microbial transfer to study the role of parasite-microbiota axis in this context.

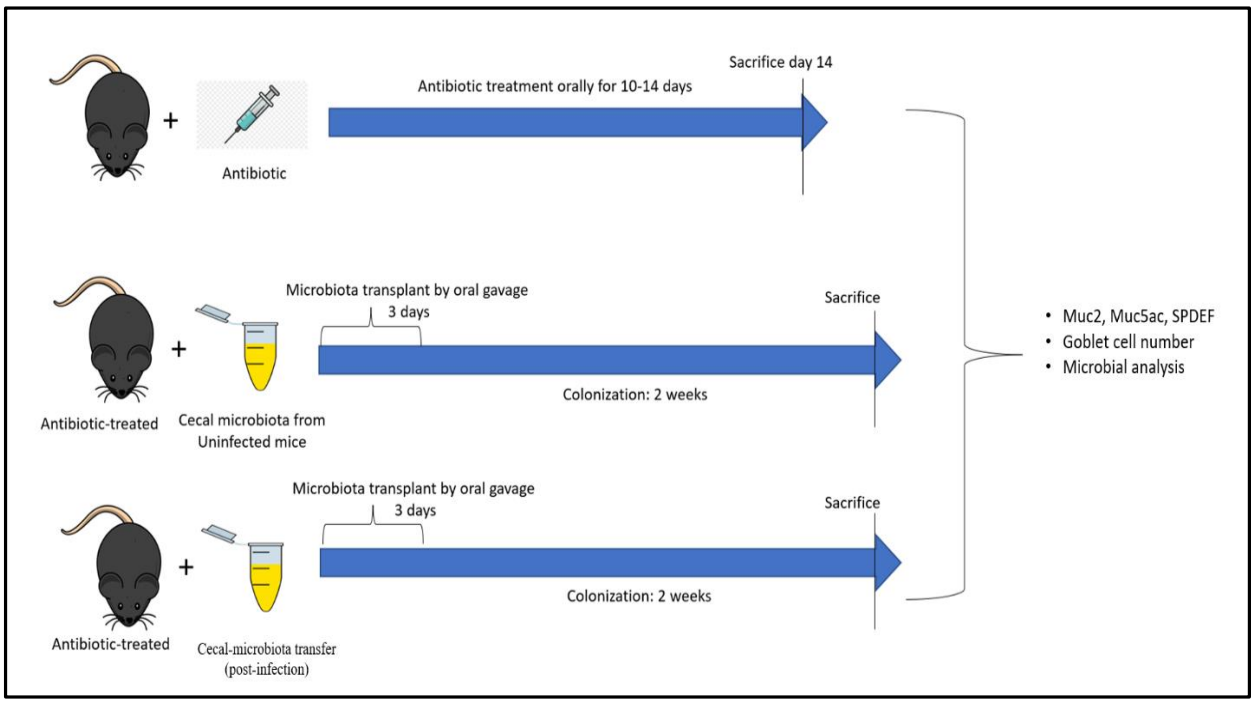

Figure 7. The experimental plan carried out among 3 groups of ABX-treated mice, with or without microbial transfer to observe the role of T. muris-microbiota interplay in modulating SPDEF

Aim 3

To understand the role of SPDEF in mediating the effect of NOD/TLR innate immune signaling in mucin production during *T. muris* infection

Rationale: Our lab has shown that *T. muris* ESPs exert a direct effect on TLR2 receptors in human enterochromaffin (EC) cell line BON-1 cells [103]. TLR2 expression was also seen to be affected by gut microbiota observed in GF and ABX-treated mice [103]. The stimulation of LS174T cells with NOD1 and NOD2 agonists upregulated MUC2 expression, and treatment with NOD1, NOD2

agonists in WT and GF mice also showed increased goblet cell numbers and Muc2 expression [107]. LS174T cells possess human colonic goblet cell-like properties and secrete higher levels of MUC2. Herein, we investigated whether the change in SPDEF is mediated through NOD/TLR immune signaling pathways during *T. muris* infection utilizing this cell line **(Figure 8)**.

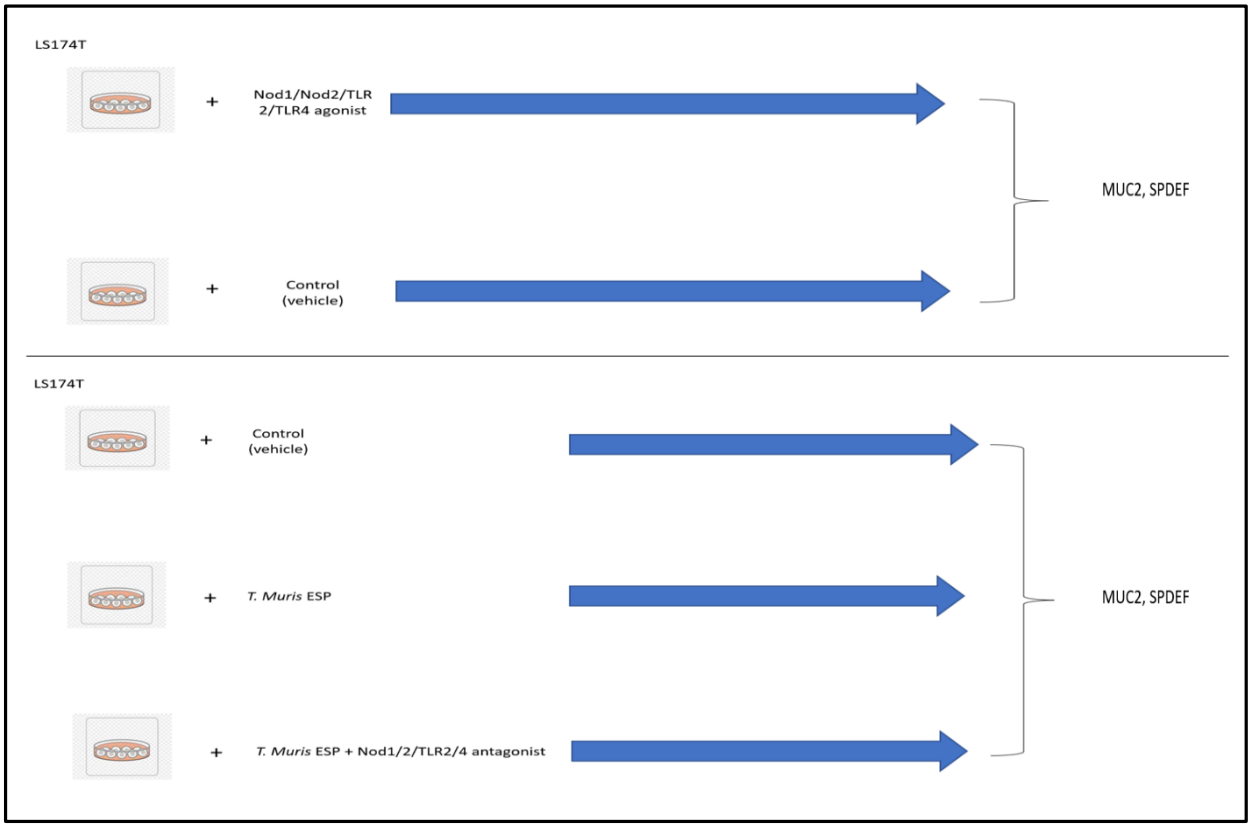

Figure 8. The experimental plan carried out using LS174T cells to observe the role of NOD/TLR signaling in modulating SPDEF during T. muris infection

Chapter 3: Methods

3.1 Animals

All the mice used in the experiments were from BALB/c background. Each group had a combination of both male and female mice and were 6-8 weeks old. The breeding pairs of WT (*SPDEF*$^{+/+}$) and *SPDEF*$^{-/-}$ mice on BALB/c background were obtained from Cincinnati Children's Hospital Medical Center (Cincinnati, Ohio, USA). The *SPDEF*$^{-/-}$ mice were produced by genetic mutation. The BALB/c mice for antibiotic treatment were purchased from The Jackson Laboratory (Bar Harbor, ME, USA). All the mice were kept in sterile, filter-topped cages at McMaster University Central Animal Facility (CAF) under specific pathogen-free (SPF) conditions where they were adapted to the environment for a duration of 7 days before starting any experiment. The mice received autoclaved food and water at 21-22°C and were kept in a 12-hour light-dark cycle. All animal experiments were conducted in accordance with Canadian guidelines for animal research and were approved by Animal Research Ethics Board (AREB) at McMaster University.

3.2 T. muris infection

To generate a batch of *T. muris* eggs, a number of immunodeficient mice (C57BL/6 SCID, The Jackson Laboratory, stock no. 001913) were infected with around 300 *T. muris* eggs by oral gavage. Following their sacrifice after day 35, *T. muris* worms were carefully removed from their cecum and were harvested in 5 ml RPMI 1640 media with 500 U/ml penicillin and 500 µg/ml streptomycin. The culture was incubated at 37°C for 4 hours and then overnight. Eggs from this culture were resuspended in autoclaved distilled water. The eggs are then stored in a 175 ml flask in dark at room temperature for 2 months before preparing them for oral gavage. To prepare the eggs for gavage, the stored eggs were washed, transferred to a 15 ml falcon tube with autoclaved distilled water and the solution was centrifuged at 1500 rpm for 5-6 minutes. The eggs were then

transferred to a foil-wrapped 15 ml falcon tube. The live, mature eggs were counted per 50 µl under a light microscope. The counting was adjusted to approximately 300 eggs for high dose (acute) infection and the eggs were suspended in 200 µl autoclaved distilled water for the preparation of gavage. A group of *SPDEF*$^{+/+}$ and *SPDEF*$^{-/-}$ mice for aim 1 experiments received a single dose of approximately 300 *T. muris* eggs per 200 µl sterile water solution to establish acute infection. In acute infection, the majority of the worms in resistant mice are expelled between 14 and 21 days, so the timepoints of sacrifice were set at day 14 and 21 p.i. for two different groups of *SPDEF*$^{+/+}$*and SPDEF*$^{-/-}$ mice (**Figure 6)**. Throughout the time of infection, the mice received adequate autoclaved food and water, and their weight and physical condition were assessed twice weekly.

After sacrifice, the cecal samples were collected and stored at -20℃ to assess the worm burden under a dissecting microscope. The counting of worms was done by scraping the tissue and suspending the cecal contents in sterile water. The colonic and fecal samples were also collected and stored in -80℃ for other experiments.

3.3 Antibiotic treatment

3 groups of BALB/c mice (each group containing 4 mice) received a cocktail of broad-spectrum antibiotics consisting of neomycin, ampicillin, vancomycin, and metronidazole (all 0.5 g/L) in sterile drinking water for 10-12 days (**Figure 7**). During the time of treatment, their body weight, water and food consumption were recorded daily. One set of mice was sacrificed at the end of the treatment period and their cecal, colonic, and fecal samples were collected for experiments.

3.4 Adoptive microbiota transfer

At the end of the antibiotic treatment, 2 sets of antibiotic treated BALB/c mice received 200 µl of cecal content diluted with sterile water from either naive BALB/c or *T. muris* infected donors by

oral gavage for 3 consecutive days. The cecal contents from *T. muris* infected donors were collected at day 35 p.i. . The cecal contents from both donors were diluted in sterile phosphate buffer saline (PBS), incubated in 37℃ water bath for 20-30 minutes with vigorous shaking every 5 minutes and were aliquoted in small tubes before transfer. The rest of the aliquoted contents were stored in -80℃ for microbial analysis.

3.5 Tissue preparation

After sacrifice, the colonic tissue was collected from each mouse. The tissue was divided into 5 sections of approximately 1.5 cm length, the sections were flash frozen in liquid nitrogen before storing them at -80℃ and was used for different assays according to the location of the sections. From proximal to distal, the sections were used for the following assays: quantitative polymerase chain reaction (qPCR), 5-HT/ serotonin assay (if needed), cytokine assays, histology, myeloperoxidase assay (if needed) and an extra segment of tissue for any other supplementary experiment. For histology, tissue of 1-2 mm length was placed in histology cassettes. Some cecal contents and fecal matters were stored for subsequent microbial analysis.

3.6 Histology (goblet cell staining)

Colonic tissues (around 2 mm in length) were placed in histology cassettes following sacrifice and were fixed in 10% neural buffered formalin for 24-48 hours. The cassettes were transferred to 50% ethanol and then to 70% ethanol before embedding the tissues in paraffin wax. A periodic acid-Schiff (PAS) stain was used to stain the paraffin-embedded tissue slides in order to detect the colonic goblet cells. The PAS+ goblet cells were counted per 10 colonic crypts in 4 different quadrants (12, 3, 6, and 9 o’ clock regions) for each mouse.

3.7 Immunofluorescence (IFC)

The formalin-fixed, paraffin-embedded colonic tissues cut to around 5 μm were stained for mouse Muc2 and SPDEF to observe their expression. The sections were first deparaffinized by heating at 60°C for 40 minutes and cleaned with CitriSolv (Fisher Scientific, ON, Canada). The sections were rehydrated using a graded ethanol series in decreasing concentration from 100% to 70% and later quenched for 5 minutes in 3% hydrogen peroxide in methanol. After then, the slides were washed 3 times with PBS for 5 minutes and subjected to heat-induced epitope retrieval in 0.01 M citrate buffer (pH: 6.0) at a sub-boiling temperature for 10-15 minutes. The slides were again washed with PBS 3 times for 5 minutes and blocked with 5% normal goat serum (VECTASTAIN®) for 30 minutes before incubating them with primary antibodies overnight at 4°C. The primary antibodies were polyclonal rabbit anti-SPDEF (1:50, LSBio-C749124) and polyclonal rabbit anti-Muc2 (1:75, sc-15334, Santa Cruz Biotech). The sections were washed 3 times for 5 minutes before incubating them with secondary antibodies for 1 hour. The secondary antibodies used were Alexa Fluor 488-conjugated goat anti-rabbit Immunoglobulin G (IgG) (1:1000, Invitrogen) for SPDEF staining and Alexa Fluor 594-conjugated goat anti-rabbit IgG (1:1000, Invitrogen) for Muc2 staining. After washing 3 times with PBS for 5 minutes, the sections were mounted with 4',6-diamidino-2-phenylindole (DAPI) (Thermo Fisher, lot 2476677) for nuclear counterstaining and kept in the dark overnight. A Nikon digital camera attached to a fluorescence microscope (Nikon Eclipse 80i) with 40x magnification lens was used to capture the images and immunostaining was examined using NIS Elements Basic Research imaging software. The number of SPDEF+ and Muc2+ cells were counted per 10 crypts in 4 different quadrants for each section.

3.8 Enzyme-Linked Immunosorbent Assays (ELISA)

Approximately 15 mg of colonic tissues were first homogenized for 5 minutes at 30 Hz in 1 ml lysis buffer with protease inhibitor cocktail (PIC) (10 ml lysis buffer supplemented with 50ul of PIC) and centrifuged at 13000 rcf for 5 minutes. The supernatants were collected and stored at -80℃ for protein quantitation which was performed according to the manufacturer's instructions using the DC Protein Assay Kit (catalogue no: 5000111, Bio-Rad Laboratories). The protein concentration of each sample was compared to a standard curve of known concentration using bovine serum albumin (BSA) (BioShop® Canada Inc., Burlington, ON). Mouse anti-inflammatory cytokines IL-4 and IL-13 were measured using commercially available ELISA kits (Quantikine Murine, lot P293959 for IL-13 and lot P284248 for IL-4; R&D Systems, Minneapolis, MN, USA) according to the manufacturer's protocol. The results were normalized to the total protein concentration measured by protein assay.

3.9 Microbial analysis

To analyze the changes in microbial composition and diversity in *SPDEF*$^{+/+}$and *SPDEF*$^{-/-}$ groups at both uninfected and *T. muris* infected (14, 21 p.i.) stages for aim 1 and antibiotic-treated groups (with or without microbiota transfer) for aim 2, 16s rRNA sequencing of fecal samples was conducted via amplification of V3V4 regions. The amplicons were sequenced via Illumina Mi Seq Illumina (Farncombe Institute) and were compared against SILVA taxonomy database following the processing via DADA2 pipeline. An online tool for microbial analysis (https://www.microbiomeanalyst.ca/) developed by Xia Lab at McGill University was used for the analysis of the microbial data. This software broadly uses R package phyloseq for statistical analysis and visualization [118]. This tool has various modules to perform microbial analysis among which, Marker Data Profiling module-based 16s rRNA marker gene data was used. The

data were reduced to a minimum library size to resolve any uneven sequencing depth, or under-sampling problems in the data.

The β-diversity was shown using Bray-Curtis dissimilarity index and statistical analysis was performed via permutational multivariate analysis of variance (PERMANOVA) visualized on principal coordinates analysis (PCoA) plots and interactive 3D plots generated by the software. In terms of α-diversity analysis, Chao1 index was used to address species richness in samples. Student's unpaired t-test, one-way analysis of variance (ANOVA) and PERMANOVA were used to assess pairwise comparison for post-hoc statistical analysis. To observe the abundance of various bacterial genera separately, linear discriminant analysis effect size (LEFSe) was performed. A corrected p-value of <0.05 was considered statistically significant and was adjusted using false discovery rate (FDR). The relative abundance of phylum and genus levels was also observed to observe the changes in microbial composition.

3.10 In vitro experiment: cell culture

The human colonic adenocarcinoma cell line LS174T was utilized to investigate the role of SPDEF in mediating the effect of NOD/TLR innate immune signaling in mucin production **(Figure 8)**, which was obtained from Kris Chadee (Gastrointestinal Research Group, University of Calgary, Canada). These are adherent cells that secrete high amount of MUC2 and they were primarily cultured in a T75 tissue culture flask in Dulbecco's modified Eagle medium–nutrient mixture F-12 or DMEM F-12 (Gibco BRL Life Technologies, Burlington, Canada). The media was supplemented with 10% heat-inactivated fetal bovine serum (FBS), 1% penicillin, and streptomycin, and 20 mM of HEPES buffer (pH 7.5) (Invitrogen Life Technologies, Burlington, Canada). The cells were subcultured a few times in T175 tissue culture flasks and cells from passages 3 to 5 were chosen for subsequent seeding. The cells were seeded at half a million density

($0.5x10^6$ cells/well) in a 12-well plate and at $5.5x10^6$/dish in 100 mm culture dishes at 37°C for 24 hours in 5% CO2 and 95% relative humidity before treating them with *T. muris* ESPs, agonists and antagonists for NOD1, NOD2, TLR2 and TLR4 receptors. For these experiments, the following treatments were used and the optimum concentrations were chosen according to published papers: NOD1 agonist (C12-iE-DAP)- 1 μg/ml, NOD2 agonist (L18-MDP) and TLR2/1 agonist (Pam3CSK4)- 10 μg/ml, TLR4 agonist (LPS)- 100 ng/ml, *T. muris* antigen- 50ug/ml, NOD-1 antagonist (ML130)- 10 μM, NOD2 antagonist (GSK717)- 15 μM, TLR2 antagonist (CU-CPT22)- 1 μM and TLR4 antagonist (LPS-RS)- 5 μg/ml [103] [107] [119] [120] [121]. CU-CPT22 and ML130 were purchased from Tocris Bioscience (Burlington, ON), LPS and GSK717 from Sigma Aldrich (Oakville, ON), and others from InvivoGen (San Diego, CA). PBS was used as the reagent for control cells. The cells were incubated at 37°C for 24 hours in 5% CO2 following treatment. Trypan Blue (Thermo Fischer Scientific, Burlington, Canada) was used to perform a Trypan Blue exclusion assay to check the viability of the treated cells. Cell death is indicated by blue staining. Cells remained viable following treatment with the drug of interest.

After 24 hours of incubation, TRIzol RNA extraction was performed to extract the RNA from the samples in a12-well plate to perform qPCR to observe the expression of human MUC2 and SPDEF. Similarly, from the 100 mm culture dishes, cells were scraped out with PBS and stored at -80°C to perform protein extraction and assay for Western blot to detect the protein expression of MUC2 and SPDEF.

3.11 RNA extraction

Total RNA was extracted from the colonic samples (approximately 15 mg of tissue) and cell culture using TRIzol™ reagent (catalog no. 15596026, Thermo Fischer Scientific, Burlington, Canada). 500 μl of TRIzol was added to each sample and homogenized for 5 minutes at 30 Hz followed by

incubation at room temperature for 5 minutes. 100 µl of chloroform (lot no. l1305, APC, Montreal, Canada) was added per sample, vortexed for 10 seconds and incubated at room temperature for 5 minutes to allow phase separation. The samples were centrifuged at 12000 rcf for 15 minutes at 4°C which separated the samples into a lower phenol-chloroform layer and upper colorless, aqueous layer containing extracted RNA. The upper layer was carefully pipetted (100 µl) into a new set of tubes and 250 µl of cold isopropanol (lot no. 93501, Georgetown, Canada) was added into the layer to allow RNA precipitation. The samples were incubated for 10 minutes at room temperature and centrifuged at 12000 rcf for 10 minutes at 4°C. The supernatant was discarded after centrifugation and the RNA pellet at the bottom was washed with 75% cold ethanol twice with centrifugation at 7500 rcf for 10 minutes in between. At last, the pellet was air-dried for 15 minutes and dissolved in 20 µl RNAse-free water (UltraPure distilled water, lot 2277163, Invitrogen) per sample before storing them in -80°C for complementary DNA (cDNA) synthesis.

3.12 Quantification of RNA and purity assessment

The quantity and purity of RNA were assessed using a UV-Vis spectrophotometer- NanoDrop 2000 (Thermo Fischer Scientific, Burlington, Canada). The nucleic acid concentration is measured using 260 nm wavelength and using the 260/280 ratio, the purity of RNA was assessed. Generally, a range between 1.8 and 2.2 for 260/230 and 260/280 values are accepted as ‘pure’. Deviation from the range indicates contamination by urea, acid, or phenols that might happen during the process of extraction.

3.13 Complementary DNA (cDNA) synthesis:

cDNA synthesis was performed according to the manufacturer's protocol using High-Capacity cDNA Reverse Transcription Kit (Thermo Fisher, lot 2587565) which contains RNA H+ reverse transcriptase enzyme preventing RNA breakdown.

3.14 Real-time Quantitative Polymerase Reaction Chain (RT-qPCR)

The expression of target genes relative to the housekeeping genes (expressed in every cell at all states) was assessed by qPCR. Each 20 µl PCR reaction mixture (carried out in duplicates) contained 10 µl of 2 × SsoFast Evagreen SYBR Green PCR Master Mix (catalog no. 1725201, Bio-Rad, Mississauga, Canada), 7 µl of nuclease-free water, 1 µl of cDNA, and 1 µl of forward and reverse primers each (10 µmol/L concentration). A CFX96 qPCR system (Bio-Rad) was used to carry out qPCR. Expression of target genes was normalized to the reference gene coding for mouse 18S rRNA for aims 1 and 2, and human 18S rRNA for aim 3 experiments. The relative abundance of mRNA was analyzed by 2-ΔΔCT methods using mean ± SEM. The sequences (5'-3') of mouse and human primers are provided in the following tables **(Table 1 and 2)**.

Table 1: List of human primers

	Forward (5'-3')	Reverse (5'-3')
18S	TCCACAGGAGGCCTACACGCC	TTTCCGCCGCCCATCGATGTT
SPDEF	CGCTCCATCCGCCAGTATTA	GTGCACGAACTGGTAGACGA
MUC2	ACCCGCACTATGTCACCTTC	GGACAGGACACCTTGTCGTT

Table 2: List of mouse primers

	Forward (5'-3')	Reverse (5'-3')
18S	GTAACCCGTTGAACCCCATT	CCATCCAATCGGTAGTAGCG
Spdef	AAGGCAGCATCAGGAGCAATG	CTGTCAATGACGGGACACTG
Muc2	CTGACCAAGAGCGAACACAA	CATGACTGGAAGCAACTGGA
Muc5ac	GTGATGCACCCATGATCTATTTTG	ACTCGGAGCTATAACAGGTCATGTC
β-catenin	TTAAACTCCTGCACCCACCAT	AGGGCAAGGTTTCGAATCAA
Atoh-1 (Math-1)	GTGCGATCTCCGAGTGAGAG	GGGATAAGCCCCGAACAACA

3.15 Western blot

Protein extraction and measurement of total protein concentration of the cells scraped out with PBS from the 100 mm culture dish was performed using the DC Protein Assay Kit (catalogue no: 5000111, Bio-Rad Laboratories) as per the manufacturer's protocol. Using the protein quantitation template developed by our lab, equal amounts of protein (20 μg) for each group were loaded and separated by 8 to 12% SDS–polyacrylamide gel electrophoresis. Following the separation of protein, the gels were transferred to a polyvinylidene difluoride (PVDF) membrane (catalogue no: 1620177. Bio-Rad Laboratories) using Trans-Blot Turbo transfer system developed by Bio-Rad according to the manufacturer's instructions. Membranes were blocked with 5% bovine serum albumin or BSA (BioShop® Canada Inc., Burlington, ON) in Tris-buffered saline–Tween 20 (TBST) at room temperature for 1 hour before the membranes were incubated overnight with

primary antibodies at 4°C. The primary antibodies used were against MUC2 (1:250, sc-515032, Santa Cruz Biotech), SPDEF (1:1000, LSBio-C749124), and β-actin (1:1000; catalog no. 4970, CST). Membranes were washed 3 times with TBST at an interval of 15 minutes and incubated with anti-rabbit horseradish peroxidase–linked antibody (1:5000; catalog no. 7074, CST) for 1 hour at room temperature. Following incubation, the membranes were again washed 3 times and the proteins were treated with Clarity Max^{TM} Western enhanced chemiluminescence (ECL) substrate (catalog no. 1705062, Bio-Rad Laboratories). The membranes were exposed to a luminescent image analyzer (ChemiDoc Touch Imaging System) where the proteins could be visualized. The analysis of the bands was performed using GelQuantNET software, normalized to housekeeping protein β-actin.

3.16 Statistical analysis

The statistical analysis of all data was performed using GraphPad Prism version 9.0.0 for Windows (GraphPad Software, San Diego, California, USA) and the results were expressed as mean ± standard error of the mean (SEM). Unpaired Student's *t*-test was used for comparison between the two groups. One-way ANOVA with Tukey's post-hoc multiple comparison test was used when comparing more than two groups with a single variable and two-way ANOVA with Tukey's post-hoc test applied for two variables. *P* value of <0.05 was presented as statically significant.

Chapter 4: Results

4.1 SPDEF regulates intestinal goblet cell response and mucin production following T. muris infection associated with TH2-mediated immune response

To explore the role of SPDEF in goblet cell response and mucin production during *T. muris* infection, the number of PAS+ goblet cells, mRNA expression of *Spdef*, *Muc2* and *Muc5ac,* and the number of Muc2+ and SPDEF+ cells were determined in WT ($SPDEF^{+/+}$) and $SPDEF^{-/-}$ mice with or without *T. muris* infection (day 14 and 21 p.i.) **(Figure 9-12)**. The number of PAS+ goblet cells significantly increased following infection with *T. muris* in $SPDEF^{+/+}$ mice at day 14 p.i. which remained unaltered at day 21 **(Figure 9A, B)**. The $SPDEF^{-/-}$ mice did not show any significant increase in PAS+ goblet cells after infection. Moreover, fewer PAS+ goblet cells were observed in $SPDEF^{-/-}$ mice compared to $SPDEF^{+/+}$ **(Figure 9A, B)**. Since SPDEF, Muc2 and Muc5ac are important markers of goblet cells and were seen to be upregulated during *T. muris* infection in mice in previous studies, their mRNA expression was observed via qPCR **(Figure 10A-C)**. The $SPDEF^{+/+}$ mice showed significant upregulation of *Spdef* at day 14 p.i. and downregulation by day 21 **(Figure 10A)**. The $SPDEF^{+/+}$ mice also showed increased expression of *Muc2* at day 14 p.i. which remained unchanged at day 21 **(Figure 10B)**. *Muc2* expression was also significantly lower in $SPDEF^{-/-}$ mice as opposed to $SPDEF^{+/+}$ mice during both uninfected and infected periods **(Figure 10B).** *Muc5ac*, a mucin normally expressed in stomachs and lungs but seen to be increased in colons in the resistant mice following *T. muris* infection did not, however, show any significant change in its expression **(Figure 10C)**.

Since the genetic expression of *Spdef* was higher in $SPDEF^{+/+}$ mice after infection, the number of SPDEF+ cells per 10 crypts was then assessed via immunofluorescence (IFC) in $SPDEF^{+/+}$ mice. The data presented a similar trend regards to protein expression of SPDEF following *T. muris*

infection, which showed that SPDEF+ cells significantly increased at day 14 p.i. and were depleted by day 21 **(Figure 11A, B)**. The number of Muc2+ cells in *SPDEF*$^{+/+}$ and *SPDEF*$^{-/-}$ mice was also determined via IFC, which showed that Muc2+ cells in *SPDEF*$^{+/+}$ mice increased at day 14 and remained unchanged at day 21 p.i. **(Figure 12A, B)**. The downregulation of SPDEF and higher expression of Muc2 at day 21 in *SPDEF*$^{+/+}$ mice might suggest that there are other factors which induce Muc2 expression in goblet cells. In addition, *SPDEF*$^{-/-}$ mice showed lower number of Muc2+ cells compared to *SPDEF*$^{+/+}$ mice **(Figure 12A, B)**. All these findings suggest that SPDEF modulates goblet cell response and secretion of mucin (Muc2) following *T. muris* infection.

The BALB/c mice are the resistant strains which show TH2 immune response with a higher dose of *T. muris* infection (>150 eggs) by secreting TH2 cytokines (IL-4, IL-13) that helps in expulsion of worms. To see if the changes in SPDEF and Muc2 were associated with TH2-mediated immune response in *SPDEF*$^{+/+}$ and *SPDEF*$^{-/-}$ mice, the levels of IL-4 and IL-13 were assessed via ELISA. The data showed increased levels of IL-4 and IL-13 in *SPDEF*$^{+/+}$ mice at day 14 p.i. and significant depletion of both cytokines by day 21 **(Figure 13A, B)**. On the other hand, the *SPDEF*$^{-/-}$ mice showed a gradual increase in IL-4 and IL-13 levels from day 14 to day 21, which was significant for IL-4 **(Figure 13A, B)**. Compared to *SPDEF*$^{-/-}$ mice, the *SPDEF*$^{+/+}$ mice showed higher levels of IL-4 and IL-13 at day 14, but a lower level of IL-4 at day 21 **(Figure 13A, B)**.

The worm burden data showed a significantly higher number of worms in the cecum at day 14 p.i. in *SPDEF*$^{+/+}$ mice compared to *SPDEF*$^{-/-}$, which declined significantly by day 21 **(Figure 13C)**. The *SPDEF*$^{-/-}$ mice, however, started showing an elevation in their worm count from day 14 to 21. This result in combination with the TH2 cytokines data may suggest that *SPDEF*$^{+/+}$ mice show an elevated TH2 response around day 14 p.i. which helps in worm expulsion and subsequently reduces the number of worms remarkably by day 21. The increased worm count observed in

SPDEF$^{-/-}$ mice at day 21 could suggest delayed or impaired hatching of *T. muris* eggs in these mice. The delayed expulsion of worms observed in *SPDEF*$^{-/-}$ mice at day 21 p.i. may have also been associated with a delayed TH2 response, however, this needs to be determined further.

ATOH-1 (or Math-1 in mice) acts as a downstream component of Wnt canonical β-catenin signaling cascade and regulates the cell-fate differentiation of ISCs into the secretory cell-types. It activates several transcription factors and one of them is SPDEF, which differentiates the secretory progenitors into goblet cells. To observe whether these upstream regulators of SPDEF are differently expressed following *T. muris* infection, the mRNA expression of *β-catenin* and *Atoh-1/Math-1* was determined via qPCR in *SPDEF*$^{+/+}$ and *SPDEF*$^{-/-}$ mice during uninfected and infected (14 and 21 p.i.) periods **(Figure 14A, B)**. No significant difference was observed in *β-catenin* expression in *SPDEF*$^{+/+}$ and *SPDEF*$^{-/-}$ mice during *T. muris* infection **(Figure 14A).** However, *Atoh-1* showed increased expression in *SPDEF*$^{+/+}$ and *SPDEF*$^{-/-}$ mice following infection at day 21 p.i. **(Figure 14B),** indicating that the differentiation of ISCs was directed more towards the secretory cell-types during *T. muris* infection.

Figure 9. Effect of T. muris on intestinal goblet cells in SPDEF$^{+/+}$ and SPDEF $^{-/-}$ mice with (day 14 & 21 p.i.) or without infection

Representative images of (A) PAS-stained colonic goblet cells observed by microscope, and (B) Number of PAS+ goblet cells counted per 10 crypts in *SPDEF*$^{+/+}$ and *SPDEF* $^{-/-}$ mice with (day 14 & 21 p.i.) or without *T. muris* infection. Data are represented as mean+/- SEM, *$p<0.05$ is considered as statistically significant.

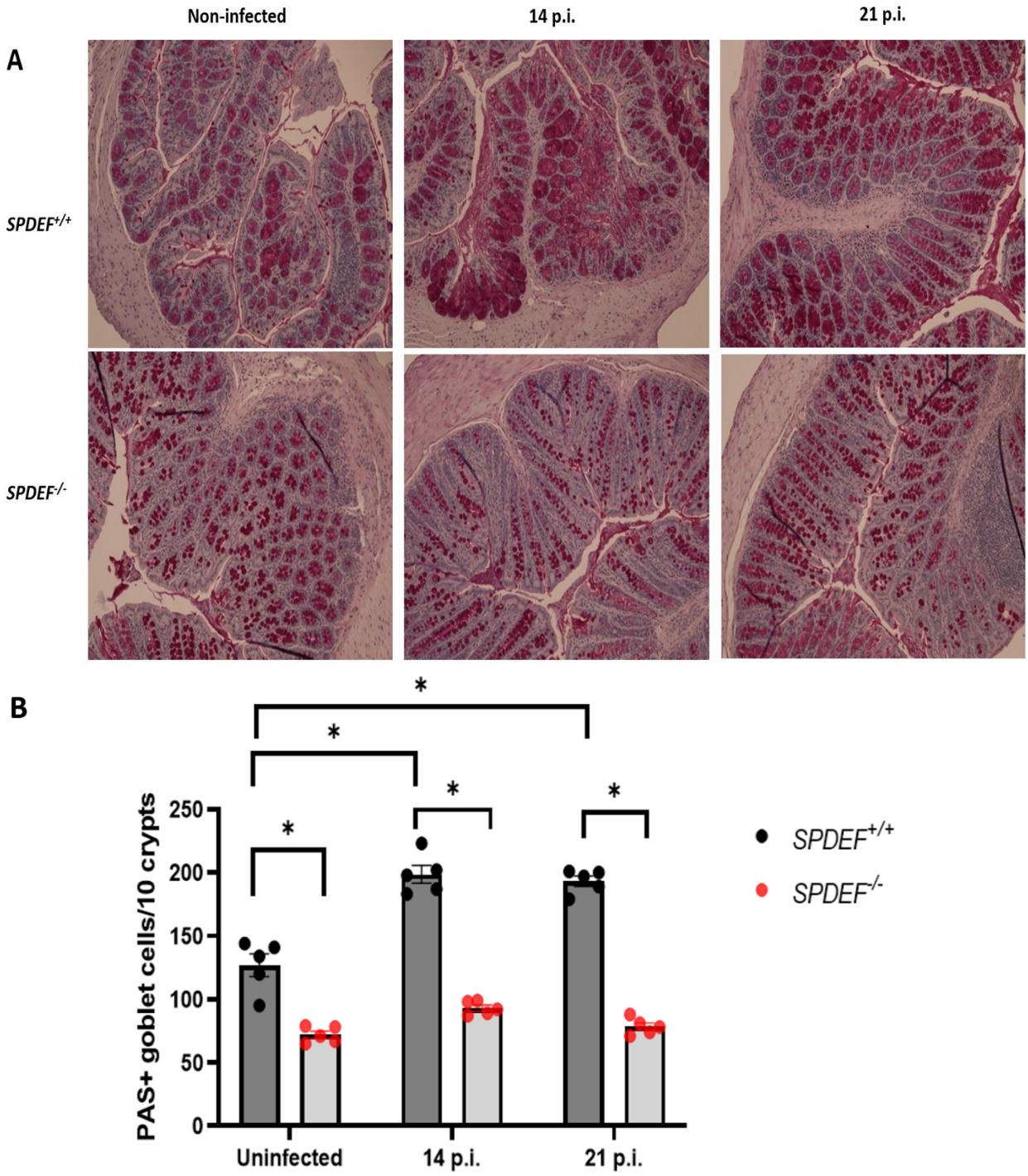
Non-infected
14 p.i.
21 p.i.
A
SPDEF+/+
SPDEF-/-
B
PAS+ goblet cells/10 crypts
250
200
150
100
50
0
Uninfected
14 p.i.
21 p.i.
SPDEF+/+
SPDEF-/-

Figure 10. Effect of T. muris on relative mRNA expression of Spdef, Muc2 and Muc5ac in SPDEF$^{+/+}$ and SPDEF $^{-/-}$ mice with (day 14 & 21 p.i.) or without infection

Relative mRNA expression of (A) *Spdef*, (B) *Muc2*, and (C) *Muc5ac* assessed by qPCR in *SPDEF*$^{+/+}$ and *SPDEF* $^{-/-}$ mice with (day 14 & 21 p.i.) or without *T. muris* infection, normalized to mouse 18s. Data are represented as mean+/- SEM, *$p<0.05$ is considered as statistically significant.

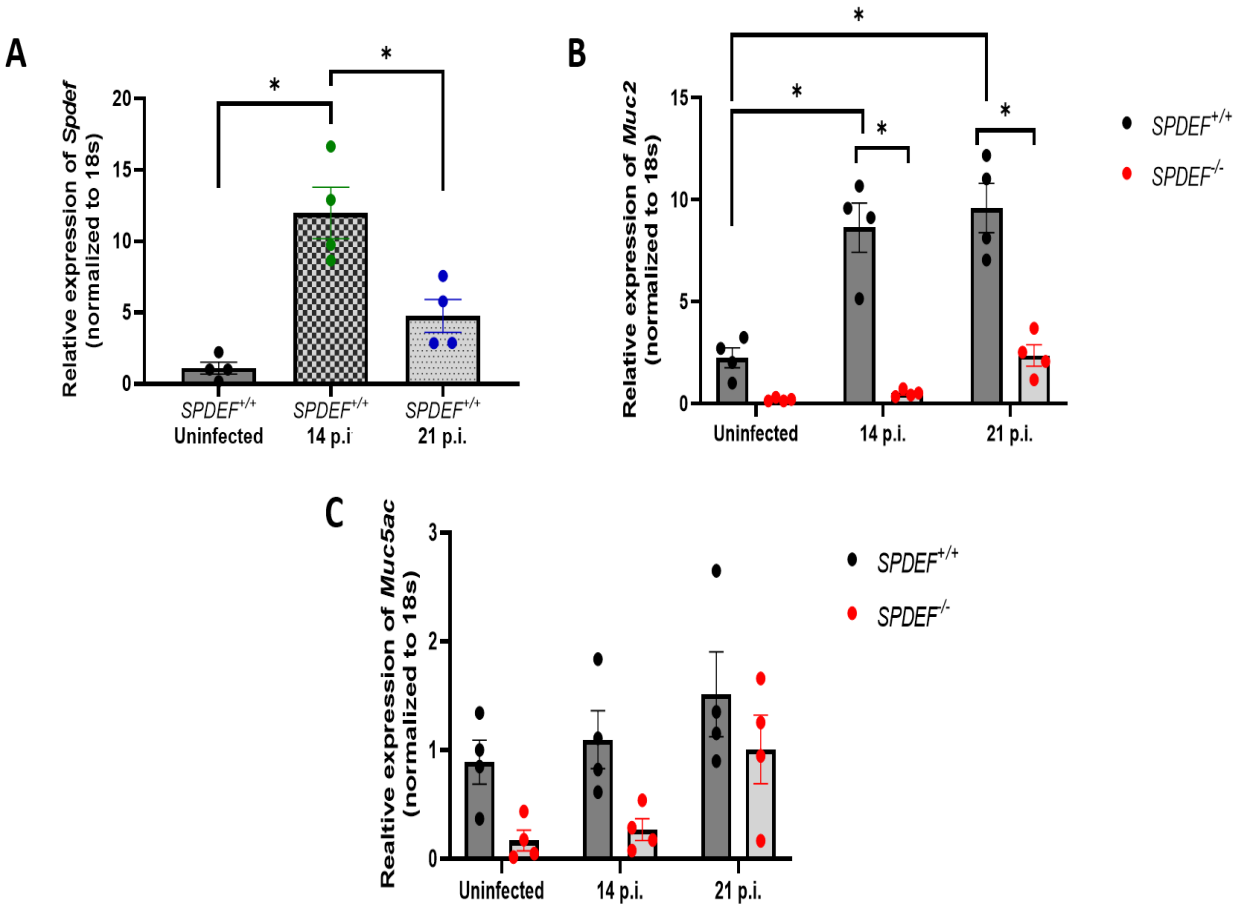
A
Relative expression of Spdef (normalized to 18s)
20
15
10
5
0
*
*
SPDEF+/+ Uninfected
SPDEF+/+ 14 p.i
SPDEF+/+ 21 p.i.
B
Relative expression of Muc2 (normalized to 18s)
15
10
5
0
*
*
*
*
Uninfected
14 p.i.
21 p.i.
SPDEF+/+
SPDEF-/-
C
Realtive expression of Muc5ac (normalized to 18s)
3
2
1
0
Uninfected
14 p.i.
21 p.i.
SPDEF+/+
SPDEF-/-

Figure 11. Effect of T. muris on SPDEF+ cells in SPDEF$^{+/+}$ mice with (day 14 & 21 p.i.) or without infection

Representative images of (A) SPDEF-stained colonic cross sections observed by IFC, and (B) Number of SPDEF+ cells counted per 10 crypts in *SPDEF*$^{+/+}$ mice with (day 14 & 21 p.i.) or without *T. muris* infection. Data are represented as mean+/- SEM, *$p<0.05$ is considered as statistically significant.

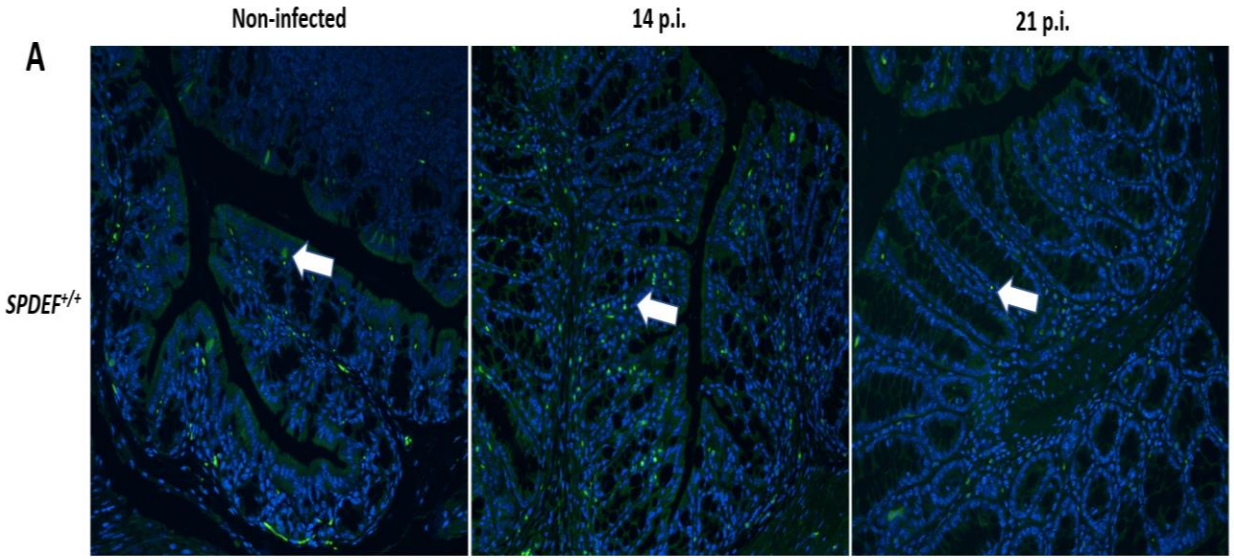
A
Non-infected
14 p.i.
21 p.i.
SPDEF+/+

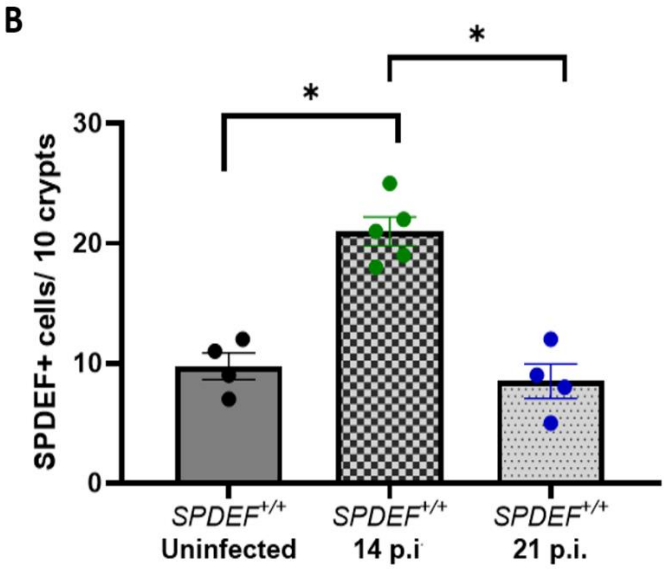
B
*
*
SPDEF+ cells/ 10 crypts
30
20
10
0
SPDEF+/+
Uninfected
SPDEF+/+
14 p.i
SPDEF+/+
21 p.i.

Figure 12. Effect of T. muris on Muc2+ cells in SPDEF$^{+/+}$ and SPDEF $^{-/-}$ mice with (day 14 & 21 p.i.) or without infection

Representative images of (A) Muc2-stained colonic cross sections observed by IFC, and (B) Number of Muc2+ cells counted per 10 crypts in *SPDEF*$^{+/+}$ and *SPDEF* $^{-/-}$ mice with (day 14 & 21 p.i.) or without *T. muris* infection. Data are represented as mean+/- SEM, *$p<0.05$ is considered as statistically significant.

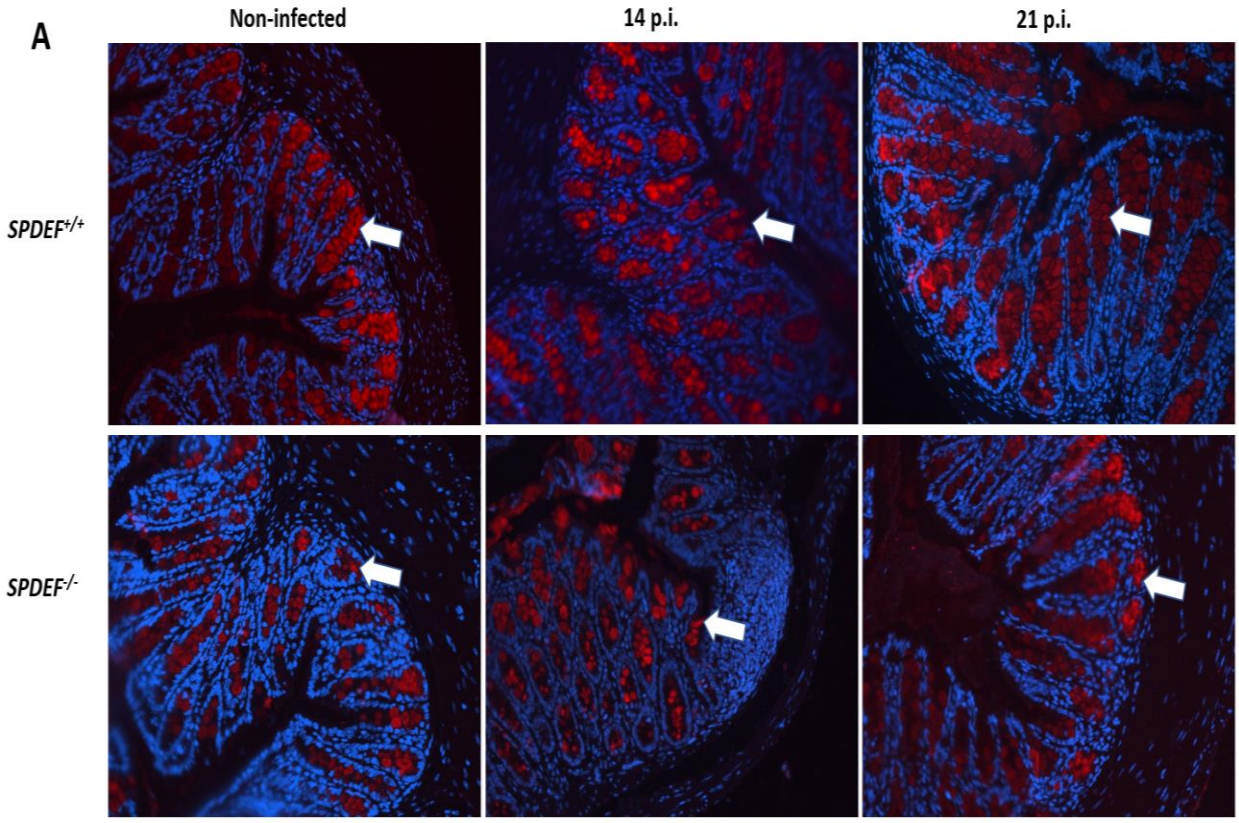
A
Non-infected
14 p.i.
21 p.i.
SPDEF+/+
SPDEF-/-

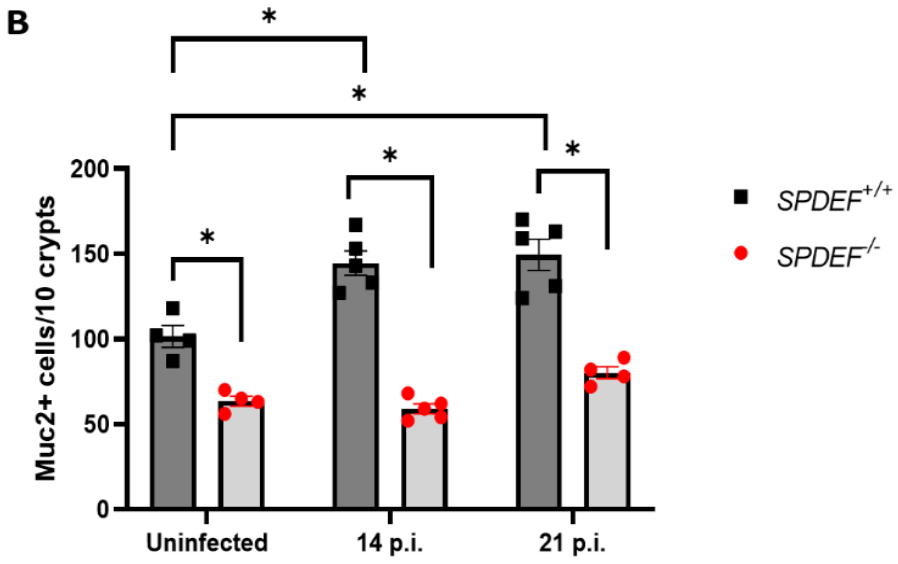
B
Muc2+ cells/10 crypts
200
150
100
50
0
Uninfected
14 p.i.
21 p.i.
SPDEF+/+
SPDEF-/-

Figure 13. Effect of T. muris on the levels of TH2 cytokines IL-4 and IL-13 in colonic tissues in SPDEF$^{+/+}$ and SPDEF $^{-/-}$ mice with (day 14 & 21 p.i.) or without infection and worm burden in SPDEF$^{+/+}$ and SPDEF $^{-/-}$ mice with T. muris infection (day 14 & 21 p.i.)

Levels of TH2 cytokines (A) IL-4, and (B) IL-13 assessed by ELISA in *SPDEF*$^{+/+}$ and *SPDEF* $^{-/-}$ mice with (day 14 & 21 p.i.) or without *T. muris* infection, and (C) Worm burden in *SPDEF*$^{+/+}$ and *SPDEF* $^{-/-}$ mice with *T. muris* infection (day 14 & 21 p.i.). Data are represented as mean+/- SEM, *$p<0.05$ is considered as statistically significant.

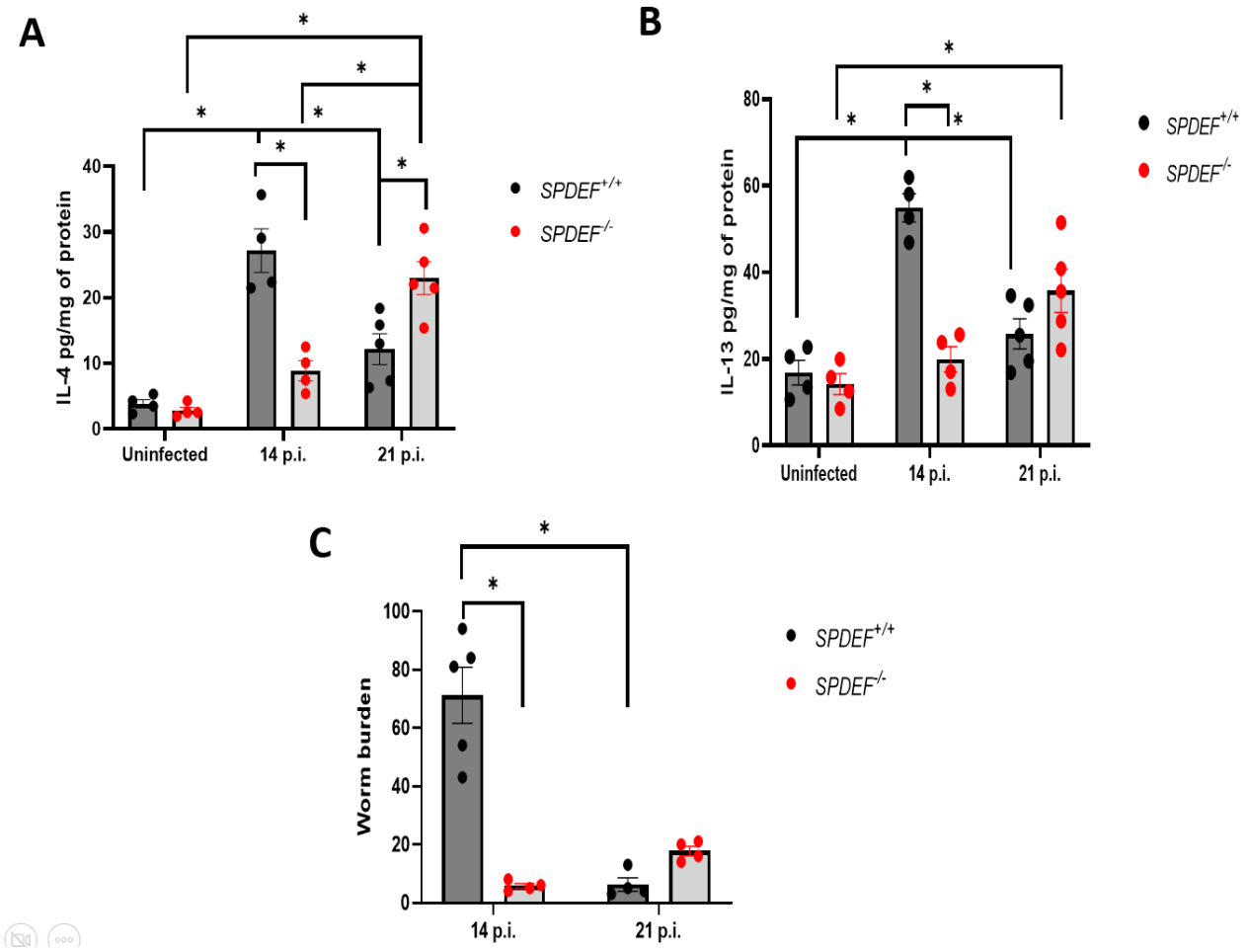
A
IL-4 pg/mg of protein
0
10
20
30
40
Uninfected
14 p.i.
21 p.i.
SPDEF+/+
SPDEF-/-
B
IL-13 pg/mg of protein
0
20
40
60
80
Uninfected
14 p.i.
21 p.i.
SPDEF+/+
SPDEF-/-
C
Worm burden
0
20
40
60
80
100
14 p.i.
21 p.i.
SPDEF+/+
SPDEF-/-

Figure 14. Effect on T. muris on relative mRNA expression of β-catenin and Atoh-1 in SPDEF$^{+/+}$ and SPDEF$^{-/-}$ mice with (day 14 & 21 p.i.) or without infection

Relative mRNA expression of (A) *β-catenin*, and (B) *Atoh-1* assessed by qPCR in *SPDEF*$^{+/+}$ and *SPDEF*$^{-/-}$ mice with (day 14 & 21 p.i.) or without *T. muris* infection, normalized to mouse 18s. Data are represented as mean+/- SEM, *$p<0.05$ is considered as statistically significant.

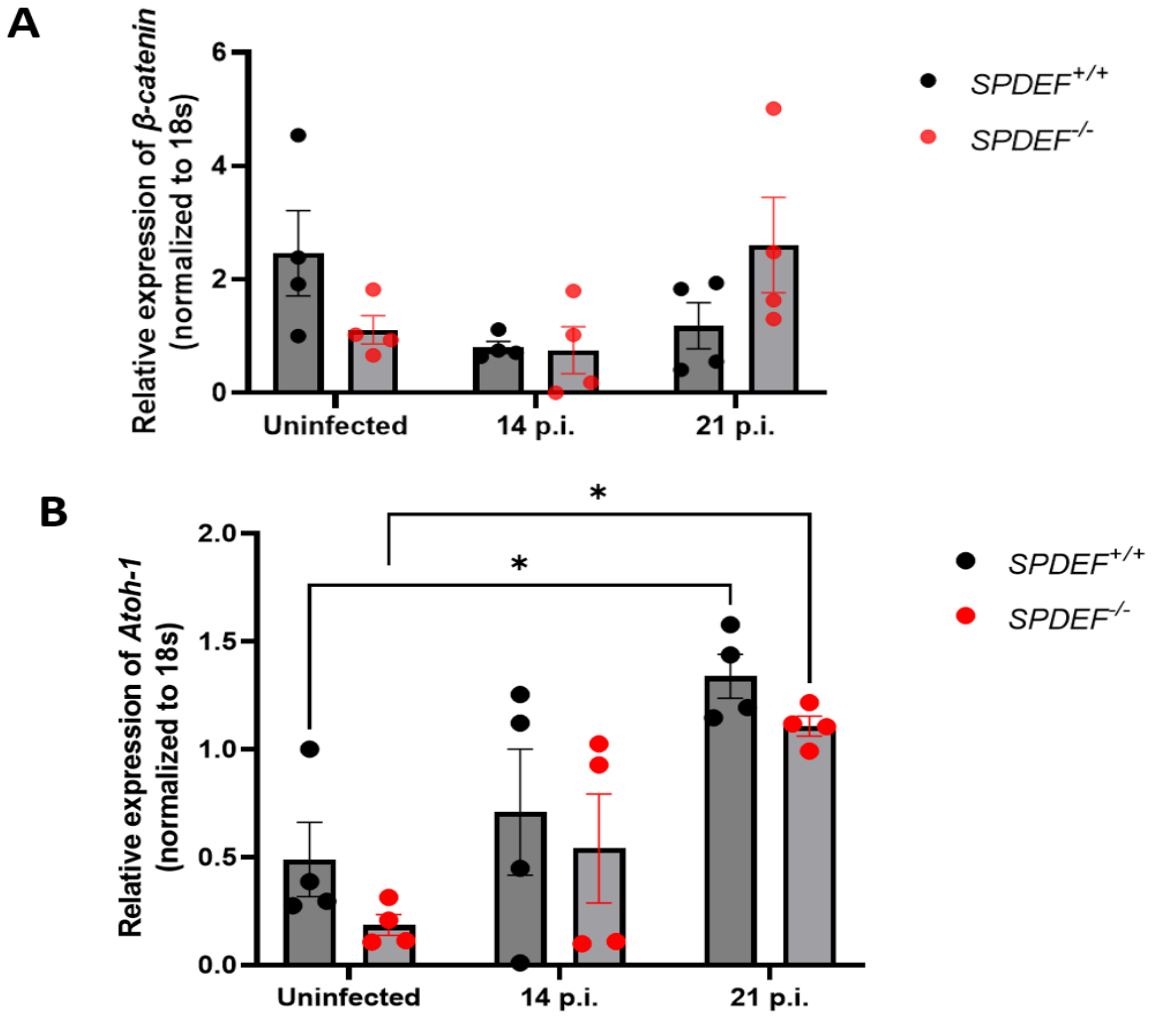
A
Relative expression of β-catenin
(normalized to 18s)
6
4
2
0
Uninfected
14 p.i.
21 p.i.
SPDEF+/+
SPDEF-/-
B
Relative expression of Atoh-1
(normalized to 18s)
2.0
1.5
1.0
0.5
0.0
*
*
Uninfected
14 p.i.
21 p.i.
SPDEF+/+
SPDEF-/-

4.2 T. muris infection alters cecal microbial community in SPDEF$^{+/+}$ and SPDEF$^{-/-}$ mice

The interaction between *T. muris* and gut microbiota is well-documented in various studies, even more so in terms of chronic infection, where it was seen that chronic *T. muris* infection in C57BL/6 mice was associated with changes in microbial diversity, a decline in the relative abundance of Bacteroidetes phylum and a rise in *Lactobacillaceae* family [109] [122]. A study from our lab conducted on C57BL/6 mice with acute *T. muris* infection demonstrated that microbial composition was altered in infected mice at day 36 p.i. compared to uninfected mice, which is yet to be published. To observe the differences in microbial community in *SPDEF*$^{+/+}$ and *SPDEF*$^{-/-}$ mice on BALB/c background following *T. muris* infection, relative abundance of microbial composition at genus level, linear discriminant analysis effect size (LEFSe) of various bacterial genera and α, β-diversities with post-hoc analysis were assessed in both groups at various timepoints **(Figure 15-17, Table 3, 4)**. The timepoints were designated as D-0 (uninfected), D-14 and D-21 (p.i). The relative abundance plots are shown in **Figure 15A**. To determine the significantly different (p-value <0.05) bacterial genera in both of these groups, linear discriminant analysis effect size was conducted **(Figure 15B, C)**. *SPDEF*$^{-/-}$ mice showed increased abundance of *Bacteroides* and *Streptococcus* after *T. muris* infection at day 14 p.i. and higher abundance of *Eubacterium, Anaerofustis, Incertae* and members from *Prevotellaceae* family without *T. muris* infection compared to *SPDEF*$^{+/+}$ mice **(Figure 15B)**. On the other hand, *SPDEF*$^{+/+}$ mice showed higher abundance of *Rikenella, Musicpirillum, Bifidobacterium* and members from *Lachnospiraceae* family without infection, while the infected *SPDEF*$^{+/+}$ mice showed increased abundance of *Oscillibacter, Faecalibaculum, Oscillospira* at day 14 and *Pseudomonas* at day 21 p.i. **(Figure 15B)**. **Figure 15C** shows the graphical presentations of some of the most abundant bacterial genera present in the gut in *SPDEF*$^{+/+}$ and *SPDEF*$^{-/-}$ mice at different timepoints.

To take a look into the changes in microbial diversity in *SPDEF*$^{+/+}$ and *SPDEF*$^{-/-}$ mice, α-diversity was determined using Chao1 index to observe species richness in each group and β-diversity was determined via Bray-Curtis distance using PCoA plot to observe the similarities in microbial distribution between different groups **(Figure 16, 17)**. Post-hoc pairwise comparison was conducted to observe the differences in diversity between multiple groups (**Table 3, 4)**. *SPDEF*$^{-/-}$ mice showed decreased α-diversity compared to *SPDEF*$^{+/+}$ mice at day 14 p.i. **(Figure 16, Table 3)**. Although the *SPDEF*$^{+/+}$ and *SPDEF*$^{-/-}$ mice did not show any significant difference in α-diversity after infection compared to their uninfected timepoints, *SPDEF*$^{+/+}$ mice showed decreased α-diversity at day 21 compared to day 14 p.i. (**Figure 16, Table 3)**. The β-diversity data showed different distribution of microbial communities between *SPDEF*$^{+/+}$ and *SPDEF*$^{-/-}$ mice at day 14 p.i. (**Figure 17, Table 4)**. Both groups also showed different distributions of microbiota at day 14 and 21 p.i. compared to their uninfected timepoints (**Figure 17, Table 4)**.

Figure 15. Analysis of microbial composition in SPDEF$^{+/+}$ and SPDEF $^{-/-}$ mice with (day 14 & 21 p.i.) or without T. muris infection

(A) Relative abundance of microbial community on genus level, (B) Graphical summary of significantly different bacterial genera in *SPDEF*$^{+/+}$ and *SPDEF* $^{-/-}$ mice with a p-value cutoff 0.05, analyzed via LEFSe, (C) Graphical presentations of the most abundant bacterial genera in *SPDEF*$^{+/+}$ and *SPDEF* $^{-/-}$ mice, analyzed via LEFSe

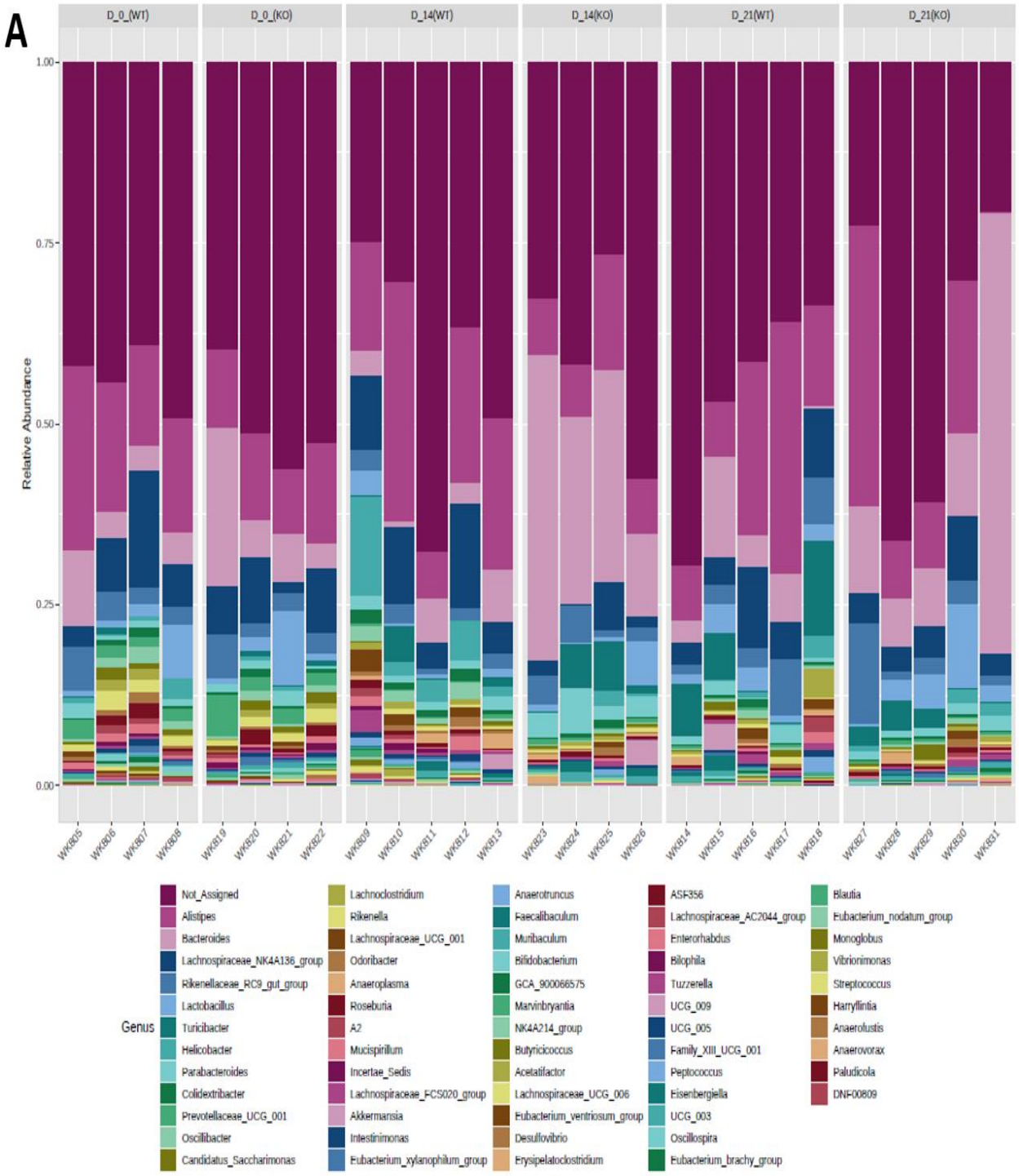
A
D_0_(WT)
D_0_(KO)
D_14(WT)
D_14(KO)
D_21(WT)
D_21(KO)
Relative Abundance
1.00
0.75
0.50
0.25
0.00
WK805
WK806
WK807
WK808
WK819
WK820
WK821
WK822
WK809
WK810
WK811
WK812
WK813
WK823
WK824
WK825
WK826
WK814
WK815
WK816
WK817
WK818
WK827
WK828
WK829
WK830
WK831
Genus
Not_Assigned
Alistipes
Bacteroides
Lachnospiraceae_NK4A136_group
Rikenellaceae_RC9_gut_group
Lactobacillus
Turicibacter
Helicobacter
Parabacteroides
Colidextribacter
Prevotellaceae_UCG_001
Oscillibacter
Candidatus_Saccharimonas
Lachnoclostridium
Rikenella
Lachnospiraceae_UCG_001
Odoribacter
Anaeroplasma
Roseburia
A2
Mucispirillum
Incertae_Sedis
Lachnospiraceae_FCS020_group
Akkermansia
Intestinimonas
Eubacterium_xylanophilum_group
Anaerotruncus
Faecalibaculum
Muribaculum
Bifidobacterium
GCA_900066575
Marvinbryantia
NK4A214_group
Butyricicoccus
Acetatifactor
Lachnospiraceae_UCG_006
Eubacterium_ventriosum_group
Desulfovibrio
Erysipelatoclostridium
ASF356
Lachnospiraceae_AC2044_group
Enterorhabdus
Bilophila
Tuzzerella
UCG_009
UCG_005
Family_XIII_UCG_001
Peptococcus
Eisenbergiella
UCG_003
Oscillospira
Eubacterium_brachy_group
Blautia
Eubacterium_nodatum_group
Monoglobus
Vibrionimonas
Streptococcus
Harryflintia
Anaerofustis
Anaerovorax
Paludicola
DNF00809

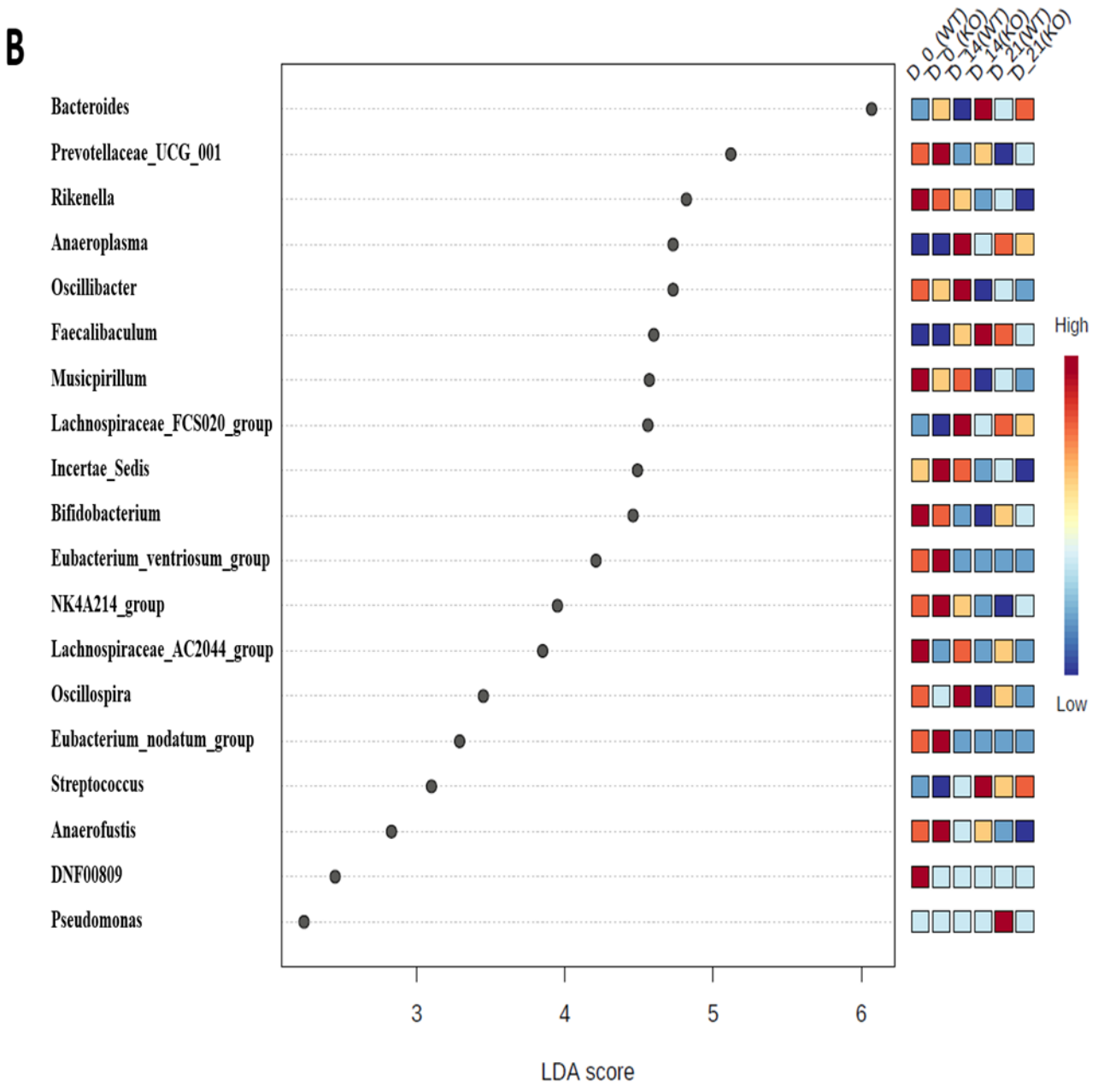
B
D_0_(WT)
D_0_(KO)
D_14(WT)
D_14(KO)
D_21(WT)
D_21(KO)
Bacteroides
Prevotellaceae_UCG_001
Rikenella
Anaeroplasma
Oscillibacter
Faecalibaculum
Musicpirillum
Lachnospiraceae_FCS020_group
Incertae_Sedis
Bifidobacterium
Eubacterium_ventriosum_group
NK4A214_group
Lachnospiraceae_AC2044_group
Oscillospira
Eubacterium_nodatum_group
Streptococcus
Anaerofustis
DNF00809
Pseudomonas
High
Low
3
4
5
6
LDA score

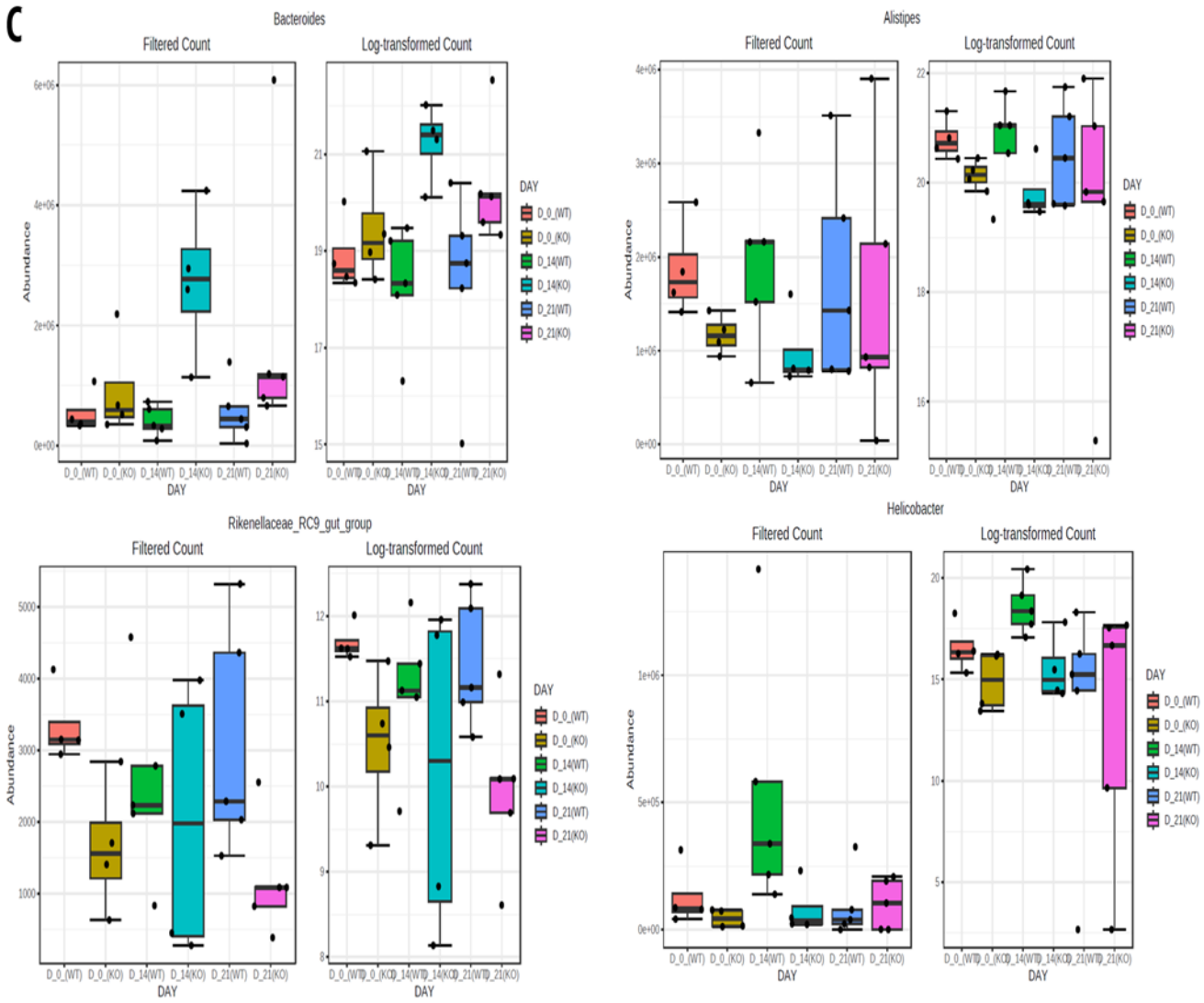
C
Bacteroides
Filtered Count
Log-transformed Count
Abundance
DAY
D_0_(WT)
D_0_(KO)
D_14(WT)
D_14(KO)
D_21(WT)
D_21(KO)
Alistipes
Filtered Count
Log-transformed Count
Abundance
DAY
Rikenellaceae_RC9_gut_group
Filtered Count
Log-transformed Count
Abundance
DAY
Helicobacter
Filtered Count
Log-transformed Count
Abundance
DAY

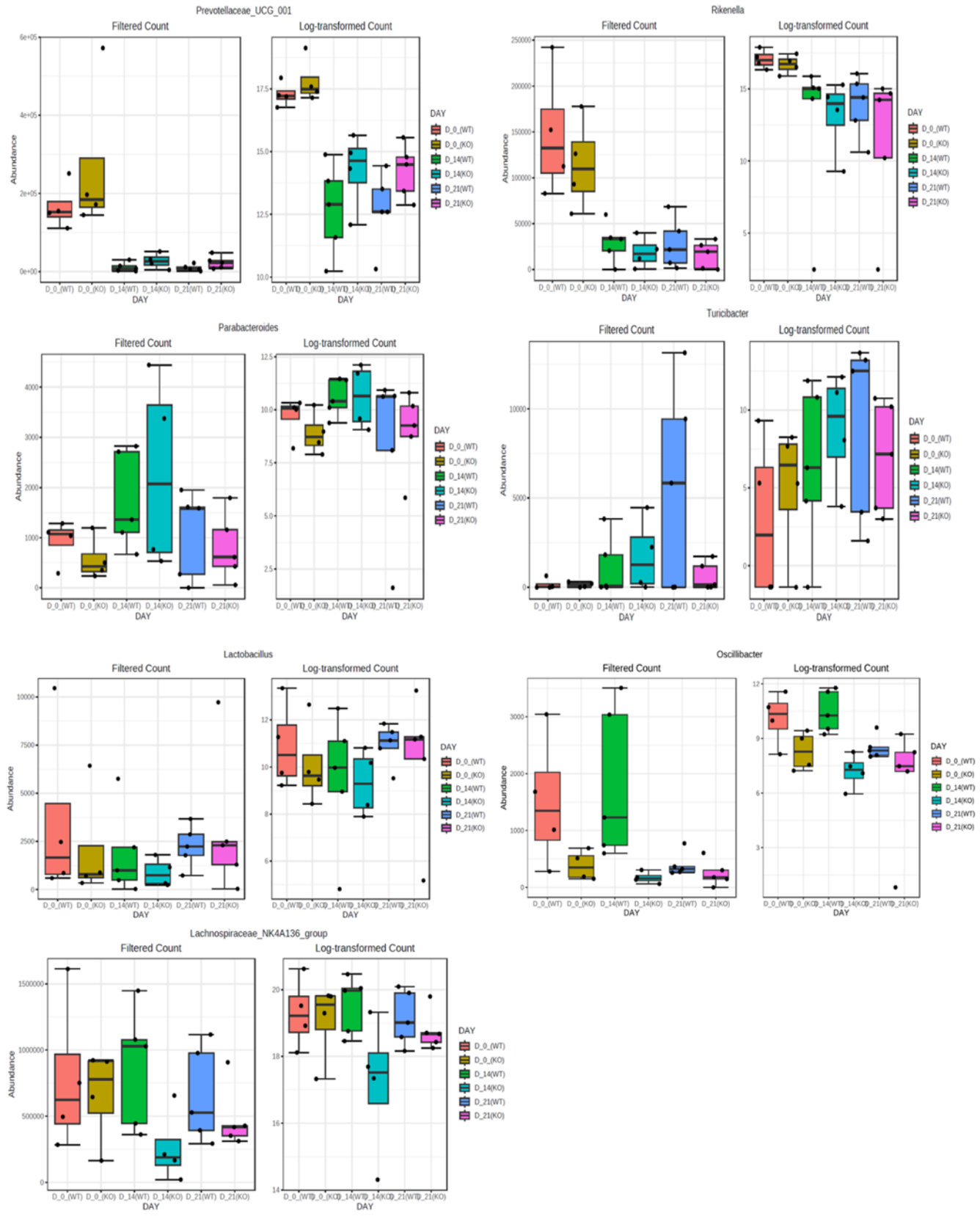
Prevotellaceae_UCG_001
Filtered Count
Log-transformed Count
Rikenella
Parabacteroides
Turicibacter
Lactobacillus
Oscillibacter
Lachnospiraceae_NK4A136_group
Abundance
DAY
D_0_(WT)
D_0_(KO)
D_14(WT)
D_14(KO)
D_21(WT)
D_21(KO)

Figure 16. Analysis of alpha-diversity in SPDEF$^{+/+}$ and SPDEF $^{-/-}$ mice with (day 14 & 21 p.i.) or without T. muris infection

Alpha-diversity assessed by Chao1 index in *SPDEF*$^{+/+}$ and *SPDEF* $^{-/-}$ mice with (day 14 & 21 p.i.) or without (day 0) *T. muris* infection.

.

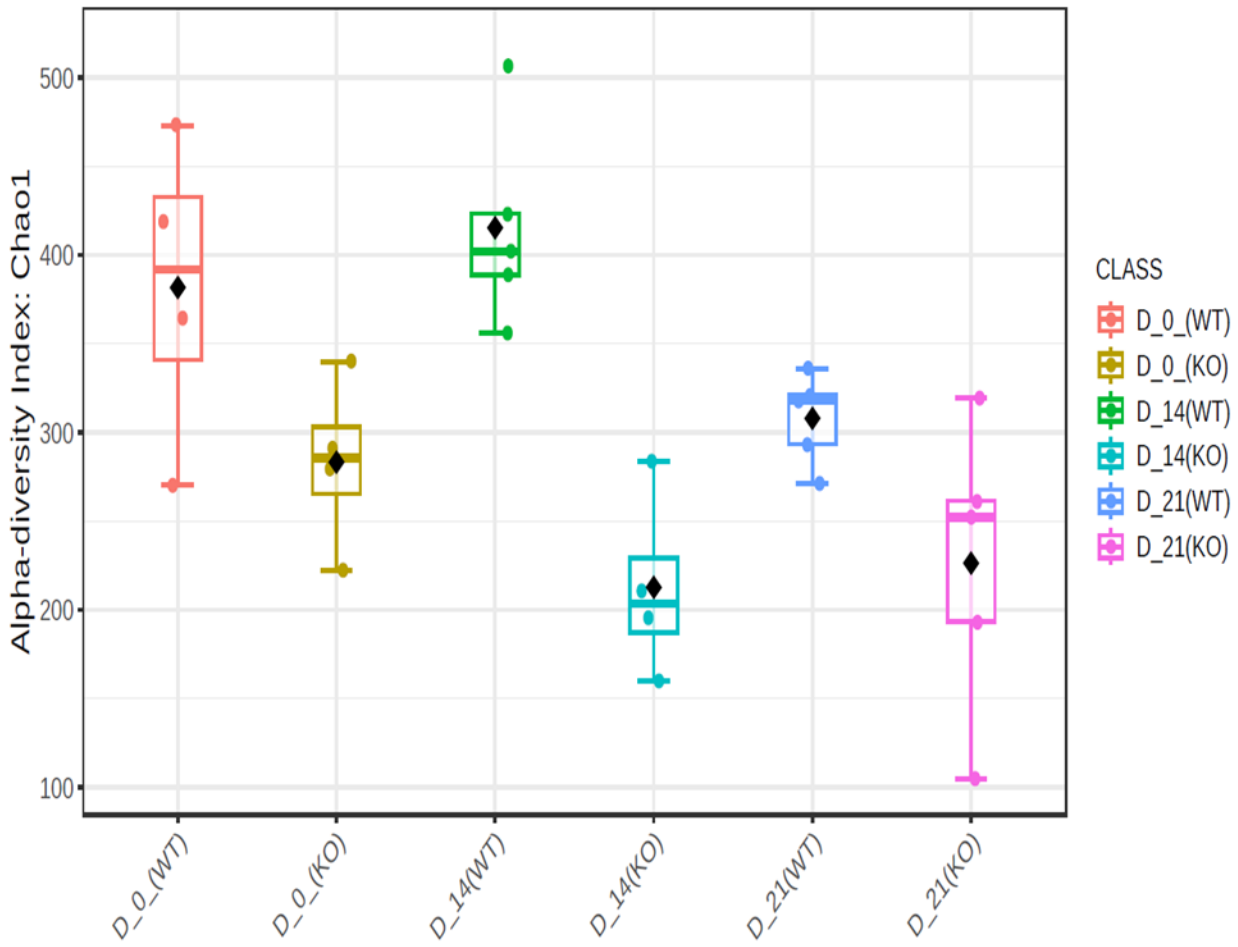
Alpha-diversity Index: Chao1
500
400
300
200
100
D_0_(WT)
D_0_(KO)
D_14(WT)
D_14(KO)
D_21(WT)
D_21(KO)
CLASS
D_0_(WT)
D_0_(KO)
D_14(WT)
D_14(KO)
D_21(WT)
D_21(KO)

Table 3: Post-hoc pairwise comparison of alpha-diversity between different groups of $SPDEF^{+/+}$ and $SPDEF^{-/-}$ mice, *p<0.05 is considered as statistically significant.

Pair	**P-value**
D_0(WT) vs D_0(KO)	0.107
D_14(WT) vs D_14(KO)	**<0.001 ***
D_21(WT) vs D_21(KO)	0.088
D_0(WT) vs D_14(WT)	0.531
D_0(WT) vs D_21(WT)	0.187
D_14(WT) vs D_21(WT)	**0.01 ***
D_0(KO) vs D_14(KO)	0.094
D_0(KO) vs D_21(KO)	0.236
D_14(KO) vs D_21(KO)	0.77

Figure 17. Analysis of beta-diversity in SPDEF$^{+/+}$ and SPDEF $^{-/-}$ mice with (day 14 & 21 p.i.) or without T. muris infection

Beta-diversity assessed by PCoA plot using Bray-Curtis dissimilarity index in *SPDEF*$^{+/+}$ and *SPDEF* $^{-/-}$ mice with (day 14 & 21 p.i.) or without (day 0) *T. muris* infection.

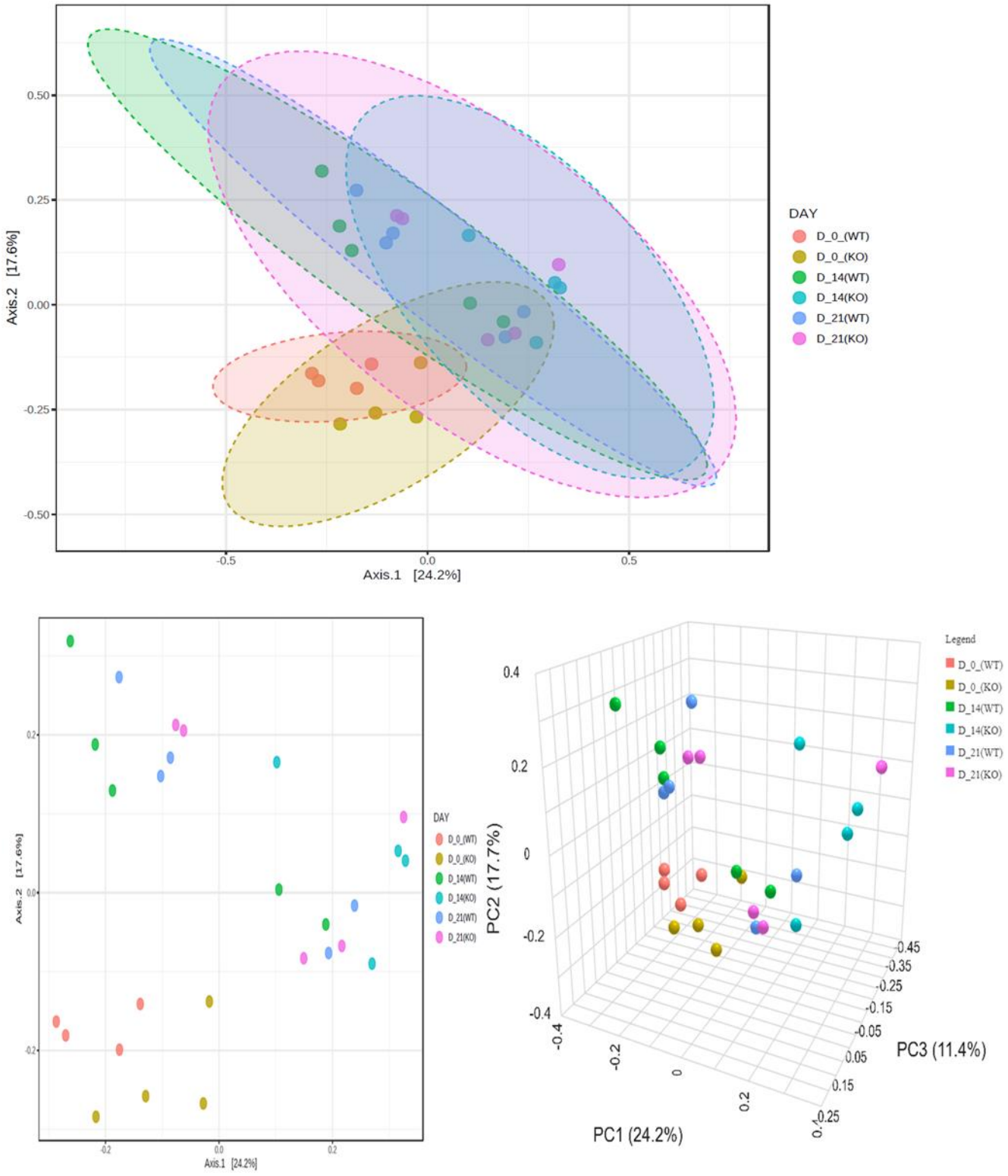
0.50
0.25
0.00
-0.25
-0.50
Axis.2 [17.6%]
-0.5
0.0
0.5
Axis.1 [24.2%]
DAY
D_0_(WT)
D_0_(KO)
D_14(WT)
D_14(KO)
D_21(WT)
D_21(KO)
Axis.2 [17.6%]
Axis.1 [24.2%]
DAY
D_0_(WT)
D_0_(KO)
D_14(WT)
D_14(KO)
D_21(WT)
D_21(KO)
PC2 (17.7%)
PC1 (24.2%)
PC3 (11.4%)
Legend
D_0_(WT)
D_0_(KO)
D_14(WT)
D_14(KO)
D_21(WT)
D_21(KO)

Table 4: Post-hoc pairwise comparison of beta-diversity between different groups of SPDEF$^{+/+}$ and SPDEF$^{-/-}$ mice, *p<0.05 is considered as statistically significant.

Pair	**P-value**
D_0_(WT) vs D_0_(KO)	0.309
D_14(WT) vs D_14(KO)	**0.026 ***
D_21(WT) vs D_21(KO)	0.858
D_0_(WT) vs D_14(WT)	**0.009 ***
D_0_(WT) vs D_21(WT)	**0.01 ***
D_14(WT) vs D_21(WT)	0.756
D_0_(KO) vs D_14(KO)	**0.029 ***
D_0_(KO) vs D_21(KO)	**0.008 ***
D_14(KO) vs D_21(KO)	0.401

4.3 T. muris-altered microbiota stimulates the expression of SPDEF and modulates goblet cell response (Muc2 secretion)

T. muris and host microbiota interaction plays a critical role in immune response. The intestinal mucus plays a major role in providing first-line defense to the host and gut microbiota also helps in proper formation and maintenance of the membrane. To determine if *T. muris*-microbiota interaction has an influence on the expression of SPDEF and goblet cell response; the number of PAS+ goblet cells, mRNA expression of *Spdef*, *Muc2* and *Muc5ac*, and the number of Muc2+ and SPDEF+ cells were assessed in the following groups of mice on BALB/c background: WT, antibiotic-treated WT (ABX-WT), ABX-WT transplanted with microbiota from naive (WT) mice, and ABX-WT transplanted with *T. muris*-altered microbiota from *T. muris* infected (WT) mice **(Figure 18-21)**. The data showed a significant increase in PAS+ goblet cells in ABX-WT mice that received microbiota either from naive or *T. muris* infected mice compared to only antibiotic-treated (ABX-WT) mice **(Figure 18A, B)**. ABX-WT mice transplanted with *T. muris*-altered microbiota showed higher number of PAS+ goblet cells in contrast to ABX-WT mice transplanted with naive microbiota **(Figure 18A, B)**. The mRNA expression of *Spdef* and *Muc2* observed via qPCR showed that both *Spdef* and *Muc2* increased in ABX-WT mice after they received microbiota from naïve or *T. muris* infected mice **(Figure 19A, B)**. Also, the mice who received altered microbiota showed higher expression of *Spdef* and *Muc2* compared to the mice who received naive microbiota **(Figure 19A, B)**. *Muc5ac* expression, however, did not show any significant increase in the mice transplanted with normal or altered microbiota **(Figure 19C)**.

In relation to the changes observed in the genetic expression of *Spdef* and *Muc2*, the number of SPDEF+ and Muc2+ cells was observed via immunofluorescence **(Figure 20,21)**. The number of SPDEF+ and Muc2+ cells showed a significant rise in ABX-WT mice after receiving microbiota

from naive or *T. muris* infected mice **(Figure 20,21)**. **Figure 20-21** also showed that after receiving *T. muris*-altered microbiota, ABX-WT mice showed greater number of SPDEF+ and Muc2+ cells compared to the group receiving naive microbiota. All these findings suggest that *T. muris*-microbiota interaction stimulates the expression of SPDEF and Muc2 with no significant alteration in Muc5ac expression.

Figure 18. Effect of T. muris-microbiota interplay on intestinal goblet cells in WT mice, antibiotic-treated WT (ABX-WT) mice, antibiotic-treated WT mice transplanted with naïve microbiota, and antibiotic-treated WT mice transplanted with T. muris-altered microbiota

Representative images of (A) PAS-stained colonic goblet cells observed by microscope, and (B) Number of PAS+ goblet cells counted per 10 crypts in WT mice, antibiotic-treated WT (ABX-WT) mice, ABX-WT mice transplanted with naïve microbiota, and ABX-WT mice transplanted with *T. muris*-altered microbiota. Data are represented as mean+/- SEM, *$p<0.05$ is considered as statistically significant.

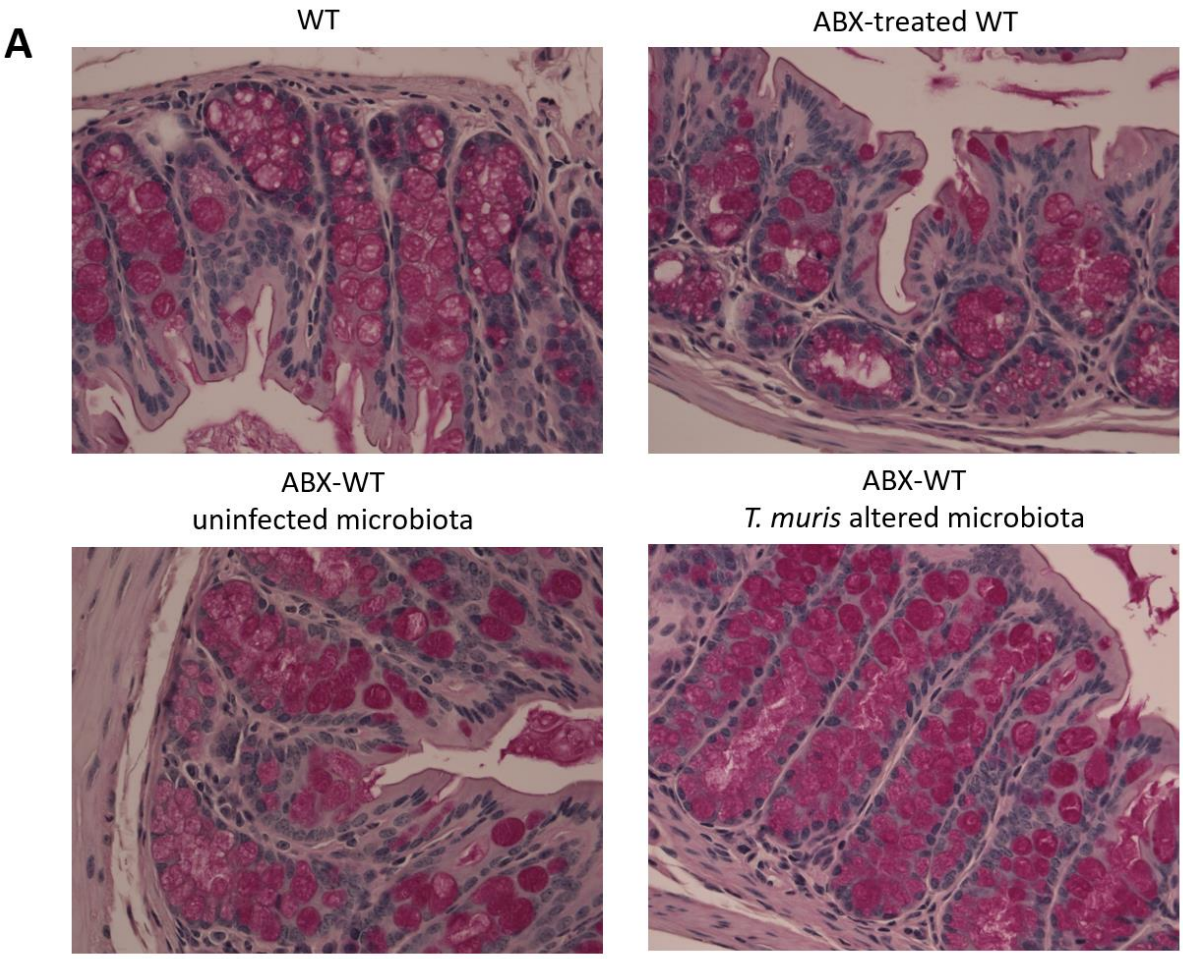
A
WT
ABX-treated WT
ABX-WT
uninfected microbiota
ABX-WT
T. muris altered microbiota

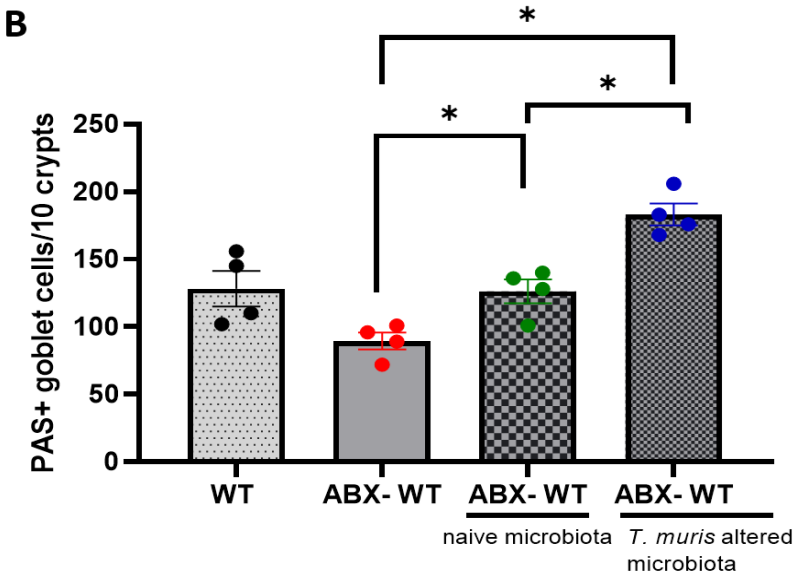
B
PAS+ goblet cells/10 crypts
250
200
150
100
50
0
*
*
*
WT
ABX- WT
ABX- WT
naive microbiota
ABX- WT
T. muris altered microbiota

Figure 19. Effect of T. muris-microbiota interplay on relative mRNA expression of Spdef, Muc2 and Muc5ac in WT mice, antibiotic-treated WT (ABX-WT) mice, antibiotic-treated WT mice transplanted with naïve microbiota, and antibiotic-treated WT mice transplanted with T. muris-altered microbiota

Relative mRNA expression of (A) *Spdef,* (B) *Muc2*, and (C) *Muc5ac* assessed by qPCR in WT mice, antibiotic-treated WT (ABX-WT) mice, ABX-WT mice transplanted with naïve microbiota, and ABX-WT mice transplanted with *T. muris*-altered microbiota, normalized to mouse 18s. Data are represented as mean+/- SEM, *$p<0.05$ is considered as statistically significant.

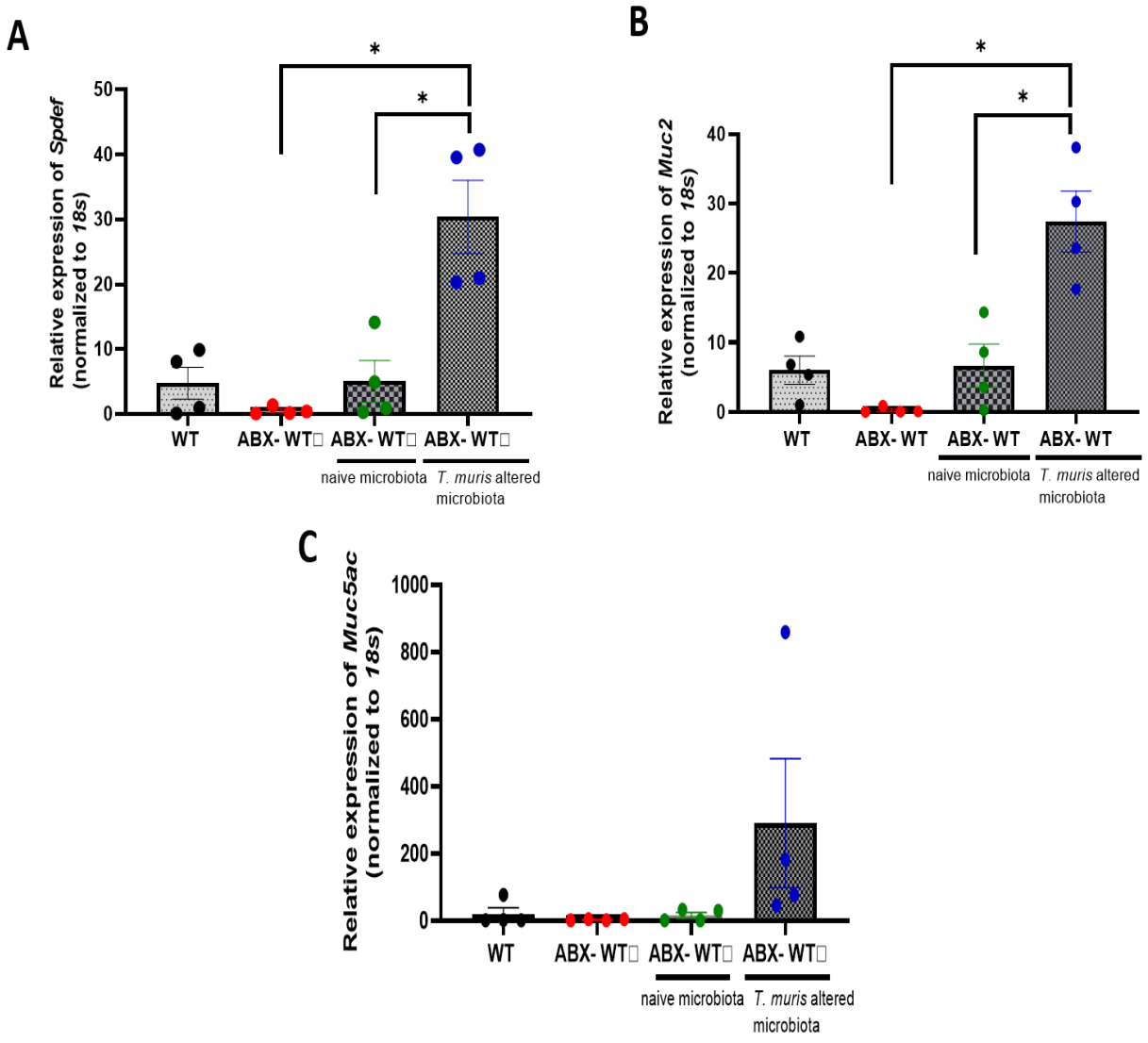
A
Relative expression of Spdef (normalized to 18s)
50
40
30
20
10
0
*
*
WT
ABX- WT
ABX- WT
ABX- WT
naive microbiota
T. muris altered microbiota
B
Relative expression of Muc2 (normalized to 18s)
40
30
20
10
0
*
*
WT
ABX- WT
ABX- WT
ABX- WT
naive microbiota
T. muris altered microbiota
C
Relative expression of Muc5ac (normalized to 18s)
1000
800
600
400
200
0
WT
ABX- WT
ABX- WT
ABX- WT
naive microbiota
T. muris altered microbiota

Figure 20. Effect of T. muris-microbiota interplay on SPDEF+ cells in WT mice, antibiotic-treated WT (ABX-WT) mice, antibiotic-treated WT mice transplanted with naïve microbiota, and antibiotic-treated WT mice transplanted with T. muris-altered microbiota

Representative images of (A) SPDEF-stained colonic cross sections observed by IFC, and (B) Number of SPDEF+ cells counted per 10 crypts in WT mice, antibiotic-treated WT (ABX-WT) mice, ABX-WT mice transplanted with naïve microbiota, and ABX-WT mice transplanted with *T. muris*-altered microbiota. Data are represented as mean+/- SEM, *$p<0.05$ is considered as statistically significant.

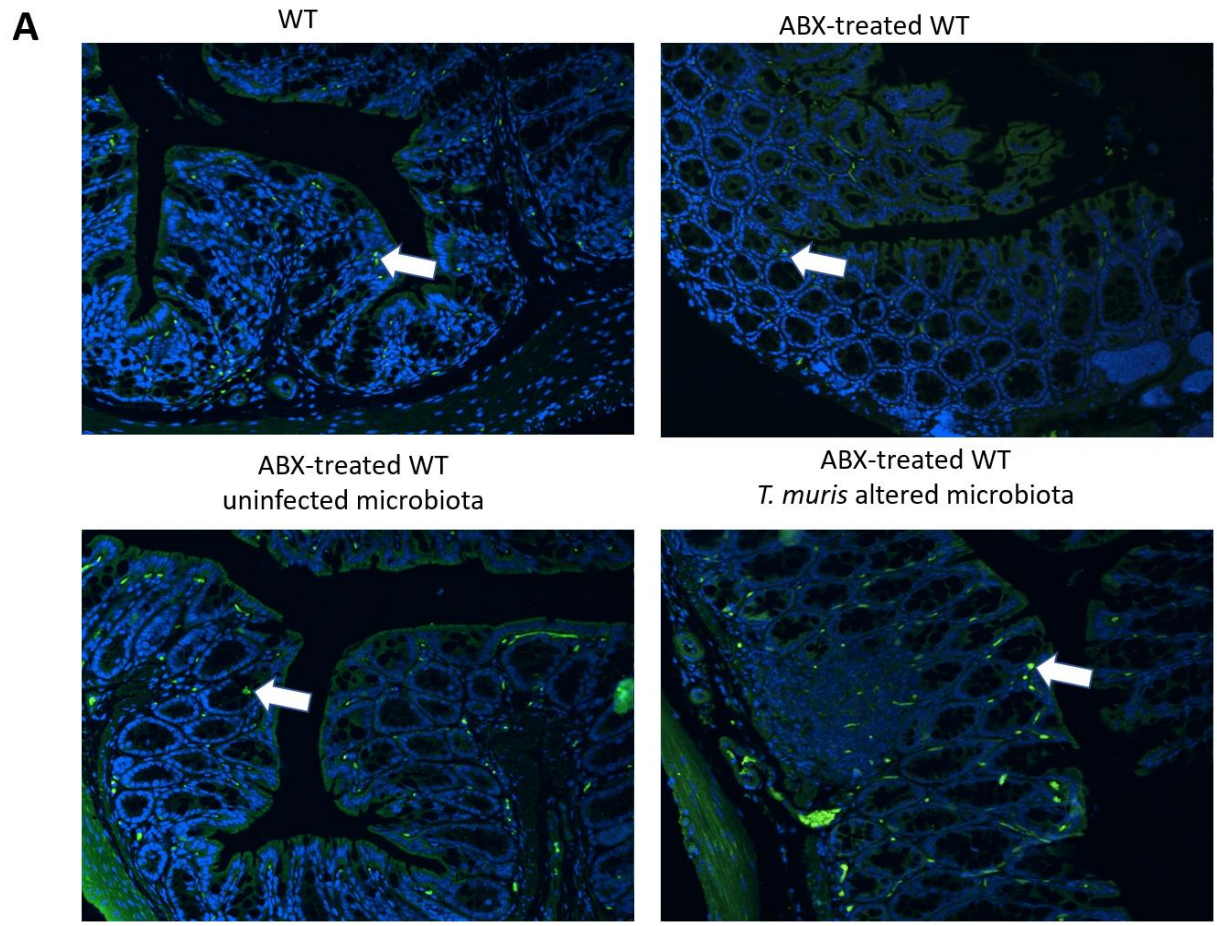
A
WT
ABX-treated WT
ABX-treated WT
uninfected microbiota
ABX-treated WT
T. muris altered microbiota

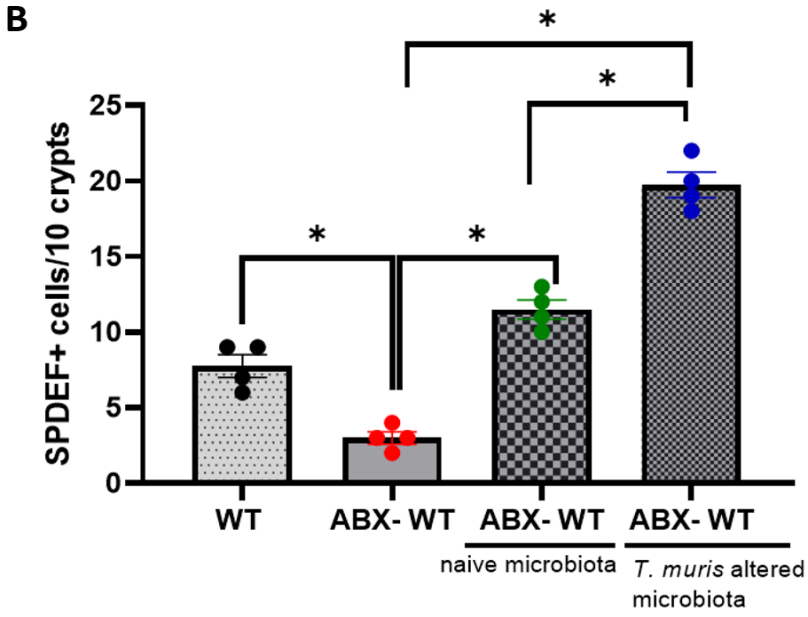
B
SPDEF+ cells/10 crypts
25
20
15
10
5
0
*
*
*
*
WT
ABX- WT
ABX- WT
ABX- WT
naive microbiota
T. muris altered microbiota

Figure 21. Effect of T. muris-microbiota interplay on Muc2+ cells in WT mice, antibiotic-treated WT (ABX-WT) mice, antibiotic-treated WT mice transplanted with naïve microbiota, and antibiotic-treated WT mice transplanted with T. muris-altered microbiota

Representative images of (A) Muc2-stained colonic cross sections observed by IFC, and (B) Number of Muc2+ cells counted per 10 crypts in WT mice, antibiotic-treated WT (ABX-WT) mice, ABX-WT mice transplanted with naïve microbiota, and ABX-WT mice transplanted with *T. muris*-altered microbiota. Data are represented as mean+/- SEM, *$p<0.05$ is considered as statistically significant.

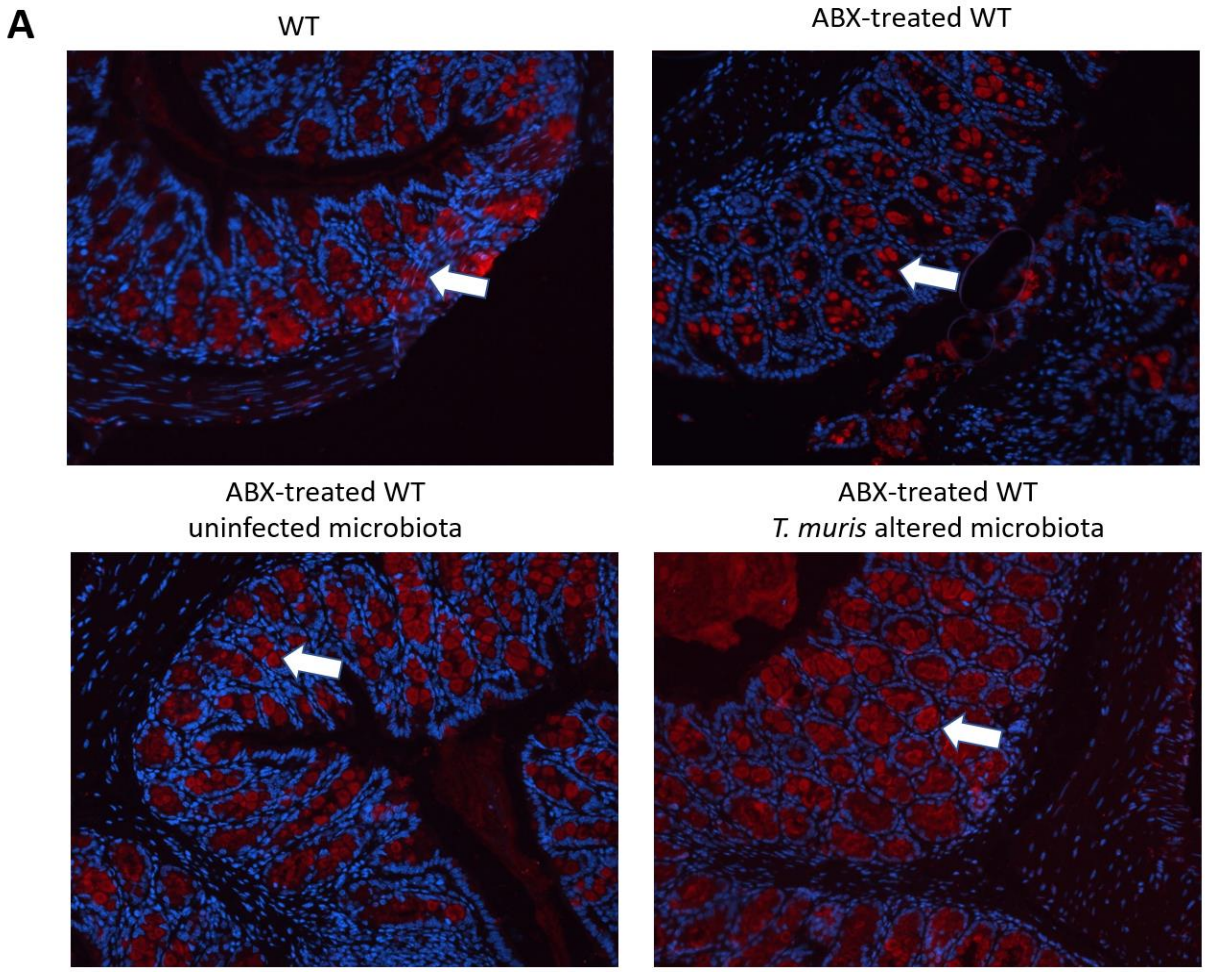
A
WT
ABX-treated WT
ABX-treated WT
uninfected microbiota
ABX-treated WT
T. muris altered microbiota

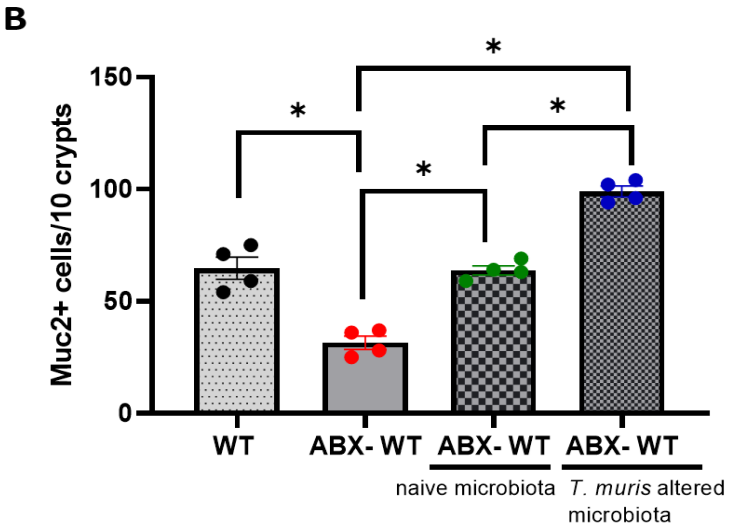
B
Muc2+ cells/10 crypts
150
100
50
0
*
*
*
*
WT
ABX- WT
ABX- WT
ABX- WT
naive microbiota
T. muris altered microbiota

4.4 T. muris-altered cecal microbiota shows difference in composition compared to naïve microbiota following microbial transplantation in antibiotic-treated mice

The antibiotic-treated WT (ABX-WT) mice showed increased number of PAS+ goblet cells and higher expression of SPDEF and Muc2 after they received *T. muris*-altered microbiota, compared to the mice that received naïve microbiota **(Result 4.3)**. To observe the differences in microbial community, bacterial profiling of the cecal contents was performed in the following groups: WT, ABX-WT, ABX-WT with naïve microbiota transplant, and ABX-WT with *T. muris*-altered microbiota transplant. Relative abundance of microbial composition on genus level, α-diversity using Chao1 index, β-diversity using Bray-Curtis dissimilarity index and post-hoc pairwise comparison of microbial diversity were assessed in those groups of mice **(Figure 22-24, Table 5,6)**. The relative abundance data on genus level showed that there was relatively higher abundance of Gram-positive bacteria *Enterococcus* in ABX-WT group compared to WT or naïve/*T. muris*-altered microbiota transplant groups **(Figure 22)**. The ABX-WT group did not show any relative presence of certain Gram-negative bacteria such as *Alistipes, Helicobacter, Odoribacter, Bacteroides, Akkermansia, Anaeroplasma, Parabacteroides* and members from *Lachnospiraceae* family, which were seen to be present in other groups **(Figure 22)**. ABX-WT mice transplanted with *T. muris*-altered microbiota showed relatively higher abundance of *Alistipes*, *Odoribacter* and members from *Lachnospiracea* family; whereas the mice transplanted with naïve microbiota showed higher abundance of *Helicobacter, Intestinimonas* and members from *Rikenellaceae* and *Prevotellaceae* families **(Figure 22)**.

In regard to microbial diversity, ABX-WT group showed diminished α-diversity compared to WT and naïve/*T. muris*-altered microbiota transplant groups **(Figure 23, Table 5)**. No significant difference in α-diversity was observed between naïve and *T. muris*-altered microbiota transplant

groups. On the contrary, the β-diversity data has shown that ABX-WT group that received *T. muris*-altered microbiota are separately distributed from the naïve microbiota transplant group **(Figure 24, Table 6)**. All these data suggest that *T. muris*-altered microbiota shows different microbial composition and diversity compared to naïve microbiota following microbial transplantation in antibiotic-treated mice.

Figure 22. Analysis of microbial composition in WT mice, antibiotic-treated WT (ABX-WT) mice, antibiotic-treated WT mice transplanted with naïve microbiota, and antibiotic-treated WT mice transplanted with T. muris-altered microbiota

Relative abundance of microbial community on genus level observed in WT mice, antibiotic-treated WT (ABX-WT) mice, ABX-WT mice transplanted with naïve microbiota, and ABX-WT mice transplanted with *T. muris*-altered microbiota.

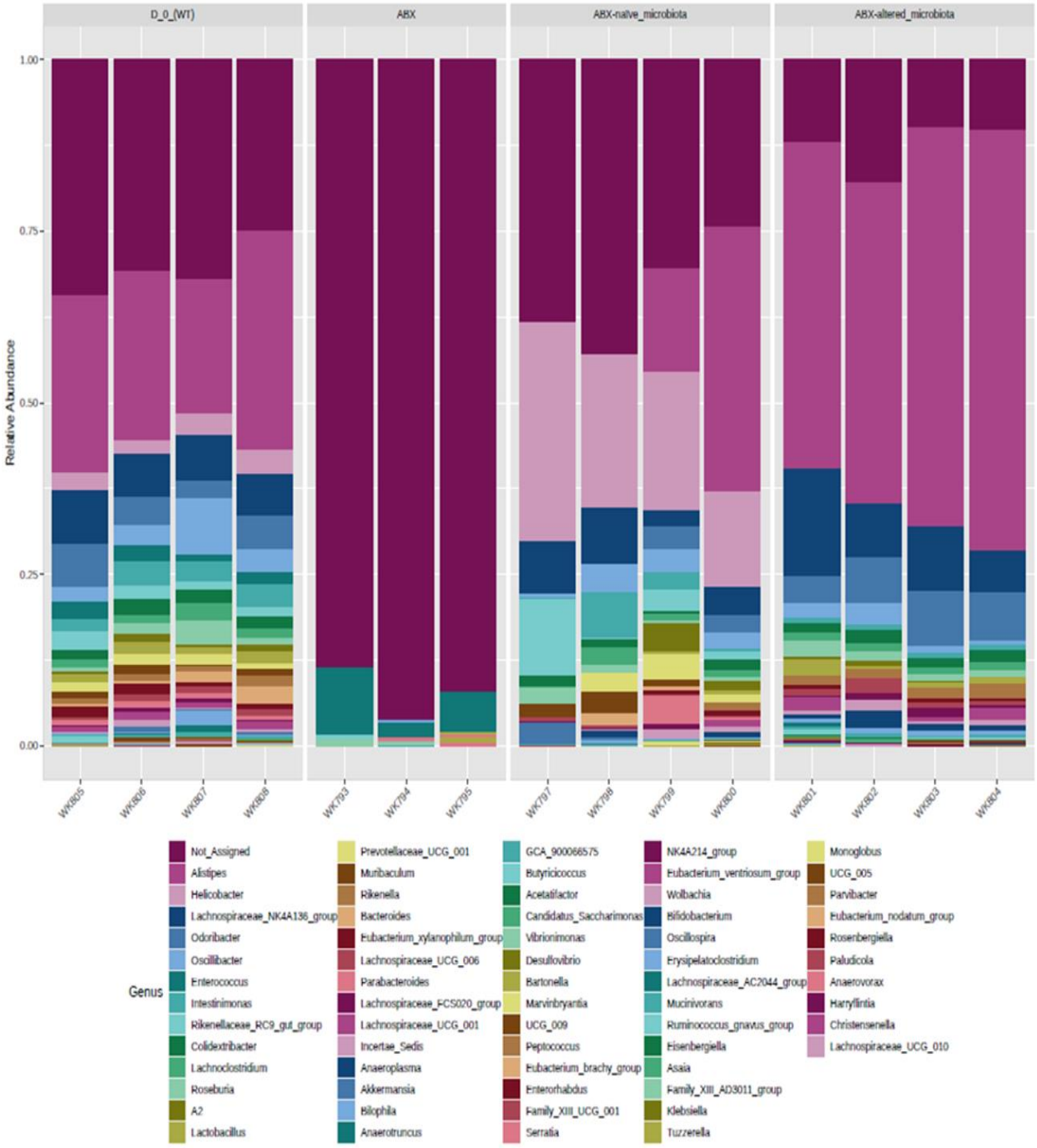
D_0_(WT)
ABX
ABX-naïve_microbiota
ABX-altered_microbiota
Relative Abundance
1.00
0.75
0.50
0.25
0.00
WK805
WK806
WK807
WK808
WK793
WK794
WK795
WK797
WK798
WK799
WK800
WK801
WK802
WK803
WK804
Genus
Not_Assigned
Alistipes
Helicobacter
Lachnospiraceae_NK4A136_group
Odoribacter
Oscillibacter
Enterococcus
Intestinimonas
Rikenellaceae_RC9_gut_group
Colidextribacter
Lachnoclostridium
Roseburia
A2
Lactobacillus
Prevotellaceae_UCG_001
Muribaculum
Rikenella
Bacteroides
Eubacterium_xylanophilum_group
Lachnospiraceae_UCG_006
Parabacteroides
Lachnospiraceae_FCS020_group
Lachnospiraceae_UCG_001
Incertae_Sedis
Anaeroplasma
Akkermansia
Bilophila
Anaerotruncus
GCA_900066575
Butyricicoccus
Acetatifactor
Candidatus_Saccharimonas
Vibrionimonas
Desulfovibrio
Bartonella
Marvinbryantia
UCG_009
Peptococcus
Eubacterium_brachy_group
Enterorhabdus
Family_XIII_UCG_001
Serratia
NK4A214_group
Eubacterium_ventriosum_group
Wolbachia
Bifidobacterium
Oscillospira
Erysipelatoclostridium
Lachnospiraceae_AC2044_group
Mucinivorans
Ruminococcus_gnavus_group
Eisenbergiella
Asaia
Family_XIII_AD3011_group
Klebsiella
Tuzzerella
Monoglobus
UCG_005
Parvibacter
Eubacterium_nodatum_group
Rosenbergiella
Paludicola
Anaerovorax
Harryflintia
Christensenella
Lachnospiraceae_UCG_010

Figure 23. Analysis of alpha-diversity in WT mice, antibiotic-treated WT (ABX-WT) mice, antibiotic-treated WT mice transplanted with naïve microbiota, and antibiotic-treated WT mice transplanted with T. muris-altered microbiota

Alpha-diversity assessed by Chao1 index in WT mice, antibiotic-treated WT (ABX-WT) mice, ABX-WT mice transplanted with naïve microbiota, and ABX-WT mice transplanted with *T. muris*-altered microbiota.

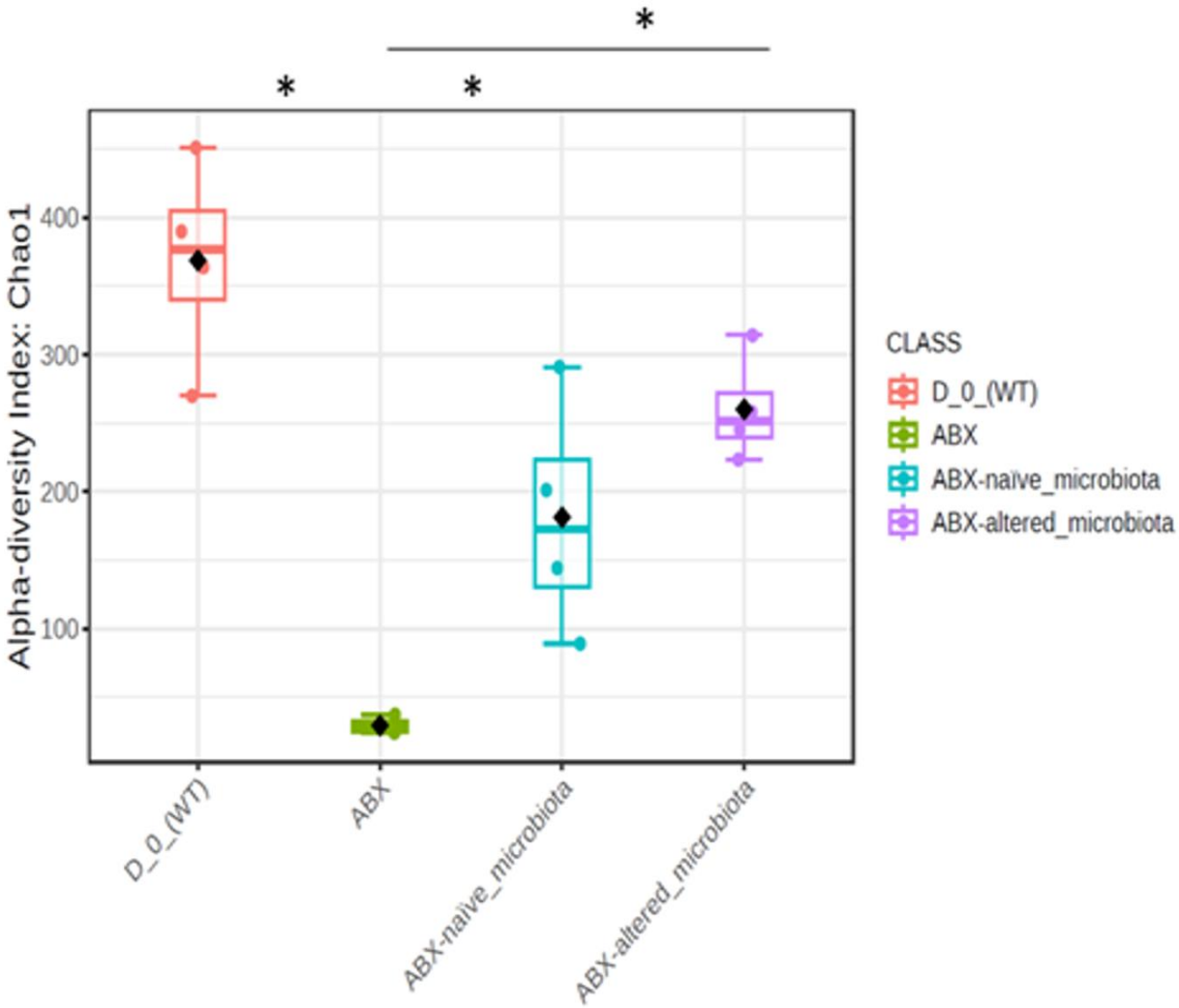
*
*
*
Alpha-diversity Index: Chao1
400
300
200
100
D_0_(WT)
ABX
ABX-naïve_microbiota
ABX-altered_microbiota
CLASS
D_0_(WT)
ABX
ABX-naïve_microbiota
ABX-altered_microbiota

Table 5: Post-hoc pairwise comparison of alpha-diversity in WT mice, antibiotic-treated WT (ABX-WT) mice, antibiotic-treated WT mice transplanted with naïve microbiota, and antibiotic-treated WT mice transplanted with T. muris-altered microbiota, *p<0.05 is considered as statistically significant.

Pair	**P-value**
D_0(WT) vs ABX	**0.003 ***
ABX vs ABX-naïve_microbiota	**0.04 ***
ABX vs ABX-altered_microbiota	**<0.001 ***
ABX-naïve_microbiota vs ABX-altered_microbiota	0.18

Figure 24. Analysis of beta-diversity in WT mice, antibiotic-treated WT (ABX-WT) mice, antibiotic-treated WT mice transplanted with naïve microbiota, and antibiotic-treated WT mice transplanted with T. muris-altered microbiota

Beta-diversity assessed by PCoA plot using Bray-Curtis dissimilarity index in WT mice, antibiotic-treated WT (ABX-WT) mice, ABX-WT mice transplanted with naïve microbiota, and ABX-WT mice transplanted with *T. muris*-altered microbiota.

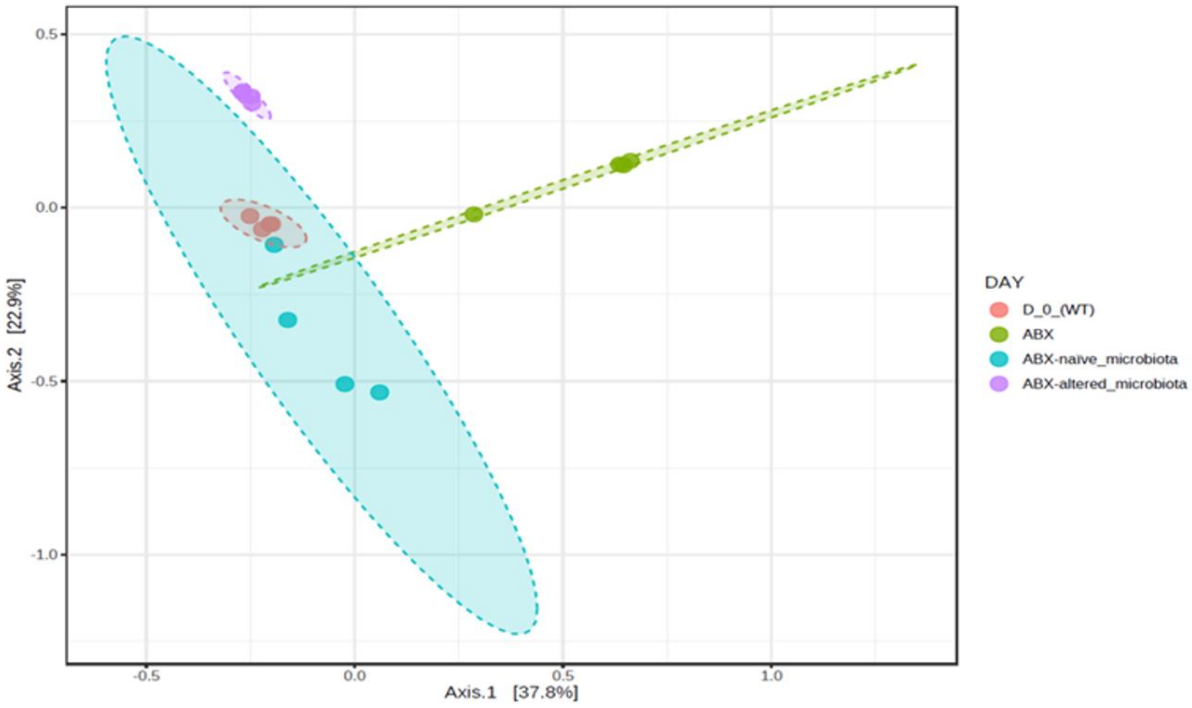
0.5
0.0
-0.5
-1.0
Axis.2 [22.9%]
-0.5
0.0
0.5
1.0
Axis.1 [37.8%]
DAY
D_0_(WT)
ABX
ABX-naive_microbiota
ABX-altered_microbiota

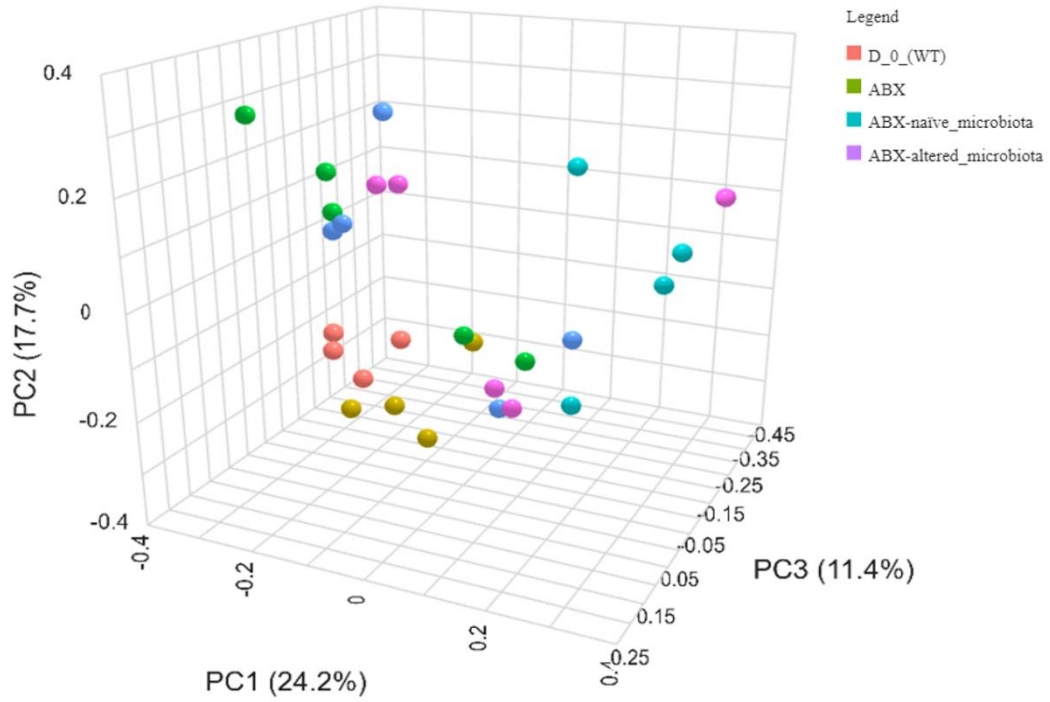
Legend
D_0_(WT)
ABX
ABX-naïve_microbiota
ABX-altered_microbiota
PC2 (17.7%)
0.4
0.2
0
-0.2
-0.4
PC1 (24.2%)
-0.4
-0.2
0
0.2
PC3 (11.4%)
-0.45
-0.35
-0.25
-0.15
-0.05
0.05
0.15
0.25

Table 6: Post-hoc pairwise comparison of beta-diversity in WT mice, antibiotic-treated WT (ABX-WT) mice, antibiotic-treated WT mice transplanted with naïve microbiota, and antibiotic-treated WT mice transplanted with T. muris-altered microbiota, *p<0.05 is considered as statistically significant.

Pair	**P-value**
D_0(WT) vs ABX	**0.026 ***
ABX vs ABX-naïve_microbiota	**0.031 ***
ABX vs ABX-altered_microbiota	**0.024 ***
ABX-naïve_microbiota vs ABX-altered_microbiota	**0.03 ***

4.5 T. muris ESPs directly stimulate the mRNA expression of SPDEF and MUC2 through NOD/TLR signaling pathways in human colonic mucin secreting cell line LS174T

As discussed in the rationale for aim 3 in chapter 2, previous research from our lab has shown how *T. muris* ESPs exert a direct effect on TLR2 expression in human EC cell line BON-1 cells and stimulate the secretion of 5-HT [103]. Our lab has also shown that treatment with NOD1 and NOD2 agonists in mice with acute *T. muris* infection resulted in increased number of goblet cells and Muc2 secretion [107]. The expression of MUC2 in human colonic LS174T cells also increased following NOD1 and NOD2 treatment [107]. The colonic goblet cells have been seen to express higher levels of TLR2, TLR4 on their surface and NOD1, NOD2 in their cytoplasm. To investigate whether *T. muris* ESPs influence the expression of SPDEF and MUC2 through NOD/TLR signaling pathways in LS174T cells, we cultured the cells and treated them in 2 different sets, each set containing cells from 3 different passages. The first set was treated with a control reagent (PBS) and agonists for NOD1, NOD2, TLR2 and TLR4 receptors; while the second set was treated with the same control, *T. muris* ESPs and the antagonists against the NOD1, NOD2, TLR2 and TLR4 receptors with *T. muris* ESPs simultaneously. **(Figure 25A)**. We assessed the mRNA expression of *SPDEF* and *MUC2* via qPCR **(Figure 25B-E)** and their protein expression via Western blot **(Figure 25A-D)** in each set.

SPDEF and *MUC2* showed higher expression in LS174T cells after treatment with TLR2 and TLR4 agonists **(Figure 25B, C)**. **Figure 25C** also showed higher *MUC2* expression in the cells after treatment with NOD2 agonist. These receptors can modulate intracellular downstream signaling cascades, such as NF-κβ or mitogen-activated protein kinase (MAPK) pathways and regulate the expression of certain genes by activating several transcription factors [123]. The cells also showed higher *SPDEF* and *MUC2* mRNA levels after being treated with *T. muris* ESPs

(Figure 25D, E). However, treatment with TLR2 antagonist and *T. muris* ESPs simultaneously showed a significantly lower expression of *SPDEF* **(Figure 25D, E**). Expression of *MUC2* was also seen to be depleted in the cells after treatment with NOD2 and TLR2 antagonists along with *T. muris* ESPs compared to only *T. muris* ESPs treatment group **(Figure 25D, E)**. These data may suggest that *T. muris* ESPs can directly stimulate the genetic expression of *SPDEF* and *MUC2* through NOD/TLR receptor-mediated pathways in human colonic cell line LS174T. On the contrary, the protein expression of SPDEF and MUC2 observed via Western blot in **Figure 26A-D** did not show any significant changes post-treatment with NOD/TLR agonists, *T. muris* ESPs or antagonists, which was one of the limitations of this study that has been discussed in the next chapter.

Figure 25. Effect of NOD/TLR signaling on relative mRNA expression of SPDEF and MUC2 in LS174T cells treated with a control reagent, agonists for NOD1, NOD2, TLR2 and TLR4 receptors, T. muris ESPs and antagonists against NOD1, NOD2, TLR2 and TLR4 receptors with T. muris ESPs

(A) Graphical image of LS174T cells cultured and treated in a 12-well plate with a control reagent, agonists for NOD1, NOD2, TLR2 and TLR4 receptors, *T. muris* ESPs and antagonists against NOD1, NOD2, TLR2 and TLR4 receptors with *T. muris* ESPs simultaneously; relative mRNA expression of (B) *SPDEF*, and (C) *MUC2* assessed by qPCR in the first set of cells treated with a control reagent and agonists for NOD1, NOD2, TLR2 and TLR4 receptors; relative mRNA expression of (D) *SPDEF*, and (E) *MUC2* assessed by qPCR in the second set of cells treated with a control reagent, *T. muris* ESPs and antagonists against NOD1, NOD2, TLR2 and TLR4 receptors with *T. muris* ESPs; normalized to human 18s. Data are represented as mean+/- SEM, *$p<0.05$ is considered as statistically significant.

A

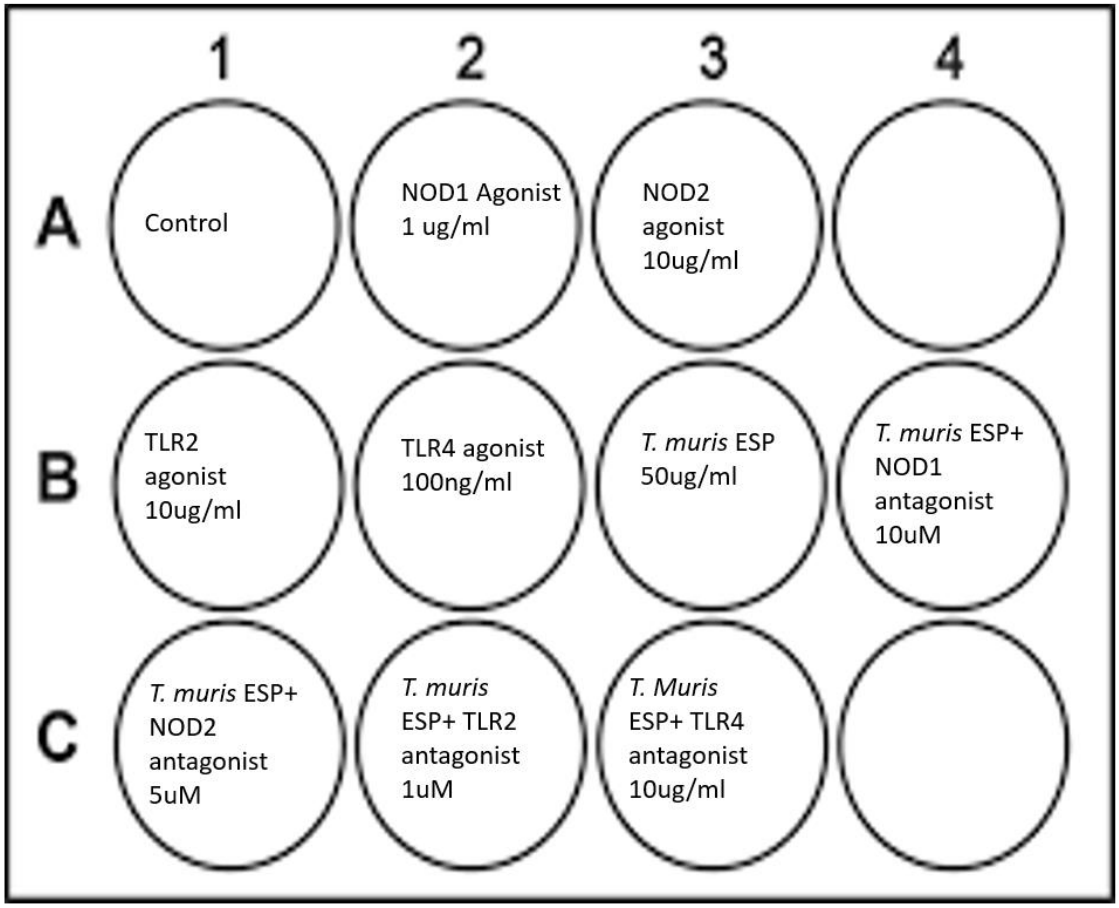
1
2
3
4
A
Control
NOD1 Agonist 1 ug/ml
NOD2 agonist 10ug/ml
B
TLR2 agonist 10ug/ml
TLR4 agonist 100ng/ml
T. muris ESP 50ug/ml
T. muris ESP+ NOD1 antagonist 10uM
C
T. muris ESP+ NOD2 antagonist 5uM
T. muris ESP+ TLR2 antagonist 1uM
T. Muris ESP+ TLR4 antagonist 10ug/ml

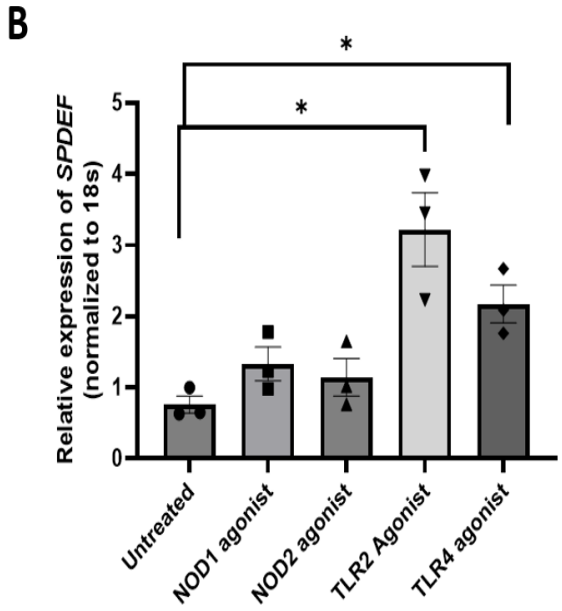
B
Relative expression of SPDEF
(normalized to 18s)
0
1
2
3
4
5
*
*
Untreated
NOD1 agonist
NOD2 agonist
TLR2 Agonist
TLR4 agonist

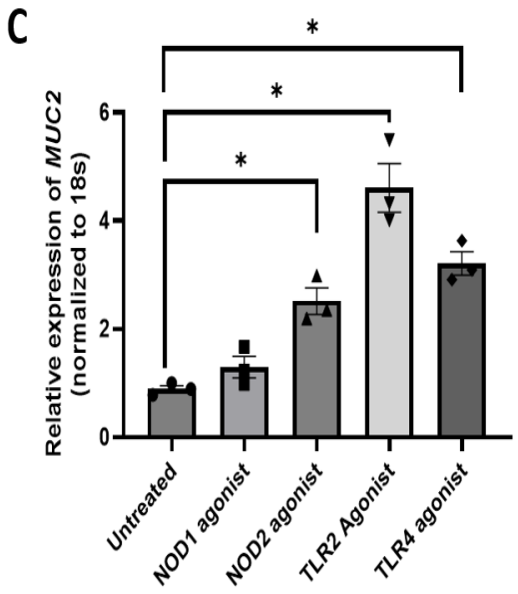
C
Relative expression of MUC2
(normalized to 18s)
0
2
4
6
*
*
*
Untreated
NOD1 agonist
NOD2 agonist
TLR2 Agonist
TLR4 agonist

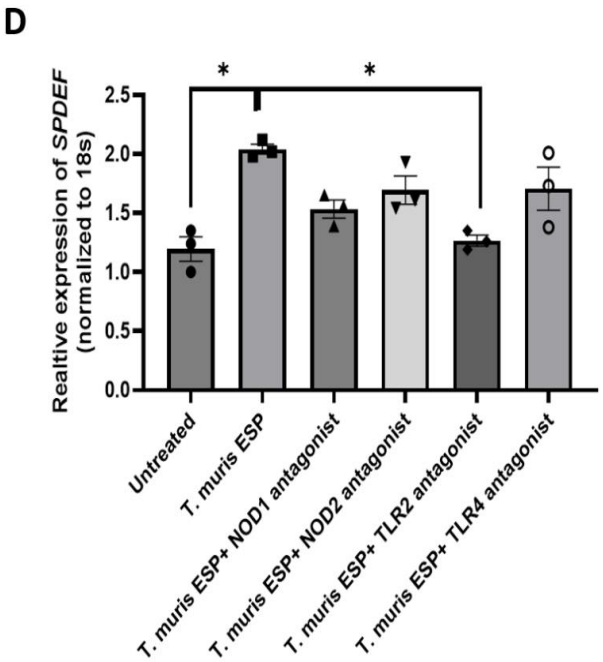
D
Realtive expression of SPDEF
(normalized to 18s)
0.0
0.5
1.0
1.5
2.0
2.5
*
*
Untreated
T. muris ESP
T. muris ESP+ NOD1 antagonist
T. muris ESP+ NOD2 antagonist
T. muris ESP+ TLR2 antagonist
T. muris ESP+ TLR4 antagonist

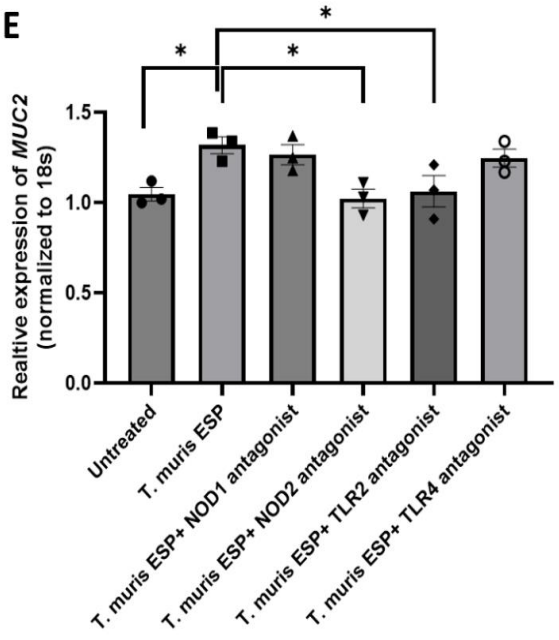
E
Realtive expression of MUC2
(normalized to 18s)
0.0
0.5
1.0
1.5
*
*
*
Untreated
T. muris ESP
T. muris ESP+ NOD1 antagonist
T. muris ESP+ NOD2 antagonist
T. muris ESP+ TLR2 antagonist
T. muris ESP+ TLR4 antagonist

Figure 26. Effect of NOD/TLR signaling on SPDEF and MUC2 protein levels in LS174T cells treated with a control reagent, agonists for NOD1, NOD2, TLR2 and TLR4 receptors, T. muris ESPs and antagonists against NOD1, NOD2, TLR2 and TLR4 receptors with T. muris ESPs

Western blot images and quantification of SPDEF protein in LS174T cells treated in 2 different sets: (A) first set with a control reagent and agonists for NOD1, NOD2, TLR2 and TLR4 receptors; (B) second set with a control reagent, *T. muris* ESPs and antagonists against NOD1, NOD2, TLR2 and TLR4 receptors with *T. muris* ESPs; Western blot images and quantification of MUC2 protein in LS174T cells treated in 2 different sets: (C) first set with a control reagent and agonists for NOD1, NOD2, TLR2 and TLR4 receptors; (D) second set with a control reagent, *T. muris* ESPs and antagonists against NOD1, NOD2, TLR2 and TLR4 receptors with *T. muris* ESPs. Data are represented as mean+/- SEM, *$p<0.05$ is considered as statistically significant.

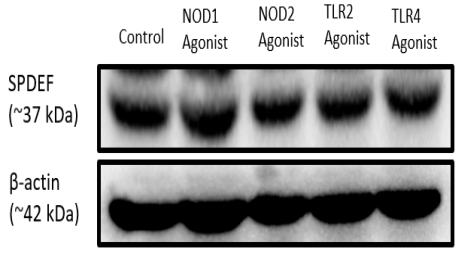
Control
NOD1 Agonist
NOD2 Agonist
TLR2 Agonist
TLR4 Agonist
SPDEF (~37 kDa)
β-actin (~42 kDa)

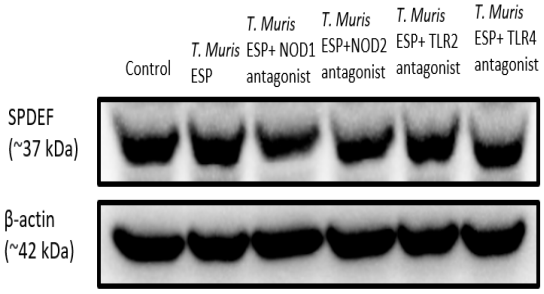
Control
T. Muris ESP
T. Muris ESP+ NOD1 antagonist
T. Muris ESP+NOD2 antagonist
T. Muris ESP+ TLR2 antagonist
T. Muris ESP+ TLR4 antagonist
SPDEF (~37 kDa)
β-actin (~42 kDa)

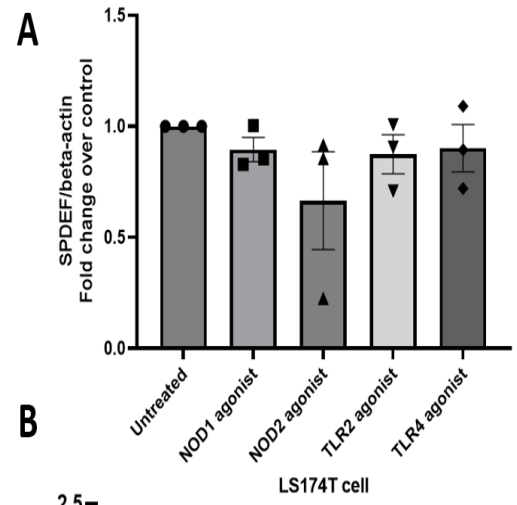
A
SPDEF/beta-actin Fold change over control
1.5
1.0
0.5
0.0
Untreated
NOD1 agonist
NOD2 agonist
TLR2 agonist
TLR4 agonist
LS174T cell

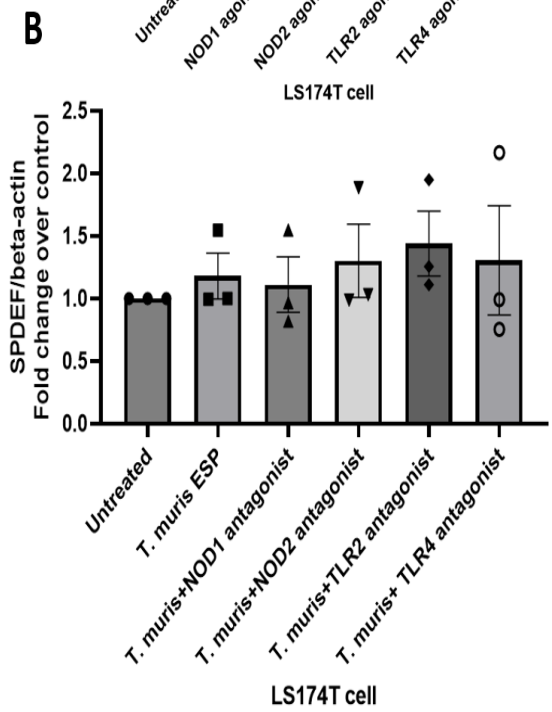
B
SPDEF/beta-actin Fold change over control
2.5
2.0
1.5
1.0
0.5
0.0
Untreated
T. muris ESP
T. muris+NOD1 antagonist
T. muris+NOD2 antagonist
T. muris+TLR2 antagonist
T. muris+ TLR4 antagonist
LS174T cell

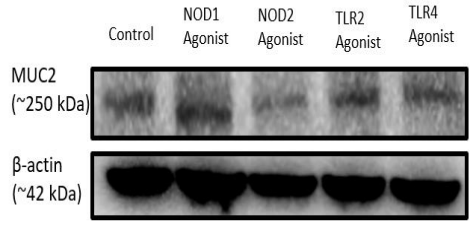
Control
NOD1 Agonist
NOD2 Agonist
TLR2 Agonist
TLR4 Agonist
MUC2 (~250 kDa)
β-actin (~42 kDa)

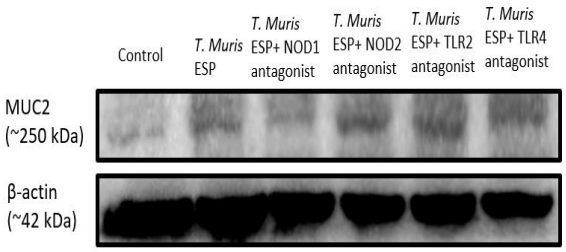
Control
T. Muris ESP
T. Muris ESP+ NOD1 antagonist
T. Muris ESP+ NOD2 antagonist
T. Muris ESP+ TLR2 antagonist
T. Muris ESP+ TLR4 antagonist
MUC2 (~250 kDa)
β-actin (~42 kDa)

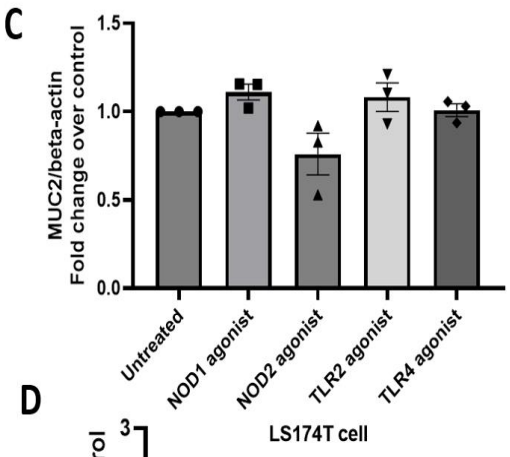
C
MUC2/beta-actin Fold change over control
1.5
1.0
0.5
0.0
Untreated
NOD1 agonist
NOD2 agonist
TLR2 agonist
TLR4 agonist
LS174T cell

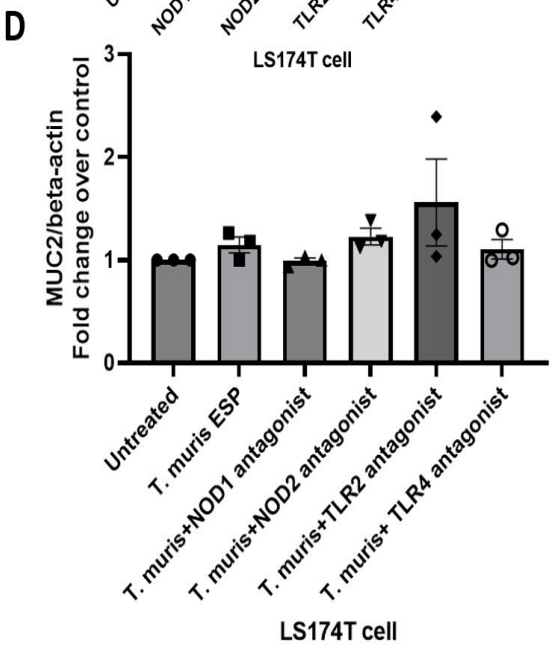
D
MUC2/beta-actin Fold change over control
3
2
1
0
Untreated
T. muris ESP
T. muris+NOD1 antagonist
T. muris+NOD2 antagonist
T. muris+TLR2 antagonist
T. muris+ TLR4 antagonist
LS174T cell

Chapter 5: Discussion

Goblet cells and the secreted mucins play important roles in providing innate defense to the host in several enteric parasitic infections, the most common of them being the soil-transmitted helminths/STH in mammals. The stimulated mucin secretion from these cells ensures a robust mucosal barrier that helps in parasite expulsion from the gut. *T. muris* in mice has been well-studied for many years as a common laboratory model for *T. trichiura* in humans, which affects more than a billion people worldwide [51]. Changes in goblet cell response and other immunological and pathophysiological changes with reference to acute and chronic *T. muris* infections have been well-documented across several studies. Goblet cell hyperplasia during acute *T. muris* infection is observed in resistant mice who are capable of worm expulsion, whereas hyperplasia of absorptive enterocytes is observed during chronic infection and in susceptible mice which results in failure in worm expulsion [27] [74] [75]. The BALB/c mice are resistant to *T. muris* infection, which otherwise showed increased expression of Hes-1 and enterocyte differentiation during chronic infection [26]. The same resistant strain has shown upregulation of Math-1 and SPDEF during acute infection, resulting in increased goblet cell differentiation [26]. Hyperplasia of goblet cells is an immune-protective mechanism against parasites which helps in trapping the worms and their expulsion through increased mucin secretion.

Consistent with these studies, we have witnessed increased PAS+ goblet, SPDEF+ and Muc2+ cells and higher expression of *Spdef* and *Muc2* in resistant (BALB/c) $SPDEF^{+/+}$ mice following acute infection with *T. muris* at day 14 and 21 p.i., compared to $SPDEF^{-/-}$ mice. The resistant mice start expelling the worms from day 14 and by day 21, majority of the worms are expelled, which was one of the reasons for selecting two different timepoints of infection for the experiments. SPDEF is known to be one of the major transcription factors regulating the terminal differentiation,

proliferation and maturation of intestinal goblet cells, the lack of which causes significant depletion of goblet cells and secreted mucins. In relation to this fact, we have observed significant difference between *SPDEF*$^{+/+}$ and *SPDEF*$^{-/-}$ mice in terms of number of goblet, SPDEF+ and Muc2+ cells, along with the genetic expression of their markers. In *SPDEF*$^{+/+}$ mice, however, we have witnessed lower mRNA and protein expression of SPDEF at day 21 p.i., while the expression of Muc2 remained high. This could suggest that there are other transcription factors that induced Muc2 expression in goblet cells, which could be studied for future research.

In a previous study, *Muc5ac*$^{-/-}$ mice showed delayed worm expulsion despite generating a robust TH2 response during acute *T. muris* infection. The absence of *Muc5ac* gene in mice also has a delayed effect on worm expulsion in other parasitic infections, such as *T. spiralis* and *N. brasiliensis* [28]. Also, higher expression of *Muc5ac* was observed in C57BL/6 mice around the time or worm expulsion [27]. However, our data did not show any significant changes in *Muc5ac* after infection and between *SPDEF*$^{+/+}$ and *SPDEF*$^{-/-}$ mice. Muc5ac is not typically expressed in the colon and it has a negative effect on worm viability observed in human colon cell lines, the mechanism which is yet to be explored [28]. The genetic background of mice used in our experiments was BALB/c and the expression of *Muc5ac* was not previously assessed in this particular genotype, which might be associated with such changes in this mucin. This might be a topic for future studies to elucidate the variability of its changes in our experiments.

The resistance and susceptibility of mice to *T. muris* are influenced by a variety of factors, which include the genetic background and gender of the mice, the infective dose of the antigen and various isolates of the parasite itself that can modulate different immune responses [51]. Worm expulsion is primarily associated with TH1 and TH2 immune responses, where TH2 response has been seen to modulate complete worm expulsion from the gut in resistant mice and TH1 response

helps in development of chronic infection by harboring the worms in the susceptible strains or by delaying their expulsion [51] [124]. The susceptible strains of mice produce a high amount of TH1 cytokines such as IFN-γ, IL-12, IL-18 and IgG2a antibody that help in prolonging inflammatory responses in mice resulting in organ damage from chronicity of infection. Neutralization of IFN-γ by administration of anti- IFN-γ-Ab was seen to promote resistant phenotype even in susceptible mice [93] [94] [95] [99]. Resistance to *T. muris* is seen to be strongly associated with TH2 cytokines such as IL-4, IL-5, IL-9, IL-13, and production of IgG1 and IgE antibodies under the control of IL-4 and IL-13. IL-4 and IL-13 are considered as major cytokines involved in the process of worm expulsion and both IL-4 and IL-13 KO mice have shown susceptibility to *T. muris*, where administration of any of these cytokines has restored their resistance [76] [99] [125].

The mechanisms by which IL-4 and IL-13 regulate increased expression of SPDEF, goblet cell hyperplasia and mucin secretion include STAT-6 pathways. However, there are other pathways independent of STAT-6 that might also be responsible in the process, which include MAPK or PI3K pathways [77] [78] [126]. With regard to these facts, our results have shown increased production of IL-4 and IL-13 in $SPDEF^{+/+}$ mice at day 14 p.i. compared to $SPDEF^{-/-}$ mice, which were significantly reduced at day 21. The $SPDEF^{-/-}$ mice, on the other hand, showed a significant increase in IL-4 and IL-13 levels from day 14 to day 21 p.i., compared to $SPDEF^{+/+}$ mice. The absence of SPDEF and decreased mucin secretion from goblet cells might suggest delayed expulsion of worms in $SPDEF^{-/-}$ mice with increased TH2 cytokine levels at day 21 p.i.. Interestingly, in $SPDEF^{-/-}$ mice, we observed higher presence of worms at day 21 p.i. compared to that on day 14 p.i.. This may be due to delayed or impaired worm hatching and poor larval development in the $SPDEF^{-/-}$ mice due to downregulated mucin secretion. Further assessments on

the worm hatching at earlier timepoints of infection are warranted to understand the underlying mechanisms.

Acute *T. muris* infection in BALB/c mice is associated with upregulation of Atoh-1, leading to hyperproliferation of goblet cells [26]. Consistent with this study, we also observed increased mRNA expression of *Atoh-1* in $SPDEF^{+/+}$ and $SPDEF^{-/-}$ mice after infection. Our experiments did not show any significant difference of *β-catenin* expression after infection in both groups. As the major intracellular signal transducer and effector protein of Wnt canonical cascade, β-catenin has many different functions, which include maintaining cellular integrity at the adherens junction linked with E-cadherins and other catenin proteins, and regulating the transcription of a variety of genes [127]. This data may suggest that *T. muris* shows effects on the signaling cascade involved in differentiation of ISCs, downstream of β-catenin.

There are more than 1000 different species of bacteria in the gut along with viruses and protozoa, which form a complex environment inside our body. Numerically, the bacteria are the most abundant in the GI tract, most of which are anaerobes that perform a variety of functions associated with host metabolism, immune system development, host behavior, limiting pathogen invasion and so on [128]. The symbiotic relationship between host and gut microbiome is subject to alteration by various factors such as host's age, gender and diet, physiology and immune system of the host, antibiotic usage, infective and inflammatory conditions, presence of autoimmune diseases, etc.; which can lead to development of chronic inflammatory diseases such as IBD, diabetes, and allergy [33]. As discussed in chapter 1, the changes in gut microbiota and the interaction between parasites and host microbial environment have been widely studied in relation to many enteric parasitic infections both in humans and mice, Moreover, changes in the mucus following parasitic infection can lead to microbial change, which has also been discussed. In

previous studies, chronic *T. muris* infection in resistant mice was seen to alter the gut microbial composition by reducing the phylum Bacteroidetes and increasing the *Lactobacillaceae* family [109]. Decreased α-diversity and changes in β-diversity were observed in relation to chronic infection which were apparent between 14 and 28 days. Although acute infection did not show any significant changes in diversity, it has shown increased abundance of *Clostridia* strains that inhibited *Bacteroides vulgatus* colonization in mice [63] [109] [110] [129].

The changes in microbiota have been more broadly studied in regard to chronic *T. muris* infection possibly for the reason that humans usually suffer from chronic infection with *T. trichiura* and the prolonged infective timeline in mice during chronic infection is more representative of microbial changes that happen in humans with *T. trichiura* infection. The duration of infection also plays an important role in changing the microbial community to a greater extent than it does in acute infection. Furthermore, during chronic infection, the pathological changes in the intestinal epithelium are more pronounced, that may lead to changes in the microbial community. Considering all these facts and speculations, we investigated the changes in microbial community in $SPDEF^{+/+}$ and $SPDEF^{-/-}$ mice at different timepoints. There were no observable significant changes in relative abundance on genus level between the 2 groups of mice, except for *Bacteroides* and *Alistipes*. Both of them belong to Bacteroidetes phylum, which is one of the most abundant phyla present in the mammalian gut. $SPDEF^{+/+}$ mice showed higher abundance of *Alistipes* species, whereas $SPDEF^{-/-}$ mice showed higher abundance of *Bacteroides.* Abundance data on phylum level showed a relatively higher abundance of Campylobacterota and decreased abundance of Bacteroidetes in $SPDEF^{+/+}$ mice compared to other timepoints in the same group and to $SPDEF^{-/-}$ group. Variations in α and β-diversity were also significant at day 14 p.i. between $SPDEF^{+/+}$ and $SPDEF^{-/-}$ mice. We further analyzed the microbiota separately in both groups, which has shown

that α-diversity has decreased significantly in *SPDEF*$^{+/+}$ mice at day 21 after infection, while it happened at day 14 in *SPDEF*$^{-/-}$ mice with higher abundance of Bacteroidetes. A possible reason for showing changes in microbial community at day 14 could be that in resistant mice, day 14 p.i. is considered as the peak timepoint of infection when changes in goblet cell markers and TH2 cytokine levels become notable compared to uninfected stage. The mice also start expelling worms from their gut from this period of time, which might suggest that day 14 p.i. is a critical period for *SPDEF*$^{+/+}$ mice to show more variations in diversity in contrast to *SPDEF*$^{-/-}$ mice. The absence of SPDEF has effects on the mucus with lower goblet cell differentiation and less mucin secretion. The mucin property bears effect on bacterial adhesion to the mucus, which could also explain the microbial differences between these 2 groups. However, since the timeline of acute infection is significantly shorter than chronic, it might be a reason why no significant visible changes were observed in several bacterial genera between these groups. It is important to note here that a number of variables can also contribute to contrasting results obtained from targeted 16s sequencing which include housing condition of the mice, diet, age, gender, body weight and so on. GF mice models are considered as the gold standard in gaining insight into the parasite-microbiota interaction and are being used in many studies. However, since microbial exposure is fully blocked in GF mice since birth which grossly impairs their immune system development, studying the role of microbiota in regulating cellular functions and signaling pathways becomes difficult in the context of parasitic infection. Therefore, antibiotic-treated or ABX mice come into play. Broad-spectrum antibiotics can be applied to mice regardless of any genotype and physiological condition, which can block some specific microbes in a specific organ without impairing gross microbial environment in the body. We have assessed the changes in SPDEF and mucin in antibiotic-treated mice after naïve and *T. muris*-altered cecal microbiota transplant where we

observed higher number of goblet cells and increased expression of SPDEF and Muc2 in ABX mice after *T. muris*-altered microbiota transplant compared to naïve microbiota transplant. *T. muris*-microbiota interaction generates downstream signaling cascades, causing changes in expression of goblet cell markers in contrast to naïve microbiota. The microbial composition and diversity analysis showed changes in β-diversity between naïve and *T. muris*-altered microbiota, although no significant difference was observed in α-diversity between the 2 groups. Our lab has shown that antibiotic treatment in C57BL/6 mice resulted in diminished abundance of Gram-negative bacteria and increased relative abundance of Gram-positive bacteria [103], which was contradictory to the changes we observed in ABX mice on BALB/c background. We have observed a higher abundance of Gram-positive *Enterococcus* and decreased abundance of a couple of Gram-negative bacteria such as *Alistipes, Bacteroides, Helicobacter,* which showed their presence following naïve and *T. muris*-altered microbiota transplant. Between the transplant groups, higher abundance of Campylobacterota was observed after naïve microbiota transplant, which showed no visible abundance in mice after *T. muris*-altered microbiota transplant. The microbial community is unique to individuals and variation in microbiota is subject to many different factors, which include the genetic background and associated phenotypic changes in mice, colonization period of microbiota and other environmental conditions, so it is important to keep the variability in check as much as possible.

Both naïve and *T. muris*-altered microbiota were collected from the cecal samples of *SPDEF*$^{+/+}$ or WT mice, as discussed in chapter 3. Our lab has shown the absence of worms in *T. muris* infected C57BL/6 mice after day 35 (unpublished data) and hence, the cecal content for the altered microbiota by *T. muris* was collected after day 35 p.i. to exclude the possibility of transferring worms from the cecum to the antibiotic-treated mice. However, the microbial community after

complete worm expulsion might show differences with the community that is being altered when the worms are still persisting in the gut. This could lead us to do future experiments with *T. muris*-altered microbiota while the worms are still present. Moreover, microbiota transplant from *SPDEF*$^{-/-}$mice into antibiotic-treated mice can also be conducted in the future to see if the expression of SPDEF in ABX mice after microbiota transplant from *SPDEF*$^{-/-}$mice has any notable difference from *SPDEF*$^{+/+}$ mice.

Goblet cells in the intestine express several pattern recognition receptors which help in microbial recognition, binding and generation of subsequent downstream intracellular cascade that provide immunity to the host. As discussed in chapter 1 and chapter 4: section 4.5, our lab study has shown that treatment with NOD1 and NOD2 agonists produced more Muc2 mucin from goblet cells in mice with acute *T. muris* infection, which was also consistent with previous studies done in this context where NOD2 was seen to play an important role in epithelial cell response to *T. muris* [106]. In human colon cell line, NOD1 and NOD2 agonists increased the expression of MUC2 mucin [107]. The sentinel goblet cells of colonic tissue in multiple mouse strains showed that TLRs in goblet cells activate NLRP-6 inflammasome-mediated signaling cascade and MyD88-dependent ROS synthesis, which can induce transcription of several genes including Muc2 [130]. TLR4 was also seen to inhibit Notch-mediated signaling which resulted in increased goblet cell differentiation in mice [131]. In relation to the effect of *T. muris* ESPs on TLRs, a study from our lab showed that treatment with ESPs in BON-1 cells had direct effect on increased TLR2 expression [103]. *T. muris* ESPs have several immunomodulatory functions and they are considered as therapeutic candidates for inflammatory diseases like IBD and multiple sclerosis [69] [136] [133]. Considering the evidence from previous studies, we investigated whether *T. muris* can modulate changes in SPDEF and MUC2 through NOD/TLR signaling in LS174T cells.

We observed that although there was no difference in protein expression of those markers, their mRNA expression was upregulated with NOD2, TLR2 and TLR4 agonists, which was inhibited after treatment with NOD2 and TLR2 antagonists along with *T. muris* ESPs, suggesting the effect of *T. muris* on the genetic expression of goblet cell markers through NOD/TLR receptors. The variable result in their protein expression can happen due to several reasons, which include pathways involving post-translational modification or anything related to the experiment itself or antibody sensitivity that may have affected the quantification of protein levels, which can be investigated in future.

In conclusion, the study of SPDEF-mediated transcription program in *T. muris* infection will reveal important interactions among parasites, microbiota and goblet cells in the gut and enhance our understanding of the crosstalk between resident microbiota and invading intestinal parasite in the context of innate defense. Besides, there are other transcription factors that regulate cell-fate differentiation of secretory progenitors into intestinal goblet cells, such as growth factor independent-1 (Gfi1) and Kruppel-like factor-4 (KLF4), which could be studied in future in this regard [134] [135]. In turn, this data from our research may be extrapolated to the study of *T. trichiura* infection in humans, both in basic and clinical research settings. These findings may also facilitate the development of novel strategies in modulating SPDEF expression in relation to GI disorders such as colorectal cancer, inflammatory bowel disease or cystic fibrosis, that are associated with goblet cell pathology and dysregulated mucin secretion.

References

[1] B. Greenwood-Van Meerveld, A. C. Johnson, and D. Grundy, "Gastrointestinal Physiology and Function," *Handb. Exp. Pharmacol.*, vol. 239, pp. 1–16, 2017, doi: 10.1007/164_2016_118.

[2] S. Yang and M. Yu, "Role of Goblet Cells in Intestinal Barrier and Mucosal Immunity," *J. Inflamm. Res.*, vol. 14, pp. 3171–3183, Jul. 2021, doi: 10.2147/JIR.S318327.

[3] I. K. Gipson, "Goblet Cells of the Conjunctiva: A Review of Recent Findings," *Prog. Retin. Eye Res.*, vol. 54, pp. 49–63, Sep. 2016, doi: 10.1016/j.preteyeres.2016.04.005.

[4] H. A. McCauley and G. Guasch, "Three cheers for the goblet cell: maintaining homeostasis in mucosal epithelia," *Trends Mol. Med.*, vol. 21, no. 8, pp. 492–503, Aug. 2015, doi: 10.1016/j.molmed.2015.06.003.

[5] J. J. Kim and W. I. Khan, "Goblet cells and mucins: role in innate defense in enteric infections," *Pathog. Basel Switz.*, vol. 2, no. 1, pp. 55–70, Feb. 2013, doi: 10.3390/pathogens2010055.

[6] A. Kasprzak and A. Adamek, "Mucins: the Old, the New and the Promising Factors in Hepatobiliary Carcinogenesis," *Int. J. Mol. Sci.*, vol. 20, no. 6, p. E1288, Mar. 2019, doi: 10.3390/ijms20061288.

[7] M. E. V. Johansson and G. C. Hansson, "Immunological aspects of intestinal mucus and mucins," *Nat. Rev. Immunol.*, vol. 16, no. 10, pp. 639–649, Oct. 2016, doi: 10.1038/nri.2016.88.

[8] M. E. V. Johansson, H. Sjövall, and G. C. Hansson, "The gastrointestinal mucus system in health and disease," *Nat. Rev. Gastroenterol. Hepatol.*, vol. 10, no. 6, pp. 352–361, Jun. 2013, doi: 10.1038/nrgastro.2013.35.

[9] B. Deplancke and H. R. Gaskins, "Microbial modulation of innate defense: goblet cells and the intestinal mucus layer," *Am. J. Clin. Nutr.*, vol. 73, no. 6, pp. 1131S-1141S, Jun. 2001, doi: 10.1093/ajcn/73.6.1131S.

[10] D. F. Rogers, "The airway goblet cell," *Int. J. Biochem. Cell Biol.*, vol. 35, no. 1, pp. 1–6, Jan. 2003, doi: 10.1016/S1357-2725(02)00083-3.

[11] D. A. Dartt, "Control of mucin production by ocular surface epithelial cells," *Exp. Eye Res.*, vol. 78, no. 2, pp. 173–185, Feb. 2004, doi: 10.1016/j.exer.2003.10.005.

[12] J. A. Nadel, "Role of epidermal growth factor receptor activation in regulating mucin synthesis," *Respir. Res.*, vol. 2, no. 2, pp. 85–89, 2001, doi: 10.1186/rr43.

[13] Y. Diebold, J. D. Ríos, R. R. Hodges, I. Rawe, and D. A. Dartt, "Presence of nerves and their receptors in mouse and human conjunctival goblet cells," *Invest. Ophthalmol. Vis. Sci.*, vol. 42, no. 10, pp. 2270–2282, Sep. 2001.

[14] H. R. Miller, "Gastrointestinal mucus, a medium for survival and for elimination of parasitic nematodes and protozoa," *Parasitology*, vol. 94 Suppl, pp. S77-100, 1987, doi: 10.1017/s0031182000085838.

[15] S. Umar, "Intestinal Stem Cells," *Curr. Gastroenterol. Rep.*, vol. 12, no. 5, pp. 340–348, Oct. 2010, doi: 10.1007/s11894-010-0130-3.

[16] D. Pinto and H. Clevers, "Wnt control of stem cells and differentiation in the intestinal epithelium," *Exp. Cell Res.*, vol. 306, no. 2, pp. 357–363, Jun. 2005, doi: 10.1016/j.yexcr.2005.02.022.

[17] S. Koch, "Extrinsic control of Wnt signaling in the intestine," *Differ. Res. Biol. Divers.*, vol. 97, pp. 1–8, Oct. 2017, doi: 10.1016/j.diff.2017.08.003.

[18] E. Kaemmerer, M. K. Jeon, A. Berndt, C. Liedtke, and N. Gassler, "Targeting Wnt Signaling via Notch in Intestinal Carcinogenesis," *Cancers*, vol. 11, no. 4, p. 555, Apr. 2019, doi: 10.3390/cancers11040555.

[19] R. Asada *et al.*, "The Endoplasmic Reticulum Stress Transducer OASIS Is involved in the Terminal Differentiation of Goblet Cells in the Large Intestine *," *J. Biol. Chem.*, vol. 287, no. 11, pp. 8144–8153, Mar. 2012, doi: 10.1074/jbc.M111.332593.

[20] I. Y. Luk, C. M. Reehorst, and J. M. Mariadason, "ELF3, ELF5, EHF and SPDEF Transcription Factors in Tissue Homeostasis and Cancer," *Molecules*, vol. 23, no. 9, Art. no. 9, Sep. 2018, doi: 10.3390/molecules23092191.

[21] P. Oettgen *et al.*, "PDEF, a Novel Prostate Epithelium-specific Ets Transcription Factor, Interacts with the Androgen Receptor and Activates Prostate-specific Antigen Gene Expression*," *J. Biol. Chem.*, vol. 275, no. 2, pp. 1216–1225, Jan. 2000, doi: 10.1074/jbc.275.2.1216.

[22] T. K. Noah, A. Kazanjian, J. Whitsett, and N. F. Shroyer, "SAM pointed domain ETS factor (SPDEF) regulates terminal differentiation and maturation of intestinal goblet cells," *Exp. Cell Res.*, vol. 316, no. 3, pp. 452–465, Feb. 2010, doi: 10.1016/j.yexcr.2009.09.020.

[23] A. Gregorieff *et al.*, "The ets-domain transcription factor Spdef promotes maturation of goblet and paneth cells in the intestinal epithelium," *Gastroenterology*, vol. 137, no. 4, pp. 1333-1345.e1–3, Oct. 2009, doi: 10.1053/j.gastro.2009.06.044.

[24] M. Zhang and C. Wu, "The relationship between intestinal goblet cells and the immune response," *Biosci. Rep.*, vol. 40, no. 10, p. BSR20201471, Oct. 2020, doi: 10.1042/BSR20201471.

[25] J. R. McDole *et al.*, "Goblet cells deliver luminal antigen to CD103+ dendritic cells in the small intestine," *Nature*, vol. 483, no. 7389, pp. 345–349, Mar. 2012, doi: 10.1038/nature10863.

[26] S. Z. Hasnain, D. J. Thornton, and R. K. Grencis, "Changes in the mucosal barrier during acute and chronic Trichuris muris infection," *Parasite Immunol.*, vol. 33, no. 1, pp. 45–55, Jan. 2011, doi: 10.1111/j.1365-3024.2010.01258.x.

[27] S. Z. Hasnain *et al.*, "Mucin Gene Deficiency in Mice Impairs Host Resistance to an Enteric Parasitic Infection," *Gastroenterology*, vol. 138, no. 5–10, pp. 1763-1771.e5, May 2010, doi: 10.1053/j.gastro.2010.01.045.

[28] S. Z. Hasnain *et al.*, "Muc5ac: a critical component mediating the rejection of enteric nematodes," *J. Exp. Med.*, vol. 208, no. 5, pp. 893–900, May 2011, doi: 10.1084/jem.20102057.

[29] Y. Yousefi, S. Haq, S. Banskota, Y. H. Kwon, and W. I. Khan, "Trichuris muris Model: Role in Understanding Intestinal Immune Response, Inflammation and Host Defense," *Pathog. Basel Switz.*, vol. 10, no. 8, p. 925, Jul. 2021, doi: 10.3390/pathogens10080925.

[30] A. Cortés, L. Peachey, R. Scotti, T. P. Jenkins, and C. Cantacessi, "Helminth-microbiota cross-talk - A journey through the vertebrate digestive system," *Mol. Biochem. Parasitol.*, vol. 233, p. 111222, Oct. 2019, doi: 10.1016/j.molbiopara.2019.111222.

[31] P. Paone and P. D. Cani, "Mucus barrier, mucins and gut microbiota: the expected slimy partners?," *Gut*, vol. 69, no. 12, pp. 2232–2243, Dec. 2020, doi: 10.1136/gutjnl-2020-322260.

[32] F. Sommer and F. Bäckhed, "The gut microbiota — masters of host development and physiology," *Nat. Rev. Microbiol.*, vol. 11, no. 4, pp. 227–238, Apr. 2013, doi: 10.1038/nrmicro2974.

[33] M. M. Zaiss and N. L. Harris, "Interactions between the intestinal microbiome and helminth parasites," *Parasite Immunol.*, vol. 38, no. 1, pp. 5–11, Jan. 2016, doi: 10.1111/pim.12274.

[34] O. Partida-Rodríguez *et al.*, "Human Intestinal Microbiota: Interaction Between Parasites and the Host Immune Response," *Arch. Med. Res.*, vol. 48, no. 8, pp. 690–700, Nov. 2017, doi: 10.1016/j.arcmed.2017.11.015.

[35] G. P. Donaldson, S. M. Lee, and S. K. Mazmanian, "Gut biogeography of the bacterial microbiota," *Nat. Rev. Microbiol.*, vol. 14, no. 1, pp. 20–32, Jan. 2016, doi: 10.1038/nrmicro3552.

[36] B. Chassaing and A. T. Gewirtz, "Identification of Inner Mucus-Associated Bacteria by Laser Capture Microdissection," *Cell. Mol. Gastroenterol. Hepatol.*, vol. 7, no. 1, pp. 157–160, Sep. 2018, doi: 10.1016/j.jcmgh.2018.09.009.

[37] G. C. Hansson, "Mucins and the Microbiome," *Annu. Rev. Biochem.*, vol. 89, pp. 769–793, Jun. 2020, doi: 10.1146/annurev-biochem-011520-105053.

[38] M. E. V. Johansson *et al.*, "Normalization of host intestinal mucus layers requires long-term microbial colonization," *Cell Host Microbe*, vol. 18, no. 5, pp. 582–592, Nov. 2015, doi: 10.1016/j.chom.2015.10.007.

[39] A. M. Rodríguez-Piñeiro and M. E. V. Johansson, "The colonic mucus protection depends on the microbiota," *Gut Microbes*, vol. 6, no. 5, pp. 326–330, Aug. 2015, doi: 10.1080/19490976.2015.1086057.

[40] H. E. Jakobsson *et al.*, "The composition of the gut microbiota shapes the colon mucus barrier," *EMBO Rep.*, vol. 16, no. 2, pp. 164–177, Feb. 2015, doi: 10.15252/embr.201439263.

[41] L. Arike and G. C. Hansson, "The Densely O-Glycosylated MUC2 Mucin Protects the Intestine and Provides Food for the Commensal Bacteria," *J. Mol. Biol.*, vol. 428, no. 16, pp. 3221–3229, Aug. 2016, doi: 10.1016/j.jmb.2016.02.010.

[42] B. Schroeder, "Fight them or feed them: How the intestinal mucus layer manages the gut microbiota," *Gastroenterol. Rep.*, vol. 7, pp. 3–12, Feb. 2019, doi: 10.1093/gastro/goy052.

[43] L. Etienne-Mesmin *et al.*, "Experimental models to study intestinal microbes-mucus interactions in health and disease," *FEMS Microbiol. Rev.*, vol. 43, no. 5, pp. 457–489, Sep. 2019, doi: 10.1093/femsre/fuz013.

[44] K. S. B. Bergstrom and L. Xia, "Mucin-type O-glycans and their roles in intestinal homeostasis," *Glycobiology*, vol. 23, no. 9, pp. 1026–1037, Sep. 2013, doi: 10.1093/glycob/cwt045.

[45] J. P. Ouwerkerk, W. M. de Vos, and C. Belzer, "Glycobiome: bacteria and mucus at the epithelial interface," *Best Pract. Res. Clin. Gastroenterol.*, vol. 27, no. 1, pp. 25–38, Feb. 2013, doi: 10.1016/j.bpg.2013.03.001.

[46] T. Pelaseyed and G. C. Hansson, "Membrane mucins of the intestine at a glance," *J. Cell Sci.*, vol. 133, no. 5, p. jcs240929, Mar. 2020, doi: 10.1242/jcs.240929.

[47] H. Li *et al.*, "The outer mucus layer hosts a distinct intestinal microbial niche," *Nat. Commun.*, vol. 6, p. 8292, Sep. 2015, doi: 10.1038/ncomms9292.

[48] M. E. V. Johansson *et al.*, "Composition and functional role of the mucus layers in the intestine," *Cell. Mol. Life Sci. CMLS*, vol. 68, no. 22, pp. 3635–3641, Nov. 2011, doi: 10.1007/s00018-011-0822-3.

[49] G. C. Hansson, "Mucus and mucins in diseases of the intestinal and respiratory tracts," *J. Intern. Med.*, vol. 285, no. 5, pp. 479–490, May 2019, doi: 10.1111/joim.12910.

[50] G. Birchenough, B. O. Schroeder, F. Bäckhed, and G. C. Hansson, "Dietary destabilisation of the balance between the microbiota and the colonic mucus barrier," *Gut Microbes*, vol. 10, no. 2, pp. 246–250, Sep. 2018, doi: 10.1080/19490976.2018.1513765.

[51] J. E. Klementowicz, M. A. Travis, and R. K. Grencis, "Trichuris muris: a model of gastrointestinal parasite infection," *Semin. Immunopathol.*, vol. 34, no. 6, pp. 815–828, Nov. 2012, doi: 10.1007/s00281-012-0348-2.

[52] I. L. King and Y. Li, "Host-Parasite Interactions Promote Disease Tolerance to Intestinal Helminth Infection," *Front. Immunol.*, vol. 9, p. 2128, 2018, doi: 10.3389/fimmu.2018.02128.

[53] T. P. Brosschot and L. A. Reynolds, "The impact of a helminth-modified microbiome on host immunity," *Mucosal Immunol.*, vol. 11, no. 4, pp. 1039–1046, Jul. 2018, doi: 10.1038/s41385-018-0008-5.

[54] P. J. Hotez, A. Fenwick, S. E. Ray, S. I. Hay, and D. H. Molyneux, "'Rapid impact' 10 years after: The first 'decade' (2006–2016) of integrated neglected tropical disease control," *PLoS Negl. Trop. Dis.*, vol. 12, no. 5, p. e0006137, May 2018, doi: 10.1371/journal.pntd.0006137.

[55] P. J. Hotez, P. J. Brindley, J. M. Bethony, C. H. King, E. J. Pearce, and J. Jacobson, "Helminth infections: the great neglected tropical diseases," *J. Clin. Invest.*, vol. 118, no. 4, pp. 1311–1321, Apr. 2008, doi: 10.1172/JCI34261.

[56] A. Rapin and N. L. Harris, "Helminth-Bacterial Interactions: Cause and Consequence," *Trends Immunol.*, vol. 39, no. 9, pp. 724–733, Sep. 2018, doi: 10.1016/j.it.2018.06.002.

[57] S. T. Walk, A. M. Blum, S. A.-S. Ewing, J. V. Weinstock, and V. B. Young, "Alteration of the murine gut microbiota during infection with the parasitic helminth Heligmosomoides polygyrus," *Inflamm. Bowel Dis.*, vol. 16, no. 11, pp. 1841–1849, Nov. 2010, doi: 10.1002/ibd.21299.

[58] A. Araujo, K. J. Reinhard, L. F. Ferreira, and S. L. Gardner, "Parasites as probes for prehistoric human migrations?," *Trends Parasitol.*, vol. 24, no. 3, pp. 112–115, Mar. 2008, doi: 10.1016/j.pt.2007.11.007.

[59] M. Chabé, A. Lokmer, and L. Ségurel, "Gut Protozoa: Friends or Foes of the Human Gut Microbiota?," *Trends Parasitol.*, vol. 33, no. 12, pp. 925–934, Dec. 2017, doi: 10.1016/j.pt.2017.08.005.

[60] A. G. M. Tielens, K. W. A. van Grinsven, K. Henze, J. J. van Hellemond, and W. Martin, "Acetate formation in the energy metabolism of parasitic helminths and protists," *Int. J. Parasitol.*, vol. 40, no. 4, pp. 387–397, Mar. 2010, doi: 10.1016/j.ijpara.2009.12.006.

[61] M. H. Kogut, A. Lee, and E. Santin, "Microbiome and pathogen interaction with the immune system," *Poult. Sci.*, vol. 99, no. 4, pp. 1906–1913, Apr. 2020, doi: 10.1016/j.psj.2019.12.011.

[62] W. C. Gause and R. M. Maizels, "Macrobiota — helminths as active participants and partners of the microbiota in host intestinal homeostasis," *Curr. Opin. Microbiol.*, vol. 32, pp. 14–18, Aug. 2016, doi: 10.1016/j.mib.2016.04.004.

[63] A. Houlden *et al.*, "Chronic Trichuris muris Infection in C57BL/6 Mice Causes Significant Changes in Host Microbiota and Metabolome: Effects Reversed by Pathogen Clearance," *PLOS ONE*, vol. 10, no. 5, p. e0125945, May 2015, doi: 10.1371/journal.pone.0125945.

[64] L. Glendinning, N. Nausch, A. Free, D. W. Taylor, and F. Mutapi, "The microbiota and helminths: sharing the same niche in the human host," *Parasitology*, vol. 141, no. 10, pp. 1255–1271, Sep. 2014, doi: 10.1017/S0031182014000699.

[65] S. K. Menzies *et al.*, "Risk Factors for Soil-Transmitted Helminth Infections during the First 3 Years of Life in the Tropics; Findings from a Birth Cohort," *PLoS Negl. Trop. Dis.*, vol. 8, no. 2, p. e2718, Feb. 2014, doi: 10.1371/journal.pntd.0002718.

[66] M. J. Broadhurst *et al.*, "Therapeutic helminth infection of macaques with idiopathic chronic diarrhea alters the inflammatory signature and mucosal microbiota of the colon," *PLoS Pathog.*, vol. 8, no. 11, p. e1003000, 2012, doi: 10.1371/journal.ppat.1003000.

[67] A. Spor, O. Koren, and R. Ley, "Unravelling the effects of the environment and host genotype on the gut microbiome," *Nat. Rev. Microbiol.*, vol. 9, no. 4, pp. 279–290, Apr. 2011, doi: 10.1038/nrmicro2540.

[68] M. Yazdanbakhsh, A. van den Biggelaar, and R. M. Maizels, "Th2 responses without atopy: immunoregulation in chronic helminth infections and reduced allergic disease," *Trends Immunol.*, vol. 22, no. 7, pp. 372–377, Jul. 2001, doi: 10.1016/s1471-4906(01)01958-5.

[69] C. M. Trujillo-Vargas *et al.*, "Helminth-derived products inhibit the development of allergic responses in mice," *Am. J. Respir. Crit. Care Med.*, vol. 175, no. 4, pp. 336–344, Feb. 2007, doi: 10.1164/rccm.200601-054OC.

[70] J. Bethony *et al.*, "Soil-transmitted helminth infections: ascariasis, trichuriasis, and hookworm," *Lancet Lond. Engl.*, vol. 367, no. 9521, pp. 1521–1532, May 2006, doi: 10.1016/S0140-6736(06)68653-4.

[71] A. J. Bancroft and R. K. Grencis, "Immunoregulatory molecules secreted by Trichuris muris," *Parasitology*, vol. 148, no. 14, pp. 1757–1763, doi: 10.1017/S0031182021000846.

[72] C. Zaph, P. J. Cooper, and N. L. Harris, "Mucosal immune responses following intestinal nematode infection," *Parasite Immunol.*, vol. 36, no. 9, pp. 439–452, Sep. 2014, doi: 10.1111/pim.12090.

[73] W. I. Khan, "Physiological changes in the gastrointestinal tract and host protective immunity: learning from the mouse-Trichinella spiralis model," *Parasitology*, vol. 135, no. 6, pp. 671–682, May 2008, doi: 10.1017/S0031182008004381.

[74] K. J. Else, "Have gastrointestinal nematodes outwitted the immune system?," *Parasite Immunol.*, vol. 27, no. 10–11, pp. 407–415, Nov. 2005, doi: 10.1111/j.1365-3024.2005.00788.x.

[75] D. Artis, C. S. Potten, K. J. Else, F. D. Finkelman, and R. K. Grencis, "Trichuris muris: host intestinal epithelial cell hyperproliferation during chronic infection is regulated by interferon-gamma," *Exp. Parasitol.*, vol. 92, no. 2, pp. 144–153, Jun. 1999, doi: 10.1006/expr.1999.4407.

[76] G. J. McKenzie, A. Bancroft, R. K. Grencis, and A. N. J. McKenzie, "A distinct role for interleukin-13 in Th2-cell-mediated immune responses," *Curr. Biol.*, vol. 8, no. 6, pp. 339–342, Mar. 1998, doi: 10.1016/S0960-9822(98)70134-4.

[77] W. I. Khan, P. Blennerhasset, C. Ma, K. I. Matthaei, and S. M. Collins, "Stat6 dependent goblet cell hyperplasia during intestinal nematode infection," *Parasite Immunol.*, vol. 23, no. 1, pp. 39–42, Jan. 2001, doi: 10.1046/j.1365-3024.2001.00353.x.

[78] "IL-4/IL-13 independent goblet cell hyperplasia in experimental helminth infections | BMC Immunology | Full Text." https://bmcimmunol.biomedcentral.com/articles/10.1186/1471-2172-9-11 (accessed Apr. 04, 2022).

[79] M. Van der Sluis *et al.*, "Muc2-Deficient Mice Spontaneously Develop Colitis, Indicating That MUC2 Is Critical for Colonic Protection," *Gastroenterology*, vol. 131, no. 1, pp. 117–129, Jul. 2006, doi: 10.1053/j.gastro.2006.04.020.

[80] N. L. Harris and P. Loke, "Recent Advances in Type-2-Cell-Mediated Immunity: Insights from Helminth Infection," *Immunity*, vol. 47, no. 6, pp. 1024–1036, Dec. 2017, doi: 10.1016/j.immuni.2017.11.015.

[81] S. A. Saenz *et al.*, "IL25 elicits a multipotent progenitor cell population that promotes T(H)2 cytokine responses," *Nature*, vol. 464, no. 7293, pp. 1362–1366, Apr. 2010, doi: 10.1038/nature08901.

[82] N. E. Humphreys, D. Xu, M. R. Hepworth, F. Y. Liew, and R. K. Grencis, "IL-33, a potent inducer of adaptive immunity to intestinal nematodes," *J. Immunol. Baltim. Md 1950*, vol. 180, no. 4, pp. 2443–2449, Feb. 2008, doi: 10.4049/jimmunol.180.4.2443.

[83] D. R. Neill and A. N. J. McKenzie, "Nuocytes and beyond: new insights into helminth expulsion," *Trends Parasitol.*, vol. 27, no. 5, pp. 214–221, May 2011, doi: 10.1016/j.pt.2011.01.001.

[84] S. M. Cruickshank *et al.*, "Rapid Dendritic Cell Mobilization to the Large Intestinal Epithelium Is Associated with Resistance to Trichuris muris Infection1," *J. Immunol.*, vol. 182, no. 5, pp. 3055–3062, Mar. 2009, doi: 10.4049/jimmunol.0802749.

[85] J. U. Mayer, M. Demiri, W. W. Agace, A. S. MacDonald, M. Svensson-Frej, and S. W. Milling, "Different populations of CD11b+ dendritic cells drive Th2 responses in the small intestine and colon," *Nat. Commun.*, vol. 8, p. 15820, Jun. 2017, doi: 10.1038/ncomms15820.

[86] A. Martín-Fontecha *et al.*, "Induced recruitment of NK cells to lymph nodes provides IFN-gamma for T(H)1 priming," *Nat. Immunol.*, vol. 5, no. 12, pp. 1260–1265, Dec. 2004, doi: 10.1038/ni1138.

[87] O. Wald *et al.*, "IFN-γ Acts on T Cells to Induce NK Cell Mobilization and Accumulation in Target Organs1," *J. Immunol.*, vol. 176, no. 8, pp. 4716–4729, Apr. 2006, doi: 10.4049/jimmunol.176.8.4716.

[88] M. R. Hepworth and R. K. Grencis, "Disruption of Th2 Immunity Results in a Gender-Specific Expansion of IL-13 Producing Accessory NK Cells during Helminth Infection1," *J. Immunol.*, vol. 183, no. 6, pp. 3906–3914, Sep. 2009, doi: 10.4049/jimmunol.0900577.

[89] M. Svensson, L. Bell, M. C. Little, M. DeSchoolmeester, R. M. Locksley, and K. J. Else, "Accumulation of eosinophils in intestine-draining mesenteric lymph nodes occurs after Trichuris muris infection," *Parasite Immunol.*, vol. 33, no. 1, pp. 1–11, Jan. 2011, doi: 10.1111/j.1365-3024.2010.01246.x.

[90] T. D. Lee, D. Wakelin, and R. K. Grencis, "Cellular mechanisms of immunity to the nematode Trichuris muris," *Int. J. Parasitol.*, vol. 13, no. 4, pp. 349–353, Aug. 1983, doi: 10.1016/s0020-7519(83)80039-3.

[91] Y. Ito, "The absence of resistance in congenitally athymic nude mice toward infection with the intestinal nematode, Trichuris muris: resistance restored by lymphoid cell transfer," *Int. J. Parasitol.*, vol. 21, no. 1, pp. 65–69, Feb. 1991, doi: 10.1016/0020-7519(91)90121-m.

[92] K. J. Else and R. K. Grencis, "Antibody-independent effector mechanisms in resistance to the intestinal nematode parasite Trichuris muris," *Infect. Immun.*, vol. 64, no. 8, pp. 2950–2954, Aug. 1996, doi: 10.1128/iai.64.8.2950-2954.1996.

[93] K. J. Else, F. D. Finkelman, C. R. Maliszewski, and R. K. Grencis, "Cytokine-mediated regulation of chronic intestinal helminth infection," *J. Exp. Med.*, vol. 179, no. 1, pp. 347–351, Jan. 1994, doi: 10.1084/jem.179.1.347.

[94] A. J. Bancroft, K. J. Else, J. P. Sypek, and R. K. Grencis, "Interleukin-12 promotes a chronic intestinal nematode infection," *Eur. J. Immunol.*, vol. 27, no. 4, pp. 866–870, Apr. 1997, doi: 10.1002/eji.1830270410.

[95] H. Helmby, K. Takeda, S. Akira, and R. K. Grencis, "Interleukin (IL)-18 promotes the development of chronic gastrointestinal helminth infection by downregulating IL-13," *J. Exp. Med.*, vol. 194, no. 3, pp. 355–364, Aug. 2001, doi: 10.1084/jem.194.3.355.

[96] A. Dénes, N. Humphreys, T. E. Lane, R. Grencis, and N. Rothwell, "Chronic systemic infection exacerbates ischemic brain damage via a CCL5 (regulated on activation, normal T-cell expressed and secreted)-mediated proinflammatory response in mice," *J. Neurosci. Off. J. Soc. Neurosci.*, vol. 30, no. 30, pp. 10086–10095, Jul. 2010, doi: 10.1523/JNEUROSCI.1227-10.2010.

[97] A. J. Bancroft, A. N. McKenzie, and R. K. Grencis, "A critical role for IL-13 in resistance to intestinal nematode infection," *J. Immunol. Baltim. Md 1950*, vol. 160, no. 7, pp. 3453–3461, Apr. 1998.

[98] A. J. Bancroft, D. Artis, D. D. Donaldson, J. P. Sypek, and R. K. Grencis, "Gastrointestinal nematode expulsion in IL-4 knockout mice is IL-13 dependent," *Eur. J. Immunol.*, vol. 30, no. 7, pp. 2083–2091, Jul. 2000, doi: 10.1002/1521-4141(200007)30:7<2083::AID-IMMU2083>3.0.CO;2-3.

[99] K. j. Else, G. m. Entwistle, and R. k. Grencis, "Correlations between worm burden and markers of Th1 and Th2 cell subset induction in an inbred strain of mouse infected with Trichuris muris," *Parasite Immunol.*, vol. 15, no. 10, pp. 595–600, 1993, doi: 10.1111/pim.1993.15.10.595.

[100] D. Li and M. Wu, "Pattern recognition receptors in health and diseases," *Signal Transduct. Target. Ther.*, vol. 6, no. 1, Art. no. 1, Aug. 2021, doi: 10.1038/s41392-021-00687-0.

[101] R. S. Mahla, M. C. Reddy, D. V. R. Prasad, and H. Kumar, "Sweeten PAMPs: Role of Sugar Complexed PAMPs in Innate Immunity and Vaccine Biology," *Front. Immunol.*, vol. 4, p. 248, Sep. 2013, doi: 10.3389/fimmu.2013.00248.

[102] L. Franchi, N. Warner, K. Viani, and G. Nuñez, "Function of Nod-like Receptors in Microbial Recognition and Host Defense," *Immunol. Rev.*, vol. 227, no. 1, pp. 106–128, Jan. 2009, doi: 10.1111/j.1600-065X.2008.00734.x.

[103] H. Wang *et al.*, "TLR2 Plays a Pivotal Role in Mediating Mucosal Serotonin Production in the Gut," *J. Immunol.*, vol. 202, no. 10, pp. 3041–3052, May 2019, doi: 10.4049/jimmunol.1801034.

[104] C. M. Kane *et al.*, "Helminth antigens modulate TLR-initiated dendritic cell activation," *J. Immunol. Baltim. Md 1950*, vol. 173, no. 12, pp. 7454–7461, Dec. 2004, doi: 10.4049/jimmunol.173.12.7454.

[105] Y. Gao, M. Zhang, L. Chen, M. Hou, M. Ji, and G. Wu, "Deficiency in TLR2 but not in TLR4 impairs dendritic cells derived IL-10 responses to schistosome antigens," *Cell. Immunol.*, vol. 272, no. 2, pp. 242–250, 2012, doi: 10.1016/j.cellimm.2011.10.007.

[106] R. Bowcutt *et al.*, "A role for the pattern recognition receptor Nod2 in promoting recruitment of CD103+ dendritic cells to the colon in response to Trichuris muris infection," *Mucosal Immunol.*, vol. 7, no. 5, pp. 1094–1105, Sep. 2014, doi: 10.1038/mi.2013.125.

[107] H. Wang *et al.*, "New Role of Nod Proteins in Regulation of Intestinal Goblet Cell Response in the Context of Innate Host Defense in an Enteric Parasite Infection," *Infect. Immun.*, vol. 84, no. 1, pp. 275–285, Jan. 2016, doi: 10.1128/IAI.01187-15.

[108] P. L. Devine *et al.*, "Production of MUC1 and MUC2 mucins by human tumor cell lines," *Biochem. Biophys. Res. Commun.*, vol. 178, no. 2, pp. 593–599, Jul. 1991, doi: 10.1016/0006-291x(91)90149-2.

[109] J. B. Holm *et al.*, "Chronic Trichuris muris Infection Decreases Diversity of the Intestinal Microbiota and Concomitantly Increases the Abundance of Lactobacilli," *PLOS ONE*, vol. 10, no. 5, p. e0125495, May 2015, doi: 10.1371/journal.pone.0125495.

[110] "Exclusive dependence of IL-10Rα signalling on intestinal microbiota homeostasis and control of whipworm infection." https://journals.plos.org/plospathogens/article?id=10.1371/journal.ppat.1007265 (accessed Jan. 14, 2022).

[111] R. W. Li *et al.*, "Alterations in the porcine colon microbiota induced by the gastrointestinal nematode Trichuris suis," *Infect. Immun.*, vol. 80, no. 6, pp. 2150–2157, Jun. 2012, doi: 10.1128/IAI.00141-12.

[112] K. S. Hayes, A. J. Bancroft, M. Goldrick, C. Portsmouth, I. S. Roberts, and R. K. Grencis, "Exploitation of the Intestinal Microflora by the Parasitic Nematode Trichuris muris," *Science*, vol. 328, no. 5984, pp. 1391–1394, Jun. 2010, doi: 10.1126/science.1187703.

[113] M. A. Dea-Ayuela, S. Rama-Iñiguez, and F. Bolás-Fernandez, "Enhanced susceptibility to Trichuris muris infection of B10Br mice treated with the probiotic Lactobacillus casei," *Int. Immunopharmacol.*, vol. 8, no. 1, pp. 28–35, Jan. 2008, doi: 10.1016/j.intimp.2007.10.003.

[114] Y. E. Beyhan and M. R. Yıldız, "Microbiota and parasite relationship," *Diagn. Microbiol. Infect. Dis.*, vol. 106, no. 4, p. 115954, Apr. 2023, doi: 10.1016/j.diagmicrobio.2023.115954.

[115] K.-S. Park *et al.*, "SPDEF regulates goblet cell hyperplasia in the airway epithelium," *J. Clin. Invest.*, vol. 117, no. 4, pp. 978–988, Apr. 2007, doi: 10.1172/JCI29176.

[116] P. Rajavelu, G. Chen, Y. Xu, J. A. Kitzmiller, T. R. Korfhagen, and J. A. Whitsett, "Airway epithelial SPDEF integrates goblet cell differentiation and pulmonary Th2 inflammation," *J. Clin. Invest.*, vol. 125, no. 5, pp. 2021–2031, May 2015, doi: 10.1172/JCI79422.

[117] T. Aivelo and A. Norberg, "Parasite-microbiota interactions potentially affect intestinal communities in wild mammals," *J. Anim. Ecol.*, vol. 87, no. 2, pp. 438–447, Mar. 2018, doi: 10.1111/1365-2656.12708.

[118] A. Dhariwal, J. Chong, S. Habib, I. L. King, L. B. Agellon, and J. Xia, "MicrobiomeAnalyst: a web-based tool for comprehensive statistical, visual and meta-analysis of microbiome data," *Nucleic Acids Res.*, vol. 45, no. W1, pp. W180–W188, Jul. 2017, doi: 10.1093/nar/gkx295.

[119] H. Y. Jiang *et al.*, "Activation of the pattern recognition receptor NOD1 augments colon cancer metastasis," *Protein Cell*, vol. 11, no. 3, pp. 187–201, Mar. 2020, doi: 10.1007/s13238-019-00687-5.

[120] J. Gao *et al.*, "Gut microbial DL-endopeptidase alleviates Crohn's disease via the NOD2 pathway," *Cell Host Microbe*, vol. 30, no. 10, pp. 1435-1449.e9, Oct. 2022, doi: 10.1016/j.chom.2022.08.002.

[121] M. E. Abdelmageed, M. S. El-Awady, M. Abdelrahim, and G. M. Suddek, "LPS-RS attenuation of lipopolysaccharide-induced acute lung injury involves NF-κB inhibition," *Can. J. Physiol. Pharmacol.*, vol. 94, no. 2, pp. 140–146, Feb. 2016, doi: 10.1139/cjpp-2015-0219.

[122] K. S. Hayes and R. K. Grencis, "Trichuris muris and comorbidities - within a mouse model context," *Parasitology*, vol. 148, no. 14, pp. 1–9, Jun. 2021, doi: 10.1017/S0031182021000883.

[123] M. Fukata, A. S. Vamadevan, and M. T. Abreu, "Toll-like receptors (TLRs) and Nod-like receptors (NLRs) in inflammatory disorders," *Semin. Immunol.*, vol. 21, no. 4, pp. 242–253, Aug. 2009, doi: 10.1016/j.smim.2009.06.005.

[124] T. Bellaby, K. Robinson, and D. Wakelin, "Induction of differential T-helper-cell responses in mice infected with variants of the parasitic nematode Trichuris muris.," *Infect. Immun.*, vol. 64, no. 3, pp. 791–795, Mar. 1996.

[125] A. J. Bancroft, K. J. Else, and R. K. Grencis, "Low-level infection with Trichuris muris significantly affects the polarization of the CD4 response," *Eur. J. Immunol.*, vol. 24, no. 12, pp. 3113–3118, Dec. 1994, doi: 10.1002/eji.1830241230.

[126] H. Yu, Q. Li, Victor. P. Kolosov, Juliy. M. Perelman, and X. Zhou, "Interleukin-13 Induces Mucin 5AC Production Involving STAT6/SPDEF in Human Airway Epithelial Cells," *Cell Commun. Adhes.*, vol. 17, no. 4–6, pp. 83–92, Aug. 2010, doi: 10.3109/15419061.2010.551682.

[127] T. Valenta, G. Hausmann, and K. Basler, "The many faces and functions of β-catenin," *EMBO J.*, vol. 31, no. 12, pp. 2714–2736, Jun. 2012, doi: 10.1038/emboj.2012.150.

[128] M. A. E. Lawson, I. S. Roberts, and R. K. Grencis, "The interplay between Trichuris and the microbiota," *Parasitology*, vol. 148, no. 14, pp. 1806–1813, Dec. 2021, doi: 10.1017/S0031182021000834.

[129] D. Ramanan *et al.*, "Helminth infection promotes colonization resistance via type 2 immunity," *Science*, vol. 352, no. 6285, pp. 608–612, Apr. 2016, doi: 10.1126/science.aaf3229.

[130] G. M. H. Birchenough, E. E. L. Nyström, M. E. V. Johansson, and G. C. Hansson, "A sentinel goblet cell guards the colonic crypt by triggering Nlrp6-dependent Muc2 secretion," *Science*, vol. 352, no. 6293, pp. 1535–1542, Jun. 2016, doi: 10.1126/science.aaf7419.

[131] C. P. Sodhi *et al.*, "Intestinal epithelial Toll-like receptor 4 regulates goblet cell development and is required for necrotizing enterocolitis in mice," *Gastroenterology*, vol. 143, no. 3, pp. 708-718.e5, Sep. 2012, doi: 10.1053/j.gastro.2012.05.053.

[132] R. K. Shears and R. K. Grencis, "Whipworm secretions and their roles in host-parasite interactions," *Parasit. Vectors*, vol. 15, no. 1, p. 348, Sep. 2022, doi: 10.1186/s13071-022-05483-5.

[133] B. J. Foth *et al.*, "Whipworm genome and dual-species transcriptome analyses provide molecular insights into an intimate host-parasite interaction," *Nat. Genet.*, vol. 46, no. 7, pp. 693–700, Jul. 2014, doi: 10.1038/ng.3010.

[134] A. M. Ghaleb, B. B. McConnell, K. H. Kaestner, and V. W. Yang, "Altered Intestinal Epithelial Homeostasis in Mice with Intestine-Specific Deletion of the Krüppel-Like Factor 4 Gene," *Dev. Biol.*, vol. 349, no. 2, pp. 310–320, Jan. 2011, doi: 10.1016/j.ydbio.2010.11.001.

[135] N. F. Shroyer, D. Wallis, K. J. T. Venken, H. J. Bellen, and H. Y. Zoghbi, "Gfi1 functions downstream of Math1 to control intestinal secretory cell subtype allocation and differentiation," *Genes Dev.*, vol. 19, no. 20, pp. 2412–2417, Oct. 2005, doi: 10.1101/gad.1353905.